Open access • Journal Article • DOI:10.1061/JYCEAJ.0005741

Jet Injections for Optimum Mixing in Pipe Flow — Source link

Steven D. Fitzgerald, Edward R. Holley

Institutions: University of Texas at Austin

Published on: 01 Oct 1981 - Journal of Hydraulic Engineering (ASCE)

Topics: Pipe flow, Jet (fluid), Secondary flow, Turbulence and Potential flow

WRC RESEARCH REPORT NO. 144

JET INJECTIONS FOR OPTIMUM MIXING IN PIPE FLOW

S.D. FITZGERALD AND E.R. HOLLEY
DEPARTMENT OF CIVIL ENGINEERING
UNIVERSITY OF ILLINOIS AT URBANA-CHAMPAIGN

F I N A L R E P O R T

Project No. A -- 091 -- ILL.

UNIVERSITY OF ILLINOIS
WATER RESOURCES CENTER
2535 Hydrosystems Laboratory
Urbana, Illinois 61801

December, 1979

The work upon which this publication is based is supported in part by funds provided by the Office of Water Research and Technology,(Project A-091-Ill),U.S. Department of the Interior, Washington, D.C., as authorized by the Water Research and Development Act of 1978.

TABLE OF CONTENTS

ACKNOWLEDGMENTS

Special thanks are extended to Mr. J.W. Miller who was responsible for constructing the experimental facilities and for providing valuable advice during the design of the experimental apparatus. Professor V.J. McDonald designed the concentration detection instrumentation. Ms. K. Marr and Ms. L. Dilley typed the report. The support of each person involved with this project was greatly appreciated.

LIST OF FIGURES

LIST OF TABLES

ABSTRACT

JET INJECTIONS FOR OPTIMUM MIXING IN PIPE FLOW

In order to mix an additive or a tracer with the fluid flowing in a pipe, it may be desirable to avoid the energy required and the possible maintenance problems for mixers or obstructions in a pipe and to avoid the relatively long flow length required for ambient mixing. Then, it may be advantageous to inject the additive as a jet into the pipe flow and to use the associated jet mixing to enhance the overall mixing process. Laboratory experiments were conducted to determine the rates of mixing with a single jet injection made at the pipe wall at various angles relative to the pipe wall and with two diametrically opposed jets. For uniform pipe flow, it was possible to identify an optimum momentum for each angle of injection. A few experiments with induced swirl in the pipe flow showed that the swirl had a significant effect on the jet mixing, especially when two jets were used.

Fitzgerald, Steven D. and Holley, Edward R.
JET INJECTIONS FOR OPTIMUM MIXING IN PIPE FLOW
Research Report No. 144, Water Resources Center, University of Illinois, December, 1979, Urbana, IL, 89 p.
KEYWORDS - - mixing/diffusion/jets/pipe flow/water treatment/discharge measurement/dilution method.

1. INTRODUCTION

1.1 PROBLEM DEFINITION

The mixing of a miscible substance with water flowing in the pipeline is often part of a chemical and/or biological water treatment process. Some examples include the chlorination of water supplies and of wastewaters for water quality control purposes, the addition of biocides to thermal power plant cooling water, the addition of scale and corrosion inhibitors, and the mixing of polymer gels in water to achieve an optimal hydraulic fracturing liquid for the development of oil wells. Another example not related to changing the characteristics of the water is the dilution method of measuring discharge in a pipe by injecting a tracer at a constant rate into the flow and measuring the tracer concentration downstream of the injection. The dilution method is particularly useful for situations where the flow cannot be interrupted or head losses need to be minimized. Similar types of problems exist in gas flows.

Conventional mixing devices such as batch mixers, motionless mixers (e.g. fixed blades in a pipe line), pumps, orifices, valves, etc. are used extensively in many operations. However their use may require a disruption of the flow or cause a substantial head loss (except with the pump, of course). The cost of supplying the energy to agitate the fluid and overcome the head losses, the time spent waiting for the substances to mix, and the cost of the mixing devices warrant the investigation of alternative mixing methods.

One viable alternative is to use the pipeline as a mixing chamber by injecting the substance into the pipe flow. The method is sometimes referred to as pipe-flow mixing, in-line mixing, or mixing-on-the-fly. In situations where enough pipe length is available and where the speed with

which mixing is accomplished is not important, the natural turbulence or ambient mixing in a pipe flow can ultimately provide complete mixing. Section 2.2 gives some information on the distance required to achieve a certain degree of mixing in such situations. This research was directed toward those situations in which more rapid mixing is required and, more specifically, toward use of jet injections to provide initial mixing and thereby to hasten the mixing process. With initial jet mixing, the flow distance required to achieve a certain degree of mixing is a function of both the initial mixing associated with the method of injection and the ambient mixing governed by the ambient flow characteristics. The region where initial mixing is predominant is referred to as the initial mixing zone. Likewise, the region downstream of the initial mixing zone is referred to as the ambient mixing zone.

Injection systems with jets originating at the pipe wall were the subject of this investigation because the initial mixing is greatly enhanced by the jet and many problems associated with conventional mixers are minimized. If the injection tube is at the pipe wall and does not protrude a significant distance into the pipe flow, a jet injection system can be installed, maintained, and operated with minimal interruption of the flow and piping system and there are no concerns about structural problems or flow-induced vibrations since there are no struts or tubes extending into the pipe. Also, the loss of total energy in the ambient flow due to the jet injection is usually negligible when compared to the energy requirements for operation of a batch mixer or the energy lost by placing motionless mixers in the line. Thus, with an injection system with jets originating at the wall, rapid mixing can be achieved without interrupting the ambient flow or substantially reducing the energy in the ambient flow.

For this laboratory study, the injected fluid or additive is referred to as a tracer. The mixing distance is the flow distance from the point of

injection to the point where the variation in concentration over the cross section is some small, specified amount. The expression "optimum" is used to refer to those characteristics which result in the most rapid mixing for a given type of jet injection.

1.2 RESEARCH OBJECTIVES

The research objectives for this study were to

1) experimentally investigate several jet injection systems to determine their mixing characteristics. The injections were made at the pipe wall.
2) identify those injection systems providing the most rapid mixing and determine the optimum operating conditions.
3) investigate the effects which secondary currents have on the mixing.
4) calculate the power requirements for various injection systems.

1.3 EXPERIMENTAL APPROACH

Experiments were conducted in a 6-in.I.D. galvanized steel pipe under steady, fully turbulent flow conditions. A non-buoyant, sodium chloride tracer was injected at a steady rate into the flowing water through 1/8-in. I.D. brass tubes with one end flush with the pipe wall. The distribution of tracer concentration in the ambient flow was determined by conductivity measurements on two perpendicular diameters with a total of thirteen points at various downstream cross sections spaced 10 to 20 pipe diameters apart. From the concentration data, the progress of the mixing could be followed downstream from the injection point and the mixing distance could be determined.

The two types of injection systems investigated were (1) a single jet originating at the pipe wall with the angle of injection varied from 90^{o} (cross flow) relative to the ambient flow direction to 150^{o} (almost counter flow), and (2) two jets which originated at the pipe wall, were at opposite

ends of the vertical diameter, and had an angle of injection of 90° (cross flow) relative to the ambient flow direction. After finding the optimum conditions for the jet injections, the effect which a particular secondary current had on the mixing distance was investigated by placing a fixed three-bladed outboard motor propeller upstream of the injection point.

2. THEORETICAL BACKGROUND AND LITERATURE REVIEW

2.1 SOME DEFINITIONS

A parameter which can be used to characterize the degree of mixing or the uniformity of the concentration distribution over a cross section is the coefficient of variation defined as

$$C_v = [\frac{1}{A_p}\int_{A_p} (\frac{c}{\bar{c}} - 1)^2 \, dA_p]^{1/2} \qquad (2.1)$$

where c = tracer concentration at a point in the cross section and $\bar{c}$ = cross sectional average concentration. C_v is large near the point of injection where the concentration distribution is highly non-uniform and as the concentration distribution becomes progressively more uniform, C_v decreases with increasing flow distance. For large flow distances, empirical C_v values are non-zero and are a function of the random measurement errors associated with the experimental apparatus. Eq. 2.1 written for a finite number of points in the cross section is

$$C_v = [\sum_{i=1}^{N} W_i \, (\frac{c_i}{\bar{c}} - 1)^2]^{1/2} \qquad (2.2)$$

where i = index describing the position of a measurement point,

W_i = weighting coefficient which can be used to take into account the nonuniform velocity distribution and uneven distribution of the measurement points across the cross section (Ger and Holley, 1974).

N = number of measurement points

c_i = total (measured) concentration minus background concentration

and

$$\bar{c} = \sum_{i=1}^{N} W_i c_i$$

The mixing distance can be defined as the distance from the injection to the point downstream where a desired small C_v is obtained. For a given injection system and given flow the mixing distance increases as the desired C_v decreases, i.e. as the requirement for the degree of uniformity increases. For example, the flow distance required to reach the cross section with C_v = 0.01 is longer than the flow distance to the cross section where C_v = 0.05. Both analytical and experimental evidence indicates that, for small C_v, the maximum concentration variation within a cross section, i.e. $|c - \bar{c}|_{max}$, is linearly related to C_v (Holley, 1977).

One way in which injection systems can be classified is according to the momentum of the tracer inflow. If the momentum of the injected tracer is significant, then the injection is referred to as a jet injection. If the tracer inflow has negligible momentum (and negligible buoyancy), then the injection is referred to as a source or passive source. From a physical point of view, the passive source injection does not significantly disrupt the ambient flow pattern or penetrate into the ambient flow, whereas a jet injection penetrates into the ambient flow.

From dimensional analysis, it can be shown that the penetration (y) of a nonbuoyant jet into the ambient flow can be written as

$$\frac{y}{D_p} = \phi(V_r, A_r, \mathbb{R}_j, \alpha) \qquad (2.3)$$

where V_r = velocity ratio = V_j/V_p

V_j = initial jet velocity

V_p = pipe flow velocity

A_r = area ratio = $A_j/A_p = (D_j/D_p)^2$

A_j = initial cross sectional area of jet

A_p = cross sectional area of pipe

D_j = initial diameter of jet

D_p = pipe diameter

$\mathbb{R}_j$ = initial jet Reynolds number = $V_j D_j/\nu$

ν = kinematic viscosity

α = angle of injection relative to the pipe wall

In deriving Eq. 2.3, it was assumed that the ambient turbulence and the velocity distribution in the pipe flow do not affect the jet penetration. The velocity and area ratios can be combined into a dimensionless momentum ratio, M_r:

$$M_r = \frac{M_j}{M_p} = \frac{Q_j V_j}{Q_p V_p} = \frac{V_j^2 A_j}{V_p^2 A_p} = \left(\frac{V_j D_j}{V_p D_p}\right)^2 \tag{2.4}$$

where M_j = initial jet momentum

M_p = pipe flow momentum

Q_j = initial jet discharge

Q_p = pipe flow discharge

and the densities of the two fluids are assumed to be identical. Experimental results (Chilton and Genereaux, 1930; Ger and Holley, 1974; Morgan et al, 1976) indicate that the behavior of jets injected into pipes is a function of M_r rather than being a function of V_r and A_r separately. It has been assumed that $\mathbb{R}_j$ is large enough so that kinematic similarity of the jets exists (or at least exists in an approximate sense) so that $\mathbb{R}_j$ is not a significant parameter. Eq. 2.3 can then be written as

$$\frac{y}{D_p} = \phi(M_r, \alpha) \tag{2.5}$$

This relationship is considered further in Section 2.4. Similar to Eq. 2.5, the initial mixing provided by jets is a function of M_r and α plus the number and location of the jets around the pipe wall. Passive sources can be viewed as a special case in which $M_r = 0$ so that there is zero penetration and zero initial mixing.

2.2 AMBIENT MIXING

(This section is a summary of some of the material presented by Holley and Ger, 1978.)

In order to characterize the general ambient mixing in a pipe, the flow may be assumed to be represented by a uniform velocity, V_p, and constant radial and circumferential diffusion coefficients, e_r and e_θ. Based on the analogy between momentum and mass transfer

$$e_r = \frac{0.068\, R_p U_*}{Sc_t} \tag{2.6}$$

where U_* = shear velocity = $\sqrt{f/8}\, V_p$

f = friction factor

R_p = pipe radius

Sc_t = turbulent Schmidt number.

Evaluation of e_θ is summarized later in this section. For steady injections, the longitudinal gradients of concentration are normally small enough that the effects of longitudinal diffusion are negligible relative to the advection.

Variations in pipe diameter, roughness, or Reynolds number would be expected to change the mixing distance required to achieve a certain C_v value. The effect of these variations can be considered by using a dimensionless longitudinal distance, Z, which is defined as

$$Z = \frac{e_r z}{V_p R_p} \tag{2.7}$$

where z = flow distance from injection point. Using Eq. 2.6, Eq. 2.7 can be written as

$$Z = \frac{0.048\sqrt{f}}{Sc_t} \frac{z}{D_p} \tag{2.8}$$

The friction factor is a function of both the relative roughness of the pipe and the Reynolds number ($\mathbb{R}_p$). In Section 2.3, some experimental evidence will be discussed concerning the effect which f and $\mathbb{R}_p$ have on the mixing distance. By using Z (Eqs. 2.7 or 2.8) instead of z, the mixing distance for a given source configuration and a given C_v has a Z value which is independent of the flow velocity, pipe diameter, or friction factor.

The differential mass balance equation was solved analytically to investigate the diffusion of a conservative, neutrally buoyant substance released continuously from a point source in a steady, uniform, turbulent pipe flow. Except for source configurations symmetrical about the pipe centerline, the asymptotic slope of log C_v vs Z is a function of a dimensionless parameter

$$\eta = \frac{e_\theta}{e_r} \tag{2.9}$$

Experimental results were used to evaluate η and e_θ, but the values depended on the value assumed for Sc_t. Using the concentration data collected by Filmer and Yevdjevich (1966), Clayton et al. (1968), and Ger and Holley (1974), η was found to be 1.8 assuming a turbulent Schmidt number of 1.0, or η = 1.2 assuming Sc_t = 0.77.

Figure 2.1 is a plot of log C_v versus Z with η = 1.8 and Sc_t = 1.0 for a number of different point source locations represented by $\rho' = r/R_p$ where r = radial coordinate measured from the pipe centerline. Thus, ρ' = 1 represents a source at the pipe wall and ρ' = 0 is at the centerline of the pipe. The curve for ρ' = 0 represents the best mixing for a single passive

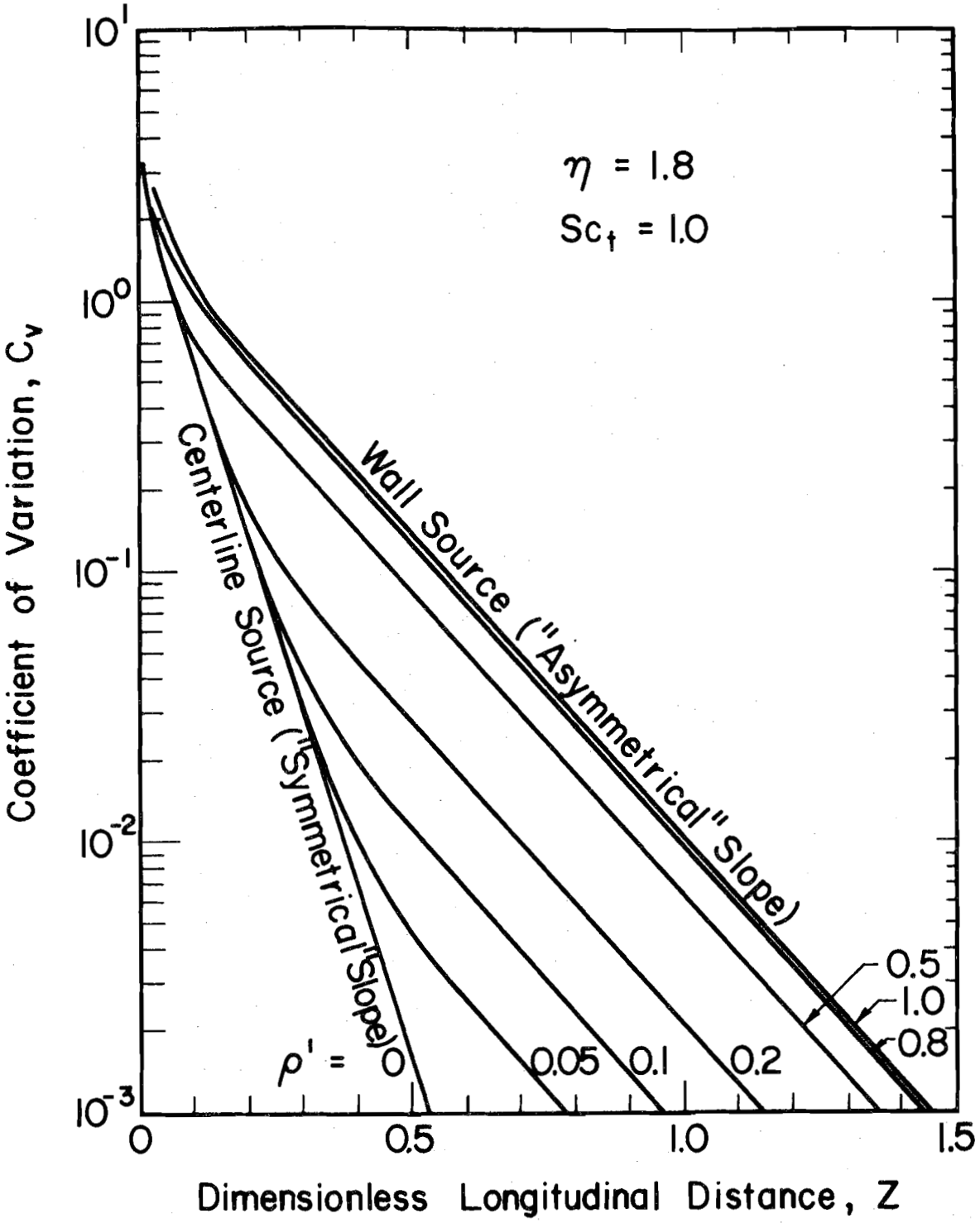

Fig. 2.1 - Calculated coefficient of variation

source because the tracer needs to mix only over a distance equal to the pipe radius, whereas the curve for $\rho' = 1$ represents the slowest mixing because the tracer must mix from one point on the wall across the entire pipe area. The asymptotic (large Z) slope for the $\rho' = 0$ curve also represents the rate of mixing or slope of log C_v vs Z for any initial concentration distributions or any number of point sources provided that the initial distributions or sources are symmetrically arranged about the pipe centerline. Similarly, the $\rho' = 1$ curve for large Z represents the asymptotic slope for all asymmetrical cases and for the slowest rate of ambient mixing. For brevity, these characteristic slopes will be called the "symmetrical" slope and the "asymmetrical" slope. For asymmetrical initial concentration distributions or point source distributions, the log C_v vs. Z curve can have somewhat different shapes for small Z. The curve can follow the centerline source curve, but eventually it will break away to the "asymmetrical" slope. See for example the curve for $\rho' = 0.2$ in Fig. 2.1. The point at which the curve changes from the "symmetrical" to the "asymmetrical" slope depends on the initial degree of asymmetry. The asymptotic slopes for symmetrical and asymmetrical distributions (Fig. 2.1) are included for comparison on the coefficient of variation graphs presented in Chapter 4 for the jet injections.

The "symmetrical" slope for $\rho' = 0$ is associated with perfect symmetry, but perfect symmetry can never be obtained in experiments. Thus, it might be expected that empirical curves for log C_v vs Z should eventually have the "asymptotic" slope for all asymmetrical conditions, but this is not necessarily the case for two reasons. First, Fig. 2.1 shows that the value of Z at which the curves for asymmetrical injections break away from the curve for $\rho' = 0$

depends on the value of ρ', or more generally, on how nearly symmetrical the initial or injection condition is. For example, for $\rho' = 0.05$ and $Z < 0.4$ (or $C_v > 0.01$), it probably would not be possible to distinguish empirically between sources corresponding to $\rho' = 0.05$ and $\rho' = 0$. Thus, a slightly asymmetrical injection could give results which followed the "symmetrical" slope. The second reason is that at some value of C_v, the empirical results begin to represent random measurement errors rather than degree of uniformity of the concentration distribution. Thus, it is normally not possible to measure extremely small values of C_v to determine if the log C_v vs Z curve has broken away from the slope for symmetrical cases. Empirical curves for nearly symmetrical situations can therefore follow the slope for symmetrical cases throughout the range of significant C_v values. Typical values of C_v below which measurement errors predominate are 0.05 for rhodamine tracers (Holley, 1977), 0.02 for conductivity (this study), and 0.003 for radioactive tracers (Clayton and Evans 1968; Holley, 1977).

2.3 PASSIVE SOURCE EXPERIMENTS

Many of the earlier experimental and analytical studies dealing with mixing of a tracer in pipe flow sought to characterize the diffusion associated with the ambient flow. Consequently, the injections were of the passive source type so as to minimize the disturbance of the ambient flow. Holley and Schuster (1967) summarized much of the earlier work on radial diffusion in pipe flow.

Filmer and Yevdjevich (1966) attempted to simulate a point source by injecting a fluorescent dye at the centerline of a 36-in. I.D. pipe at different positions along the pipeline. They measured dye distributions in order to obtain the degree of mixing as a function of flow distance from the point of

injection. The concentration distributions indicated that the tracer rose (because of buoyancy and/or the wake of the injector arm) from the point of injection at the pipe centerline toward the top of the pipe cross section. Nevertheless, their experimental work has proven valuable for subsequent studies of ambient diffusion (Holley and Ger, 1978).

Evans (1967) conducted experiments to check theoretical concentration distributions obtained by Jordan (1961). His results for a centerline source in a 6-in. I.D. copper pipe for $\mathbb{R}_p$ = 100,000, 50,000 and 10,000 agreed closely with the theoretical predictions. Evans also showed by numerical solution of the diffusion equation that the mixing distance for passive ring sources in turbulent pipe flow was minimized by locating the ring at $r/R_p = 0.62$. This result was confirmed experimentally.

Clayton et al. (1968) investigated the diffusion of a radioactive tracer in a 4-in. I.D. pipe using four different source configurations, namely a centerline source, a single wall source, four wall sources equally spaced around the pipe wall, and four sources equally spaced around a circle located at 0.63 R_p. Except for the centerline source, the measured concentration distributions agreed closely with the solutions of the theoretical diffusion equations derived by Jordan (1961). There is seldom good agreement between calculations and data for centerline sources since the calculations generally assume a perfect symmetry which is extremely difficult to simulate experimentally.

Both Evans (1966) and Clayton et al. (1968) showed experimentally and theoretically that the mixing distance increased only slightly with increasing $\mathbb{R}_p$ for smooth pipes. The range of $\mathbb{R}_p$ investigated was 5×10^3 to 1×10^7. The increase in mixing distance was due to a decrease in f and a

corresponding decrease in the diffusion coefficients relative to $V_p R_p$. The dimensionless distance Z in Eqs. 2.7 and 2.8 correctly accounted for changes in the mixing distance (Holley, 1977; Holley and Ger, 1978).

2.4 JET INJECTION EXPERIMENTS

As mentioned previously, a turbulent jet injected with significant momentum across the ambient flow can create rapid initial mixing and can significantly reduce the mixing distance. There has been a significant amount of research dealing with the trajectory and rate of spreading of jets in cross flows, but relatively little has been published concerning specific ways of using jet injection systems to produce rapid mixing in pipes.

Chilton and Genereaux (1930) published one of the first reports addressing the use of different configurations of injection systems to promote rapid mixing. They used air flowing through a glass pipe and an air jet containing smoke as the tracer so visual evaluation could be made concerning the relative mixing for each injection system. From their qualitative experiments, they concluded that the mixing with a cross-flow jet at 90^o relative to the ambient flow was as good as the other methods of injection investigated, namely, a centerline jet directed upstream, a centerline source directed downstream, diametrically opposed dual cross-flow jets, a jet directed downstream at 45^o, and a jet directed upstream at 135^o. However, quantitative data from the present study show that more rapid mixing can be obtained with dual cross-flow jets and with a jet directed at 135^o than with a single cross-flow jet. Chilton and Genereaux (1930) experimentally determined that the momentum ratio, M_r, is a more important parameter in characterizing the mixing for the cross-flow jets than the velocity ratio, V_r, or the flow area

ratio, A_r. In Section 2.1, it was mentioned that the amount of jet penetration into the pipe flow is related to M_r and that the mixing is related to the penetration and therefore to M_r. Chilton and Genereaux (1930) recognized from their qualitative experiments that a range of optimum momentum ratios existed for a given method of injection.

Some information on the relationship of jet penetration to M_r can be obtained from Wright's (1977) work on jets in cross flows. His momentum length scale (ℓ_m) can be expressed as

$$\frac{\ell_m}{D_p} = M_r^{1/2} \tag{2.10}$$

His Fig. 4, using y for the distance from the pipe wall and z for the flow distance in the pipe, indicates that for

$$\frac{\frac{y}{D_p}}{\frac{\ell_m}{D_p}} > 1.5 \tag{2.11}$$

or

$$\frac{y}{D_p} > 1.5\ M_r^{1/2} \tag{2.12}$$

the jets are in the momentum-dominated far field which is the region of interest for characterizing the penetration for most of the jet injections. For the far field, the trajectory can be written as

$$\frac{y}{D_p} = 1.6\ M_r^{1/3}\ \left(\frac{z}{D_p}\right)^{1/3} \tag{2.13}$$

after using Eq. 2.10 in re-writing Wright's equation for the trajectory. It is difficult to use Eq. 2.13 to obtain an absolute evaluation of the jet

penetration because of uncertainties concerning the point of transition from initial mixing to ambient mixing. Nevertheless, it is possible to use Eq. 2.13 to obtain relative penetrations for different M_r's by assuming that the transition can be represented by the same slope (dy/dz) of the trajectory for any two M_r values represented by sub-1 and sub-2, provided that Eq. 2.12 is satisfied. Differentiating Eq. 2.13 and setting $(dy/dz)_1 = (dy/dz)_2$ shows that

$$\frac{\frac{z_1}{D_p}}{\frac{z_2}{D_p}} = \left[\frac{M_{r_1}}{M_{r_2}}\right]^{1/2} \tag{2.14}$$

if z_1 and z_2 are the flow distances to the transition. Substituting Eq. 2.14 into a ratio of Eq. 2.13 for conditions 1 and 2 yields

$$\frac{\frac{y_1}{D_p}}{\frac{y_2}{D_p}} = \left[\frac{M_{r_1}}{M_{r_2}}\right]^{1/2} \tag{2.15}$$

so that the relative penetration of jets into the pipe should be proportional to the square root of M_r.

In addition to analytically characterizing the jet near the injection point, Ger and Holley (1974) experimentally found the optimum momentum ratio, M_r^*, to be approximately 0.016 for a single cross-flow jet. Their experiments were conducted in a 6-in. I.D. galvanized steel pipe. ($M_r^* = 0.013$ was found in this study. See Section 4.2.2.) Ger and Holley showed that for $M_r = M_r^*$, the concentration distribution of the tracer was approximately symmmetrical about the centerline of the pipe after the jet was bent over by the ambient flow. For $M_r < M_r^*$, the jet did not reach the centerline and for $M_r > M_r^*$, the jet overshot the centerline (Fig. 2.2). For M_r either greater than or less

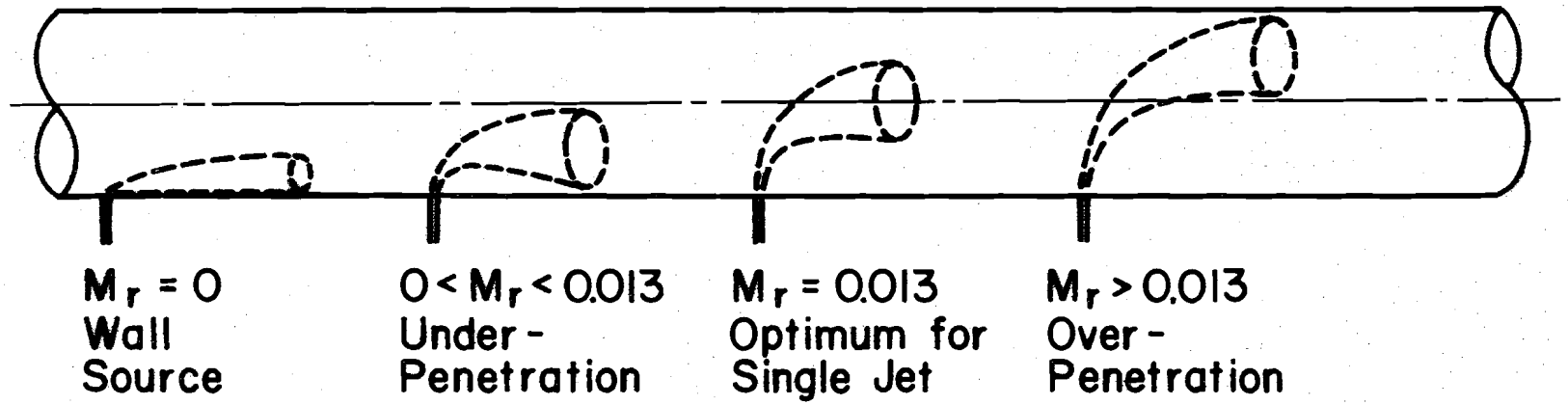

Fig. 2.2 - Penetration of Jet Perpendicular To Pipe Wall

than M_r^*, the mixing distance increased compared to the situation where $M_r = M_r^*$. Therefore, for a single jet injection system to have the maximum effectiveness as a mixing device, it must promote rapid initial mixing and distribute the tracer symmetrically about the centerline of the pipe to allow the diffusion processes to efficiently continue the mixing.

The curves in Fig. 2.1 are related only to ambient mixing since they were calculated for passive sources. The characteristic slopes are applicable for the downstream, ambient mixing part of the process even with initial jet mixing. Normally, the jet is dissipated rather rapidly so that the initial mixing region is rather short (normally only a few pipe diameters, at most, for small diameter jets). One way of viewing the effects of initial mixing is that increasing the degree of initial mixing decreases the value of C_v at the intercept if the linear part of the log C_v vs Z curves is extrapolated back to Z = 0. This can be seen in the data presented in Chap. 4.

3. DESCRIPTION OF EXPERIMENTS

3.1 THE HYDRAULIC CIRCUIT

The hydraulic circuit (Fig. 3.1) used for the experiments was a modified version of the circuit used by Ger and Holley (1974). A 6-in. I.D. galvanized steel pipe with flanged connections was used. At the point of injection, a 4-ft. long section of 6-in. I.D., clear plexiglass pipe was inserted into the piping system in order to visually observe the jet injection. The total length from elbow E2 (Fig. 3.1) to the downstream end of the pipe was 118 ft. The pipe flow was supplied by a vertical turbine pump lifting water from the laboratory sump to a constant head tank 50 ft. above the invert of the 6-in. pipe. The discharge was controlled by a gate valve as shown in Fig. 3.1. A Dall-Flowmeter (BIF, Model 0122-25) was in the line and connected to an air-water manometer, but the meter proved to be useful primarily for monitoring the steadiness of the flow during an experiment. The meter could not be used to measure the pipe discharge for each test because of difficulties in establishing a calibration curve that would remain reliable and accurate for more than a few days for the small discharges used in these experiments. The actual discharge was measured using a tank which had a capacity of 1000 lb. and which was placed on a scale balance. The accuracy of the readings was $\pm$ 7.0 lbs. It was not practical to set exactly the same discharge for each test; the range of discharges was kept between 0.132 and 0.200 cfs.

To dampen the effects of the secondary currents induced by elbow E2 (Fig. 3.1), a flow straightening system installed by Ger and Holley (1974) was used. The straighteners consisted of four vanes placed in elbow E2, followed by seven 10 ft. long, 1 5/8-in. I.D. galvanized steel pipes inserted into the 6-in. pipe, and then a series of five pieces of 5/16-in. flattened

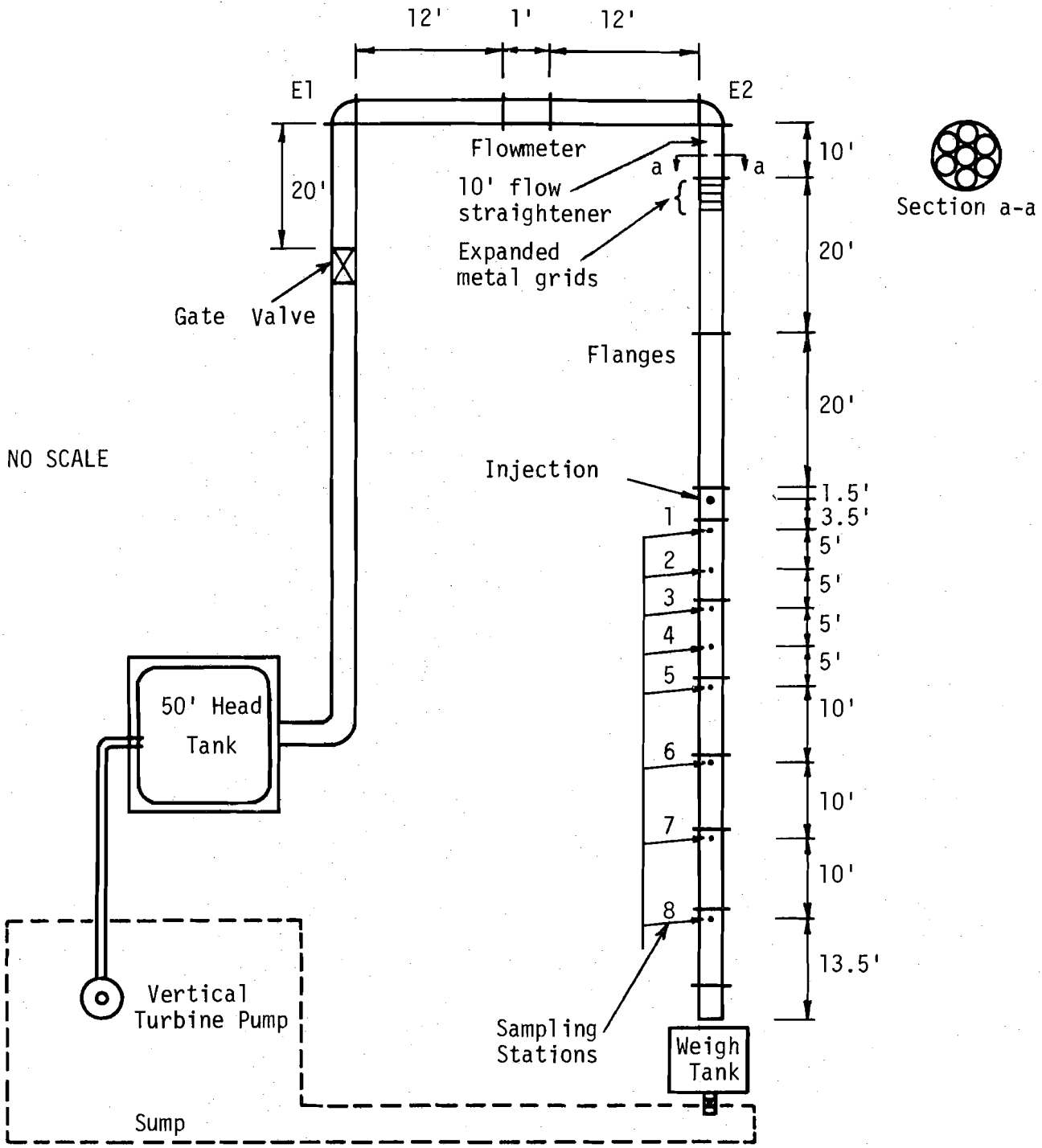

Fig. 3.1 - Schematic diagram of hydraulic circuit

expanded metal placed 6 in. apart. The distance of 79 pipe diameters from the end of the expanded metal to the injection plane was sufficient to dampen any residual secondary currents and turbulence caused by the flow straighteners and to establish fully developed turbulent flow in the pipe (Ger and Holley, 1974).

Injection of the tracer into the ambient flow took place in the 4 ft. plexiglass section, three pipe diameters from the upstream end. The injection location was determined from experiments conducted by Morgan et al. (1976) who showed that the upstream penetration of a counterflowing jet was only three pipe diameters for $M_r \simeq 25$. The five pipe diameters in the clear, plexiglass section downstream of the injection were sufficient for observing the initial behavior of dyed tracers.

The length of pipe available for sampling was 107 pipe diameters. The first sampling station was located 7 pipe diameters from the injection plane, the next four were 10 pipe diameters apart, and the last three were 20 pipe diameters apart. For most experiments, only the first five stations were needed.

At the end of the pipe, a perforated flange was used to insure that the pipe would flow full at the low discharges. The water was returned to the sump via floor channels for recirculation through the circuit.

The hydraulic roughness of the galvanized steel pipe was determined by measuring the head drop for a 50 ft. section for a range of Reynolds numbers from 3×10^4 to 3.5×10^5. The discharges were measured by the Dall-Flowmeter which could be used in this case because the calibration of the meter and the hydraulic roughness tests were conducted on the same day. The meter was calibrated using two weigh tanks with 20,000 lb capacities and 120 lb. accuracy. The relative roughness was found to be about 0.0006 which is higher than the value of 0.0001 determined by Ger and Holley (1974). Visual inspection of

the interior of the pipe wall indicated a rough surface most likely caused by additional corrosion since the last experiment by Ger and Holley (1974).

During the 12-month course of the experimental study, the water temperature ranged from 12.9°C to 25.7°C due to natural seasonal changes. The water temperature was constant during a single test which usually ran for about 4 hours. Because the water temperature covered a wide range, the temperature was taken into account when calculating the viscosity and Reynolds number. With the changing temperature and discharge from experiment to experiment, the Reynolds number varied from 27,000 to 40,100. Taking into account the errors in measuring the pipe discharge and water temperature, the Reynolds number could be calculated to within $\pm$4%. Because of the relatively small range of friction factors corresponding to the range of Reynolds numbers, an average friction factor of 0.025 was used for calculating Z (Eq. 2.8).

3.2 THE TRACER INJECTION SYSTEM

3.2.1 The Tracer

Three tracers commonly used for mixing studies in water are salt (i.e. sodium chloride), radioactive substances, and flourescent dyes. Sodium chloride (NaCl) was selected as a tracer for this experimental study for the following reasons:

a) The accuracy of the sodium chloride concentration measurements is about 1% - 3% as opposed to about 5% for fluorescent tracers. (Holley, 1977).

b) Electronic instruments and experience using NaCl were available from previous experiments conducted in the same laboratory by Ger and Holley (1974).

c) Storage facilities and detection equipment for the radioactive tracer were not available.

d) The NaCl did not require special handling and was readily available and inexpensive.

e) The detection technique chosen to measure the conductivity (amount of NaCl present in ionized form) did not require samples to be collected and analyzed. The conductivity was continuously monitored and recorded. Each experiment took about 4 hrs. and gave immediate results. With a radioactive tracer, samples would have had to be collected and analyzed separately, taking about 8 hrs. for each experiment.

The disadvantages of the salt tracer were:

a) The background conductivity level continually increased because the water flowing in the pipe was recirculated through the laboratory hydraulic circuit. This problem would have occurred for any of the tracers.

b) Adding NaCl to water increased the tracer density above the density of the ambient flow. Ger and Holley (1974) found that if the Froude Number ($F = V_j/\sqrt{(\rho_t/\rho_a - 1)D_j}$, where ρ_t = tracer density and ρ_a = density of the ambient flow) was greater than about 50, the penetration of the jet and mixing distance were independent of the initial density disparity. Hence, only for a few tests was it necessary to add methanol (s.g. = 0.79 and ionically neutral) to the salt tracer to reduce density.

c) The salt solution may have slightly accelerated the corrosion of the pipes.

Different injection flowrates were needed in different experiments in order to minimize the amount of salt being added to the recirculated water. An attempt was made to keep the ultimate salt concentration in the ambient flow close to 20 mg/ℓ above the background concentration for each experiment.

The criteria of 20 mg/ℓ was established from preliminary tests designed to determine the ultimate NaCl concentration which kept all concentration measurements within the linear range of the conductivity probe, which is discussed later in Section 3.4.2, and at the same time, was large enough to insure accurate measurements of the concentration differences. When the injection flowrate needed to be increased for an experiment, the NaCl concentration in the tracer was decreased. The salt concentrations in the injection solutions ranged from 4.2 g/ℓ to 11.1 g/ℓ for injection flowrates ranging from 2.33 x 10^{-4} cfs to 9.9 x 10^{-4} cfs. The temperature difference between the tracer solution and ambient fluid was negligible because the tracer was always prepared using the sump water.

3.2.2 The Injection Circuit

In order to inject a steady continuous flow of tracer into the pipe for a wide range of injection orientations and flow rates, it was expedient to use two separate circuits as shown in Fig. 3.2. Circuit 1 (C1) was used when a high head was required and consisted of a constant head tank which was 26.5 ft above the pipe invert and was supplied by a diaphragm pump (Chemcon, Series 1140-PUC-135). For experiments with low head requirements, Circuit 2 (C2) consisting of a constant head tank which was 5 ft. above the pipe invert and was supplied by a centrifugal pump (Cole-Palmer, U21) was used. Two different circuits were desirable because a single pump capable of meeting both the head and continuous discharge requirements was not available in the lab. The centrifugal pump maintained a steady, continuous discharge, but did not have the head necessary to reach the 26.5-ft head tank. The diaphragm pump had a sufficient head to supply the high head tank, but the pulsating discharge caused the water level to fluctuate about 0.25 in. The water level fluctuations were insignificant relative to the 26.5 ft head but might have

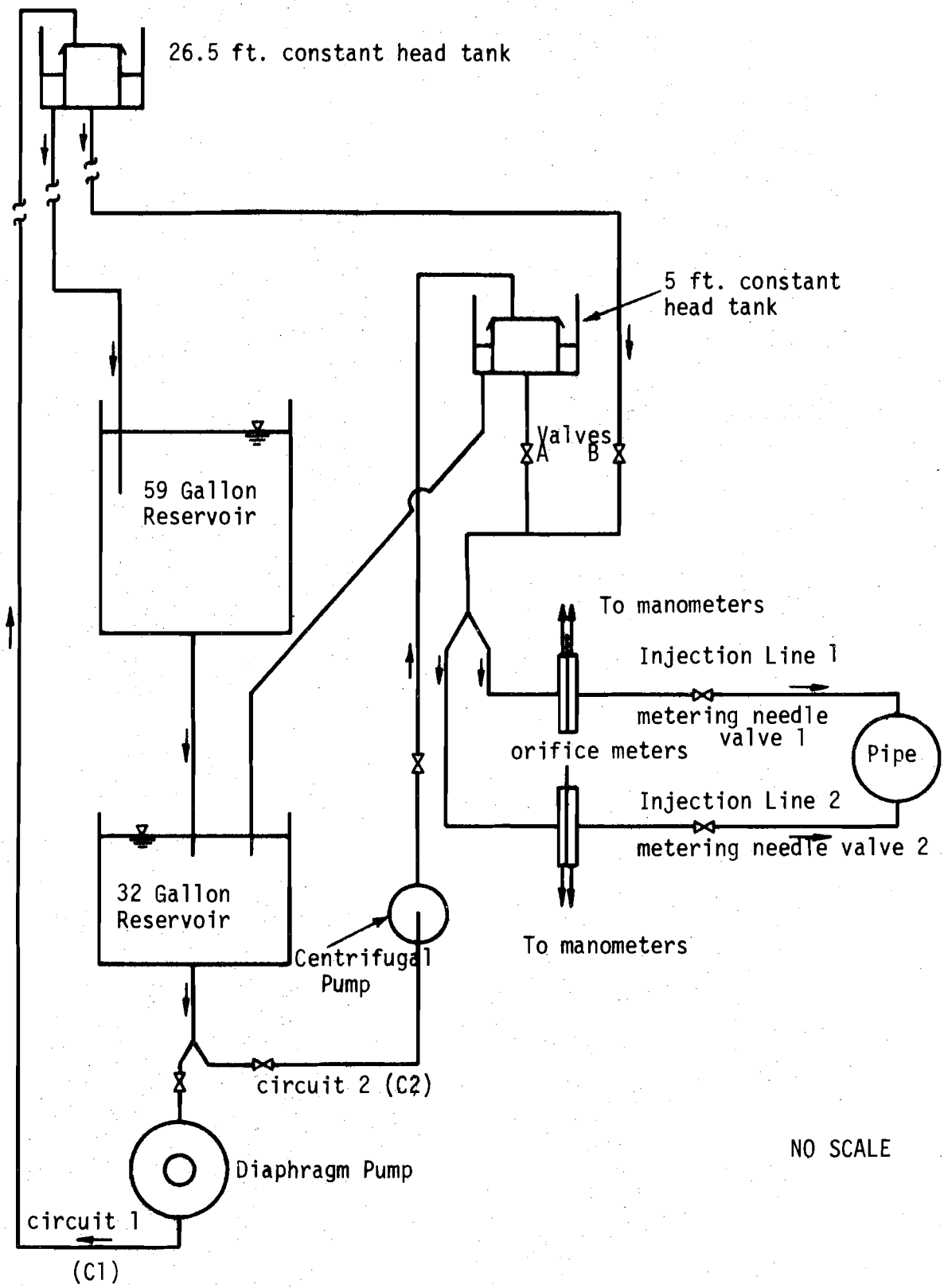

Fig. 3.2 - Schematic diagram of tracer injection circuit

caused some discharge fluctuations with the low head tank. Also, Circuit 2 (low head) was superior to Circuit 1 for two other reasons: 1) The time required for the injection discharge to become steady after readjusting the flowrate was less in C2 than C1 because the length of the tygon tubing in C2 was less than in C1. The changing pressure caused by varying the flowrate affected the flow area in the tygon tubing by stretching or shrinking the tubing and therefore affected the time required to achieve steady state. 2) The needle valves maintained a steadier flowrate in C2 since there was less head to dissipate through the valve.

The 32 gallon tracer reservoir (Fig. 3.2) used by Ger and Holley (1974) was not adequate for the larger volume of tracer required for some of the tests in this study. Therefore, a 59 gallon reservoir was placed in series with the 32 gallon reservoir. When both reservoirs were needed, the tracer solution was continually flowing from one reservoir to the other to insure a uniformly mixed tracer throughout a test.

Two different injection lines branched from the supply line. Injection line 1 was used for the single jet experiments and injection line 2 was added for the dual jet experiments. Each line had a needle valve, an orifice meter, and a U-tube manometer. Depending on the flow condition, either a 3/16" or a 1/8" bore orifice plate was placed in the orifice flanges in a section of 1-in. pipe. Ten inches of one inch pipe were provided upstream of the orifice and 5 inches downstream. Pressure taps in the flange led to a U-tube manometer filled with an indicating fluid with a specific gravity of 1.75. Each injection line had identical apparatus and was controlled independently. Small adjustments made in one line did not noticeably affect the other. Each orifice meter was calibrated independently before the tests began and recalibrated occasionally during the course of the study. No

noticeable changes in the calibration curves occurred. The injection flow rate of the tracer could be measured to within ± 2%.

3.2.3 The Injectors

For the single jet experiments, the injector was located at the top of the pipe and for the dual jet experiments the injectors were located at the top and bottom of the pipe on the same diameter. The two injectors were identical; therefore, the following description applies to both.

A 1/8"-I.D. brass tube inserted through a hole in a rubber plug (Fig. 3.3) was used as the jet injector. The rubber plug fit into a 1 3/8"-long and 1/4"-wide slot cut through the 1/4" wall of the plexiglass pipe. The end of the brass tube could be visually checked to assure that it was approximately flush with the pipe wall. A ratio of tube length to tube diameter of at least 40 is required to have fully developed turbulent flow in the jet when it enters the ambient flow; therefore, the brass tubes were five inches long. The Reynolds number in the injector tube was kept above 2100 to assure that the flow was turbulent. Only for the dual 90^{o} injection system did the Reynolds number approach 2100.

The injectors were supported by plexiglass protractors glued to the plexiglass pipe. The design, as shown in Fig. 3.3, consisted of set screws, guide slots, and collar and allowed the tube to be oriented at α angles ranging from 90^{o} (crossflow) to slightly less than 180^{o} (counter flow), where α is the angle of injection relative to the ambient flow direction. The largest α used was 150^{o}. The rubber plug allowed easy adjustment of the injector in all directions. The jet was aligned transversely by placing a small mark directly opposite the injector position and observing the jet path in an empty pipe with $\alpha = 90^{o}$. The symmetry of the jet injection about the vertical centerline of the pipe was verified by checking the symmetry

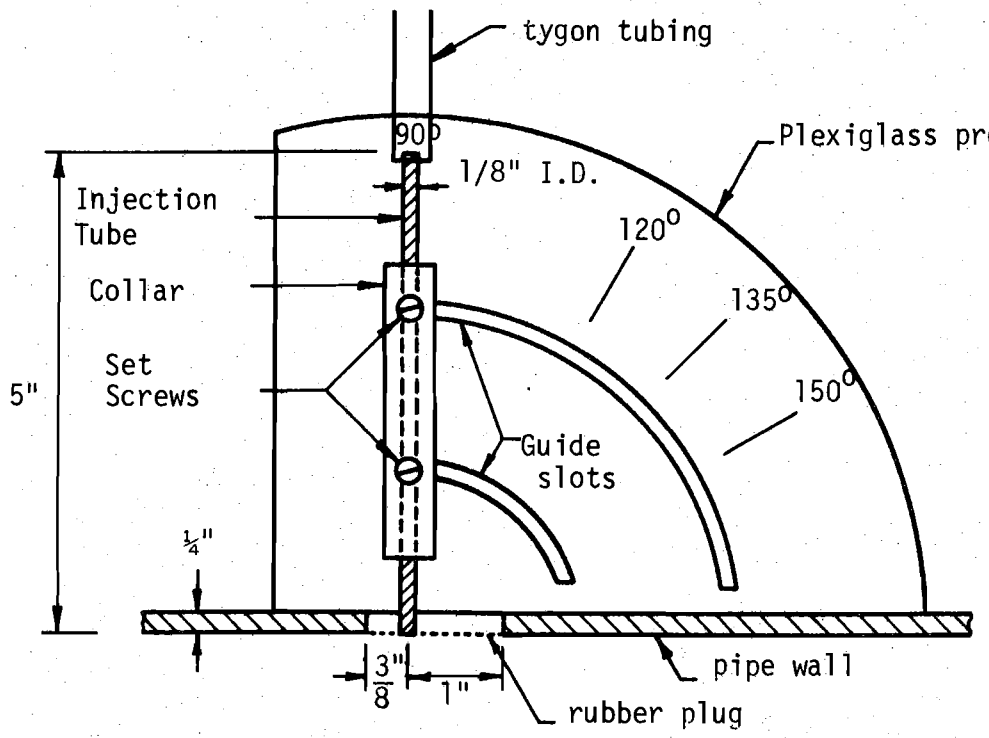

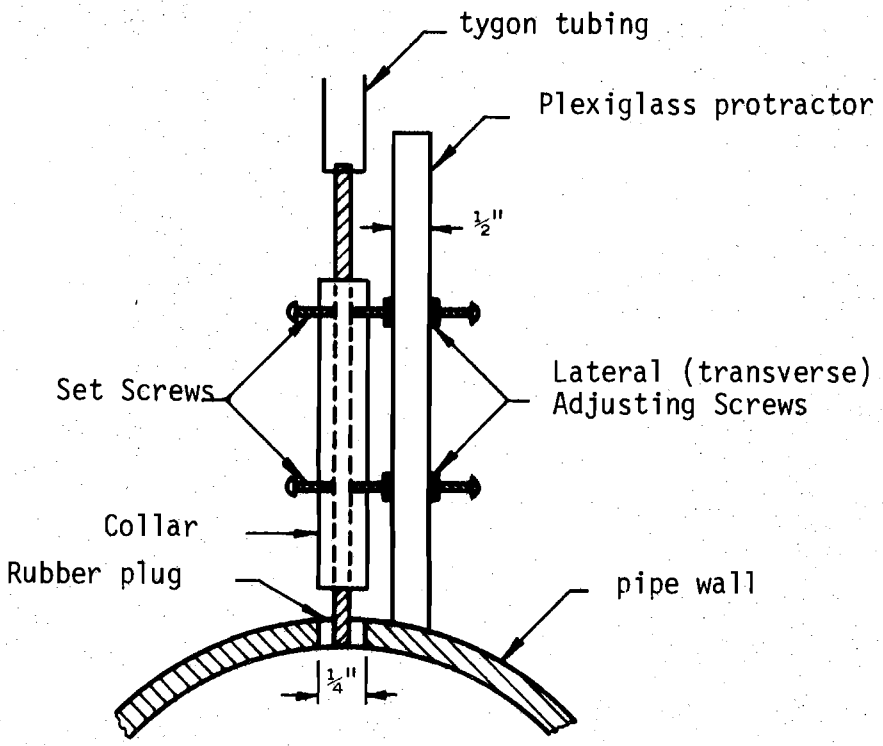

Fig. 3.3 - Schematic diagram of injector

of measured tracer concentrations along a horizontal diameter. See procedure in Section 3.5.

3.3 VISUAL OBSERVATION OF THE JET

Because of the 4 ft. long plexiglass section, it was possible to observe the jet as it entered the pipe flow and the subsequent mixing for 5 pipe diameters downstream of the injection. A potassium permanganate solution was used to dye the jet when it was desired to observe the mixing process (not during data collection).

To correct for the refraction caused by the curved pipe, a plexiglass box was built around the clear pipe and filled with water as shown in Figure 3.4. Photographs were taken for each of the injection orientations to help document the mixing characteristics of the jet in the initial mixing zone. Being able to see the behavior of the jet in the pipe was important for a better understanding of the physical mixing process.

3.4 METHOD OF MEASURING CONCENTRATIONS

3.4.1 Sampling Technique

The technique for measuring the salt concentration at different points in the pipe flow consisted of withdrawing a continuous sample from the pipe flow and measuring the concentration in a continuous flow conductivity cell. The sampling apparatus (sampler) is shown in Fig. 3.5. A 1/8"-I.D. brass tube 12 inches long with a 90^{o} bend pointing 3/8" upstream in the pipe flow was supported by a wood and metal brace bolted around the pipe. It would have been desirable to have a longer horizontal arm on the sampling tube. However, it was originally planned to insert the conductivity probe into the pipe, so the gate values mounted on the side of the pipe (see below) were selected accordingly.

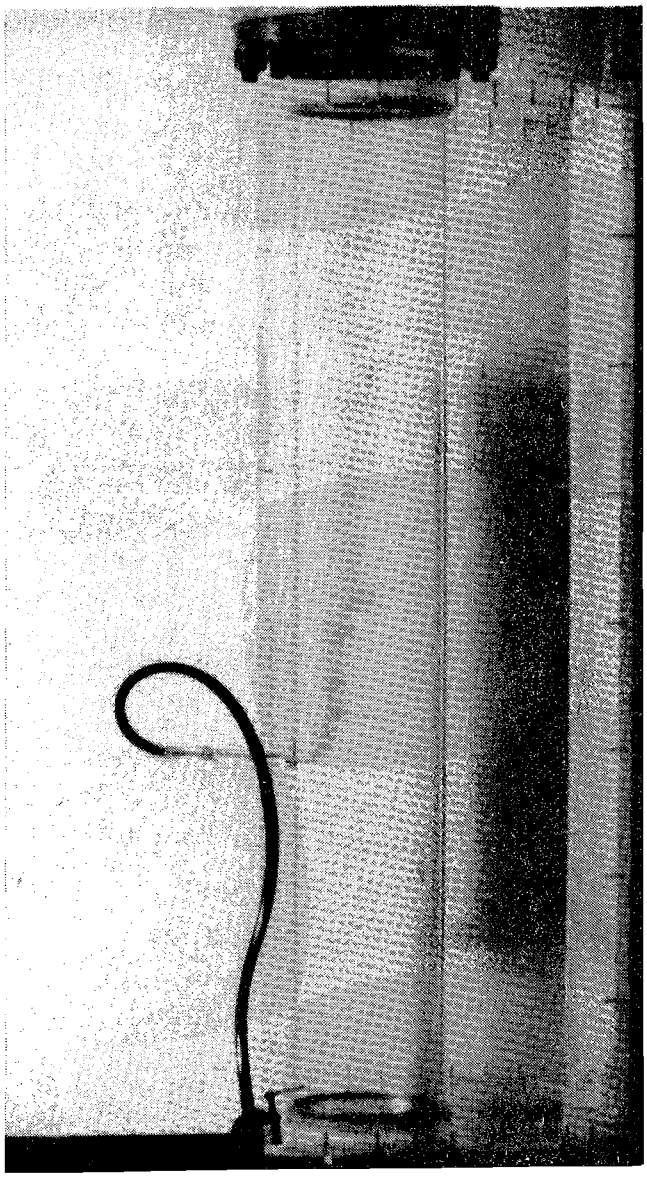

Fig. 3.4 - Plexiglass box around pipe

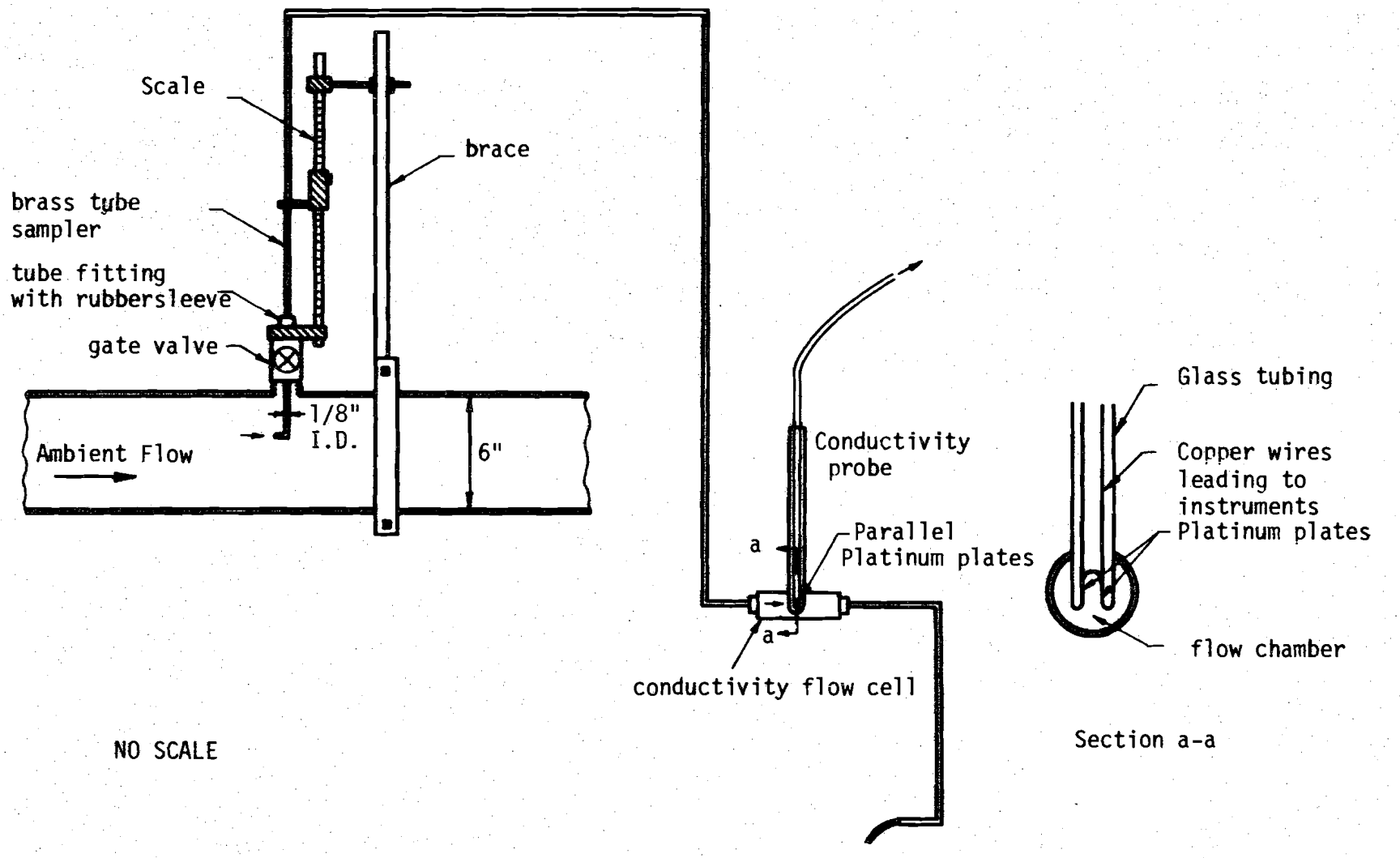

Fig. 3.5 - Schematic diagram of sampling system and conductivity flow cell

Because of electrical interference with probes in the pipe, it was decided to use the sampler tubes with a conductivity flow cell. The sampler was attached to a Lory Type-A point gage (0.001 ft scale) and entered the pipe through a 1/2 inch gate valve which was fastened to the pipe wall. By attaching a tube fitting with a rubber sleeve to each gate valve, the brass sampler tube could be inserted into and removed from the pipe without interrupting the flow or injection. This both helped to reduce the time necessary to run an experiment and helped to insure constant flow conditions during a single experimental run. Two sampling ports per cross-section allowed sampling on two perpendicular diameters (one vertical and one horizontal). The distribution of the sampling stations along the pipe is shown in Fig. 3.1.

The number of sampling points per cross section was determined by investigating the number of points used in previous pipe mixing experiments. Filmer and Yevdjevich (1966) found experimentally that their calculated coefficients of variation differed by an average of only 3.5% when 28 points were sampled instead of 84 points. Clayton et al. (1968) used three radii spaced 90^{o} apart for a total of only 10 points per cross-section. Thirteen sampling points were chosen for this study after considering the results just mentioned and after using Ger and Holley's (1974) data with 37 points per cross section to analyze the sensitivity of calculated coefficients of variation to number of data points. It was found that the use of 13 points near the injection where the concentration distribution was the most non-uniform could give errors of as much as 10% of the value of C_v, but the errors decreased rapidly downstream. Since the purpose of this project was to locate the mixing distance for different methods of injection and not to characterize the behavior of the jet near the injection, thirteen samplings points were considered to be adequate. The locations of the points were determined by

dividing each cross section into four equal concentric subareas. Sampling points were located on the pipe centerline (center of one subarea) and on the horizontal and vertical diameters at the radii which divided each of the other three subareas into two equal parts. Thus, on the four radii spaced 90^{o} apart, samples were taken at r = 1.44", 2.20", and 2.76" and one sample was taken at the center of the pipe. The sample from each subarea was assumed to represent the concentration for the entire subarea, i.e. W_i in Eq. 2.2 was taken as unity. Since the subareas were equal, using $W_i = 1$ is also equivalent to assuming a uniform velocity distribution, but this assumption has a negligible effect on the values of C_v except very near the injection (Ger and Holley, 1974).

At the downstream end of the brass sampling tube, a 1/8"-I.D. tygon tubing transmitted the flow to a 1/2"-diameter, 1" long cylindrical flow chamber where the fluid passed between the two platinum plates of a conductivity probe similar to the type used by Ger and Holley (1974). A 1/8"-tubing then discharged the sample 4 ft. below the pipe invert. This arrangement gave a head of approximately 4 ft, which was sufficient to maintain a flow rate through the sampler of about 170 ml/min, and a sampling velocity approximately 50% higher than the ambient flow velocity. The time necessary to flush the flow chamber and tubing with a new sample was approximately 15 sec.

3.4.2 Concentration Detection Circuitry and Instruments

The salt tracer concentration was detected by measuring the conductivity of a sample while it flowed between two parallel platinum plates (Fig. 3.5), which were the electrodes of a conductivity probe. Figure 3.6 shows the circuitry and instruments used to convert the conductivity measurement to a digital readout. The conductivity probe was one leg of a wheatstone bridge with 1 KΩ resistors making up the other three legs. The

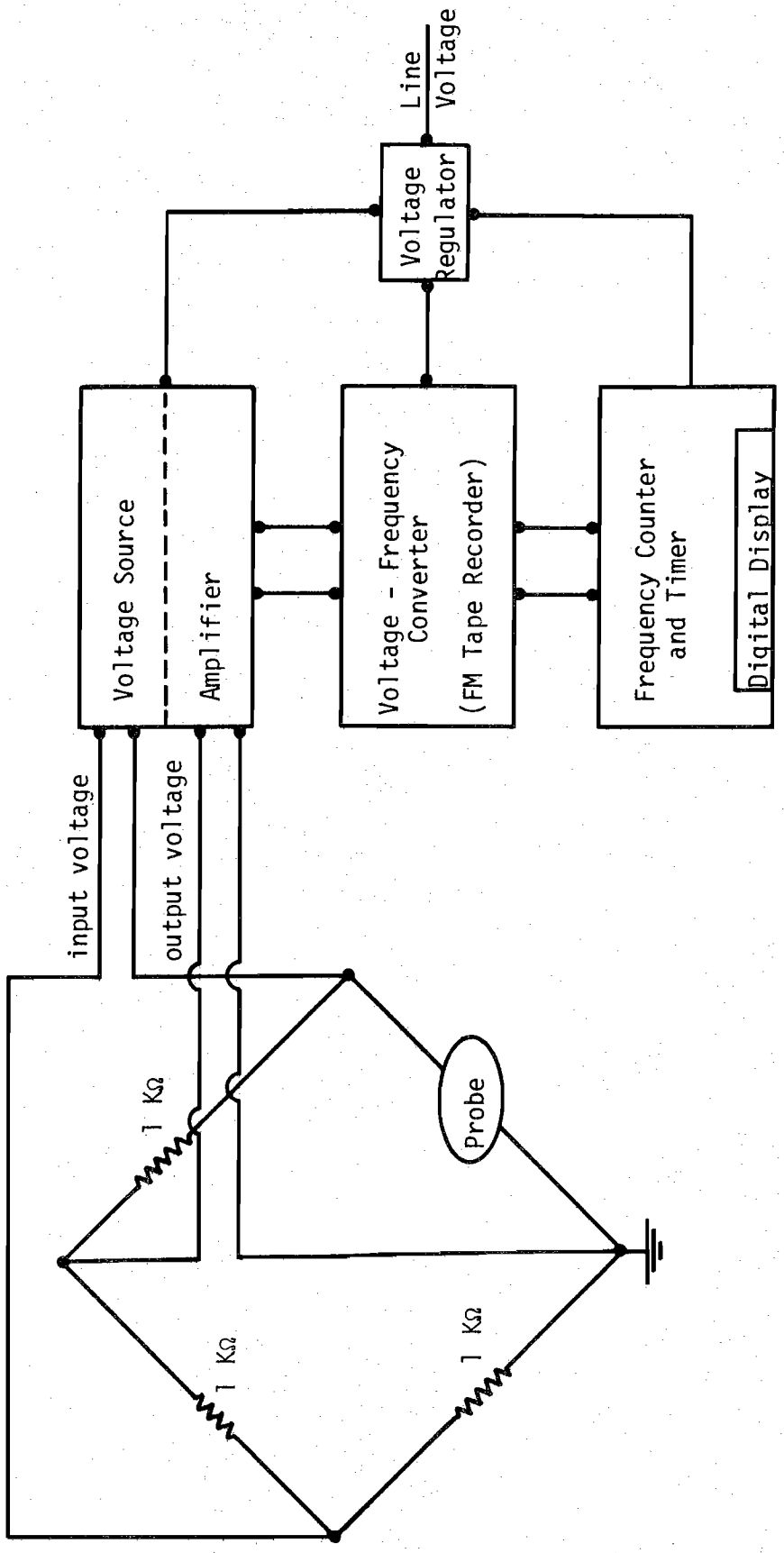

Fig. 3.6 - Schematic diagram of bridge circuitry and electronic instruments for detecting tracer concentrations.

excitation of one volt at 500 Hertz was supplied to the bridge circuit by an Endevco Signal Conditioner (Model 4470). The bridge output voltage was amplified (Carrier Amplifier, Model 4478.1A) and fed into an FM tape recorder (Precision Instruments, Model PI 6108R), part of which was used for voltage-frequency conversion. A counter and timing gate (Anadex Counter-Timer, Model CF-200R) were used to obtain a read-out proportional to the frequency. A voltage regulator was placed in the power supply line to improve the electronic stability of the instruments. The voltage-frequency conversion and the counting were used to provide integration and time averaging of the turbulent fluctuations of concentration, as explained below.

In order to check the linearity of the system, three resistors (21Ω, 1KΩ, and 125KΩ) were substituted for the conductivity probe in the bridge circuit and the corresponding frequency was read for each resistor. The frequency varied from 305 Hz to 720 Hz and the frequency-conductivity relationship was linear.

The behavior of the probe and bridge circuit was checked by calibrating the probe for total concentrations ranging from 5 mg/ℓ to 1000 mg/ℓ. Fig. 3.7 shows that the frequency (conductivity) varied linearly with total salt concentration up to approximately 100 mg/ℓ. Since the largest measured background concentration was about 250 mg/ℓ, some of the experiments were conducted with the probe operating in the nonlinear region of the calibration curve. In spite of this fact, the calibration curves were effectively assumed to be linear with a slope of 1:1 on a log-log graph for the range of concentrations encountered at a given cross section. This assumption was implied by the fact that all of the data were analyzed in terms of frequency instead of concentration when obtaining time-averaged concentrations (see below) and when calculating relative distributions and coefficients of variation. This procedure was assumed to be adequate since (1) the largest

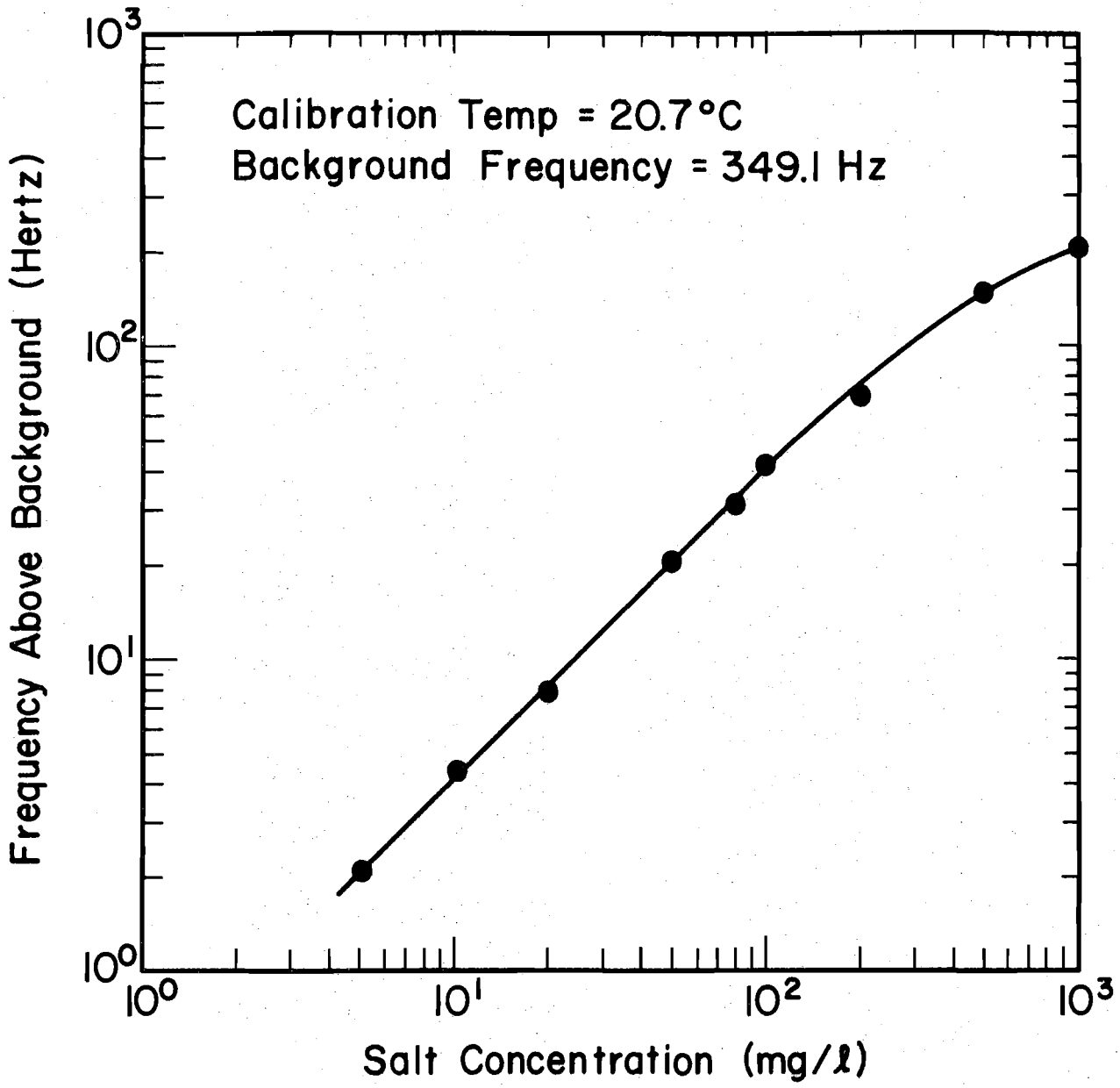

Fig. 3.7 - Typical calibration curve for conductivity probe

range of concentrations encountered was 100 mg/ℓ at Station 1, (2) for any 100 mg/ℓ interval for concentrations between 100 mg/ℓ and 350 mg/ℓ, the calibration curve can be reasonably approximated by a straight line with a 1:1 slope, and (3) for most of the cross sections, the range of measured concentrations was considerably less than 100 mg/ℓ and the degree of validity of the assumption increased with distance downstream as the range of concentrations decreased.

Sometimes readings became erratic, but this problem could be corrected by cleaning and replatinzing the electrodes according to instructions given by Ger and Holley (1974). After replatinizing, the probe was recalibrated to verify the linearity of the probe and the bridge circuit.

The minimum concentration that could be accurately measured by the probe and instruments was 0.5 mg/ℓ. The errors in the entire salt concentration measuring circuitry including the probe and instruments may have been as large as 2 1/2%. Measurement of the background concentration with no injection gave C_v values of 0.010 to 0.015 (1% to 1 1/2%) on three occasions. However, inspection of the C_v data at large Z with injection indicated possible random errors of 2 to 2 1/2%. Holley (1977) discussed indications of random errors in C_v values.

Because of the natural turbulence in the pipe flow, it was necessary to measure the salt concentration at a point for a time substantially longer than the turbulent time scale. Samples were measured for 40 to 60 sec. and then a time-average value was calculated. The shorter measuring time (40 sec.) was used for the points which were farther downstream from the injection plane and which therefore had smaller transverse gradients of concentration and smaller turbulent fluctuations of concentration. The timer on the frequency counter was set to count for 10 sec., wait 6 sec. during which the reading

was recorded manually, count 10 sec., etc. Using this technique, 4 to 6 frequency readings were taken from the digital display for each point. The time averaged values calculated for each of the 13 points at a cross section were used for further analyses.

3.5 TYPICAL EXPERIMENTAL PROCEDURE

Before a series of experiments was begun for a new injection system, the transverse alignment of the jet or jets was checked for the cases without the propeller in the line by measuring the tracer distribution along the horizontal diameter 24 pipe diameters downstream from the injection plane. Adjustments were made to the injection tube alignment until the tracer was distributed approximately symmetrically about the vertical centerline. After the injector was aligned, the typical experimental procedure outlined below was followed.

(a) The sump water was thoroughly mixed by circulating the water from the sump to the 50 ft. head tank (Fig. 3.1) to insure an initially uniform background concentration and temperature.

(b) The tracer was prepared using the sump water and a predetermined amount of salt to give an ultimate salt concentration of about 20 mg/ℓ above the background concentration. If both reservoirs were needed, the tracer solution was recirculated from one to the other for 30 min. to make sure that the salt was distributed uniformly in both reservoirs. Methanol was added if needed to adjust the density.

(c) The desired flow was established in the pipe and the discharge was measured using the weighing tank at the end of the pipeline.

(d) Based on this measured discharge, the injection flowrate was calculated for a predetermined M_r value (Eq. 2.4).

(e) The background salt concentration (background frequency) in the pipe flow was measured.

(f) Starting at the first sampling station and continuing downstream, the salt concentration for each of the 13 points at each station was measured as described in Section 3.3.2. The pipe and tracer injection flow were never turned off during the experiment. However the injection flowrate was checked frequently. Readjustments were occasionally needed to keep the flowrate constant.

(g) After completing the tracer concentration measurements for all the cross-sections, the injection was turned off and the background concentration was measured again.

The immediate availability of the frequency (concentration) readings proved to be quite useful for recognizing problems that arose with the instruments or hydraulic circuit during an experiment. For example, if the injection flowrate changed significantly, the tracer concentration measurements would deviate from the trend established before the change and immediate adjustments could be made.

3.6 DESCRIPTION AND SUMMARY OF EXPERIMENTS

Some of the experiments performed by Ger and Holley (1974) and other researchers were repeated in order to compare results and to check the experimental techniques developed for this study. One such experiment was a wall source, i.e. an injection made at the pipe wall and made with no appreciable momentum. The results obtained for C_v are shown in Figure 3.8. The data from this study are in good agreement with the data from the other studies. Therefore, it was concluded that the experimental techniques were satisfactory.

A comparison was also made between the present work and results of Ger and Holley (1974) for a 90^o jet with an optimum momentum ratio. Fig. 3.9

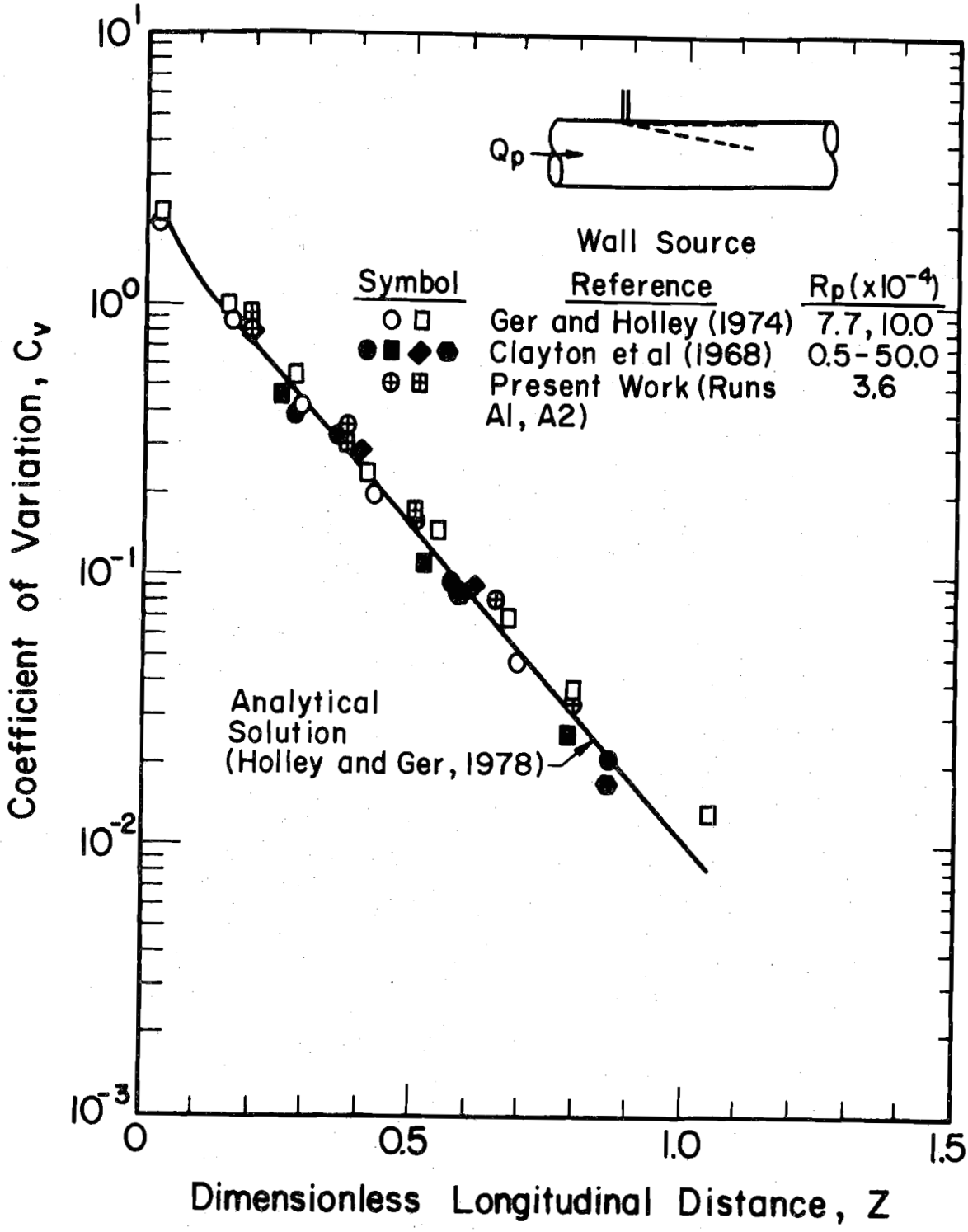

Fig. 3.8 - Coefficient of variation for one wall source

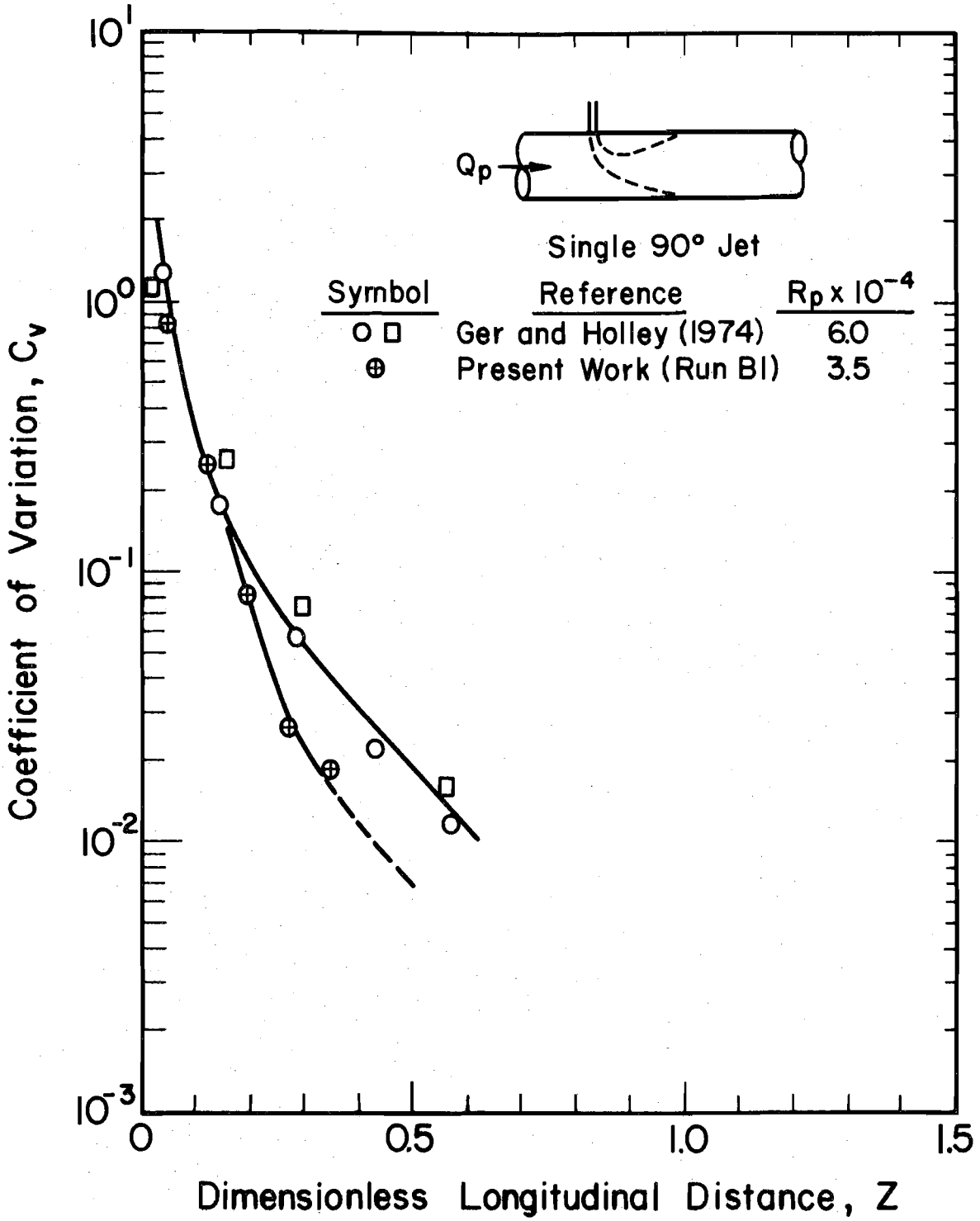

Fig. 3.9 - Coefficient of variation for optimum single 90° jet injection

shows that the mixing distance measured by the present work is significantly less than the distance measured by Ger and Holley (1974). An inspection of Ger and Holley's data reveals that the jet apparently was not aligned symmetrically about the vertical centerline of the pipe and this asymmetry resulted in a longer mixing distance (see Chapter 2). The effects of the asymmetry were also inherent in their numerical model since drag and entrainment coefficients for the jet were obtained from the measured concentration distributions (Ger and Holley, 1974).

The major objective of this research project was to identify those injection systems which promote rapid mixing in the pipe flow. The injection systems investigated fell into two categories. The first category was single jets with angles of injection (α) of 90^{o}, 120^{o}, 135^{o} and 150^{o}. By turning the jet upstream against the ambient flow ($\alpha > 90^{o}$), initial mixing was more rapid because the jet was more vigorously sheared and broken up by the pipe flow. As α increased toward 180^{o} (counterflow), the initial mixing increased, but at the cost of a greater power requirement. As pointed out in Chapter 2, the most rapid mixing, i.e. the most rapid decrease in C_v, occurred when the jet injection caused the tracer distribution to be most nearly symmetrical about the pipe centerline. For each of the four angles, the momentum ratio (M_r^*) which resulted in the most rapid decrease in C_v and in the most nearly symmetrical concentration distributions was experimentally determined.

For the second category of injections, similar experiments were conducted using two 90^{o} jets originating at the pipe wall and positioned at the top and bottom of the pipe diametrically opposite to each other. By using two jets, the tracer was initially distributed over a greater area than if one jet was used.

The effect which secondary currents in the pipe flow had on the mixing distance was studied after finding M_r^* for each of the injection systems.

A secondary current was created by a fixed, three bladed propeller which was positioned 13.5 pipe diameters upstream from the injection plane. The propeller is shown in Fig. 3.10. The propeller created a single-cell secondary current. Dye injections indicated that the water rotated 360^{o} in a flow length of 4 ft or 8 dia. (Fig.3.11). The additional turbulence created by the fixed propellor placed in the flow was not determined. However, it was apparent that the propeller and its supports created a significant disturbance.

A summary of all the successful experiments is given in Table 3.1. Unsuccessful experiments included those in which the instruments failed to operate properly or the injection became unsteady. Column 1 is a brief description of the injection type and Column 2 is the run number for each injection type. Columns 3 and 4 are the ambient flow velocity and Reynolds number and Columns 5 and 6 are the jet flow velocity and Reynolds number. The momentum ratio as defined by Eq. 2.4 is given in Column 7. The relative position of the tracer cloud with respect to the horizontal diameter at the first measurement cross section is given in Column 8 as an overpenetration (+), an underpenetration (-), or nearly symmetrical about the centerline (0) for the single jet and as a relative location for the dual jets, i.e. a = near quarter points and b = between quarter points and centerline.

TABLE 3.1 SUMMARY OF EXPERIMENTS

Type of Injection	Run #	V_p(fps)	R_p	V_j(fps)	R_j	M_r	Comments on Tracer Cloud (See Text)
1	2	3	4	5	6	7	8
Wall Source	A1	0.79	32,500	-	-	0.0038	
	A2	0.79	37,300	-	-	0.0038	
Single	B1	0.72	35,300	4.07	4160	0.0138	0
90^o jet	B2	0.69	31,500	4.07	3890	0.0151	+
	B3	0.72	32,800	4.07	3890	0.0140	+
	B4	0.73	33,500	3.91	3730	0.0124	-
	B5	0.75	34,300	4.26	4070	0.0140	+
Single	C1	0.72	37,500	4.73	5150	0.0188	-
120^o jet	C2	0.69	36,100	4.61	5020	0.0193	-
	C3	0.67	35,100	4.75	5180	0.0216	+
Single	D1	0.73	36,500	6.40	6700	0.0337	-
135^o jet	D2	0.72	35,600	6.69	6920	0.0377	-
	D3	0.72	34,800	6.75	6810	0.0382	-
	D4	0.77	35,600	7.28	7050	0.0390	-
	D5	0.76	35,400	7.72	7480	0.0446	-
	D6	0.71	33,200	7.28	7050	0.0450	0
Single	E1	0.71	32,400	11.62	11100	0.1170	+
150^o jet	E2	0.74	32,400	11.27	10320	0.1009	+
	E3	0.72	31,500	10.45	9570	0.0916	+
	E4	0.73	31,200	10.33	9200	0.0868	+
	E5	0.73	31,200	9.74	8670	0.0773	-
Dual 90^o	F1	0.96	36,800	2.93	2320	0.0040	a
jet	F2	0.97	37,600	3.13	2520	0.0045	a
	F3	1.00	38,700	2.85	2290	0.0035	a
	F4	1.04	40,100	2.73	2200	0.0030	a
	F5	0.86	33,200	2.61	2100	0.0040	a
	F6	0.80	31,000	2.98	2400	0.0060	b
	F7	0.77	30,700	3.10	2570	0.0070	b
	F8	0.69	27,500	3.32	2680	0.0100	b
Induced Swirl Single 90^o jet	G1	0.71	31,300	4.05	3700	0.0140	-
Induced Swirl Dual 90^o jet	G2	0.67	30,000	3.23	3000	0.0100	-

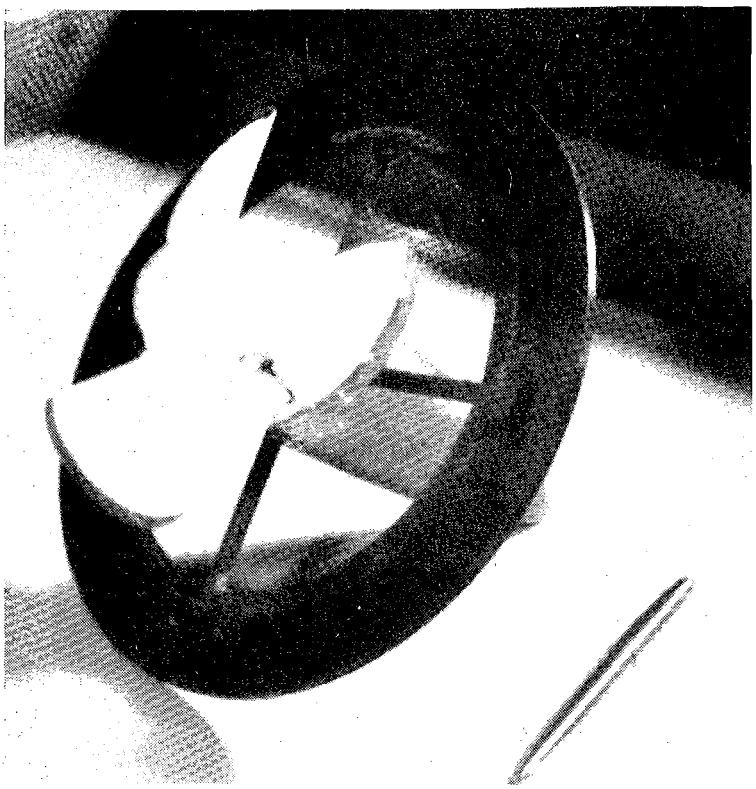

Fig. 3.10 - Propellor used in pipe

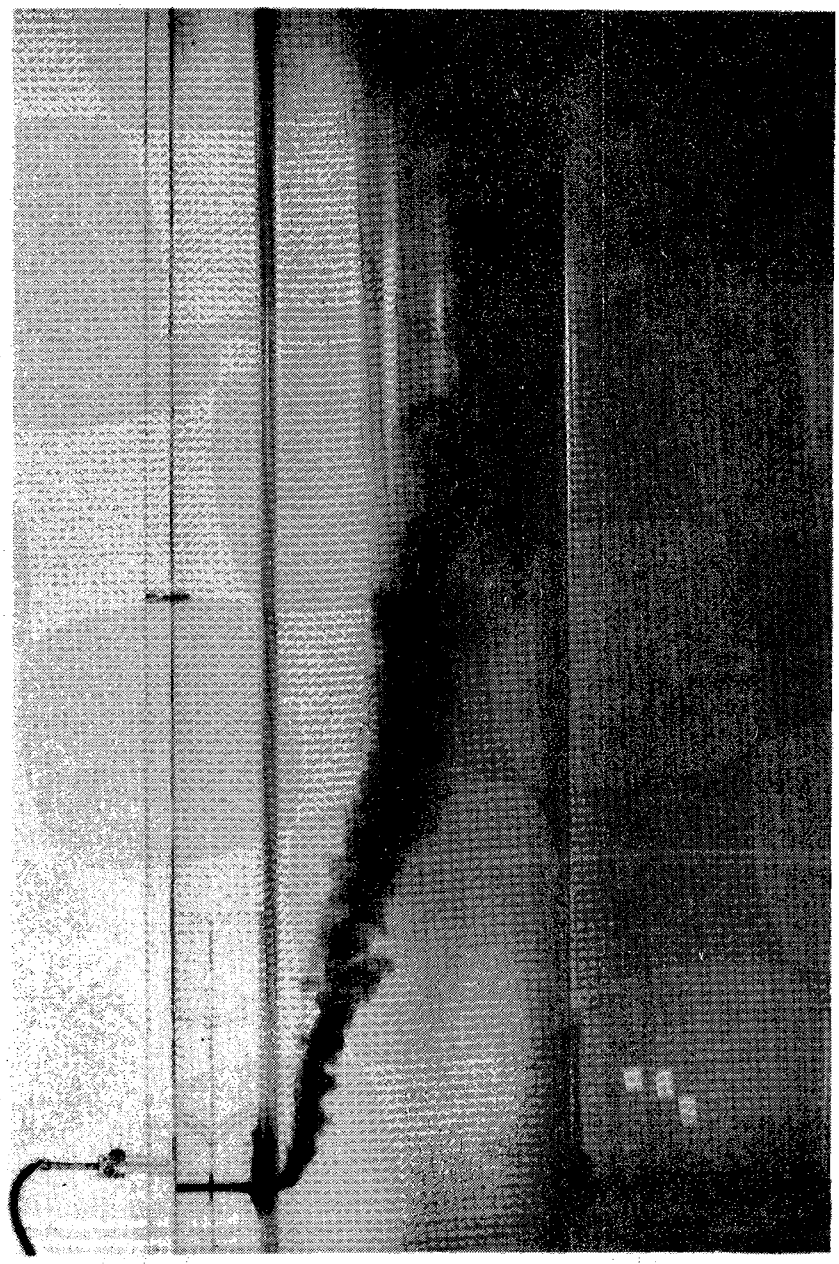

Fig. 3.11 - Photograph showing one-half wave-length of the induced swirl

4. RESULTS AND DISCUSSION

4.1 SINGLE JET INJECTIONS

The single jet injection experiments consisted of an injection tube positioned at the top of the pipe with one end flush with the pipe wall and oriented at angles of 90^{o}, 120^{o}, 135^{o} and 150^{o} relative to the ambient flow. The NaCl concentration was measured at thirteen points over the cross section (Section 3.4) for various sampling stations downstream from the injection point (Fig. 3.1). The concentration data were normalized with respect to the cross sectional average concentration. The normalized concentration data collected for each experiment are given in Appendix A. Some typical concentration distributions are discussed later.

4.1.1 Coefficient of Variation

The coefficient of variation, C_v (Eq. 2.2), was calculated using the concentration data collected for each experiment. The weighting coefficient, W_i, was set equal to unity for all i because the 13 measurement points represented equal subareas and the effects of the velocity distribution were assumed to be negligible (Holley and Ger, 1978). Figures 4.1, 4.2, 4.3 and 4.4 show semi-log graphs of C_v vs Z (Eqs. 2.7 and 2.8) for each of the angles of injection. The jet and ambient flow conditions for each of the experiments are given in Table 3.1.

The concentration distributions showed that there was an increasing amount of scatter as the distributions became more uniform. The fluctuations in the background salt concentration and the random errors in the measurements had a negligible effect on C_v for the highly nonuniform concentration distributions near the point of injection. However, the experimental inaccuracies became progressively more significant with increasing uniformity

of the concentration distributions and with increasing flow distance. By comparing the empirical log C_v vs Z curves to the general analytical behavior of log C_v vs Z curves (Fig. 2.1), it was estimated that C_v values equal to or less than approximately 0.02 represented random measurement errors rather than degree of uniformity of the concentration distribution (Section 2.2). Thus, the values of C_v below 0.02 are not necessarily reliable and some of the points for $0.02 < C_v < 0.025$ may be questionable.

4.1.2 Optimum Momentum Ratio

One objective of the single jet injection experiments was to find the optimum momentum ratio, M_r^*, for various angles of the jet relative to the ambient flow. For each α, M_r was varied to provide concentration data for estimating M_r^*. From the C_v graphs shown in Figures 4.1, 4.2, 4.3 and 4.4, approximate M_r^* values were determined. In some cases a clear definition of M_r^* could not be obtained from just the log C_v vs Z graphs. Thus, some of the M_r^* values were selected by studying both C_v and the concentration data. M_r^* could have been identified by the symmetry of the concentration distributions about the horizontal diameter if the jets maintained a circular shape as they were spreading and interacting with the ambient flow. (Symmetry about the vertical diameter relates to alignment of the jet.) However, due to the horseshoe or kidney shape which develops for jets in crossflows (Fan, 1967), the maximum measured concentration for optimum conditions could actually be somewhat below the centerline for some cross sections. For optimum conditions it was not uncommon to have the maximum concentration near the centerline at Station 1 and below the centerline (say at $r/R_p = 0.1$ to 0.2) for Stations 2 and 3. At Station 4 the concentration distribution was nearly symmetrical about the horizontal

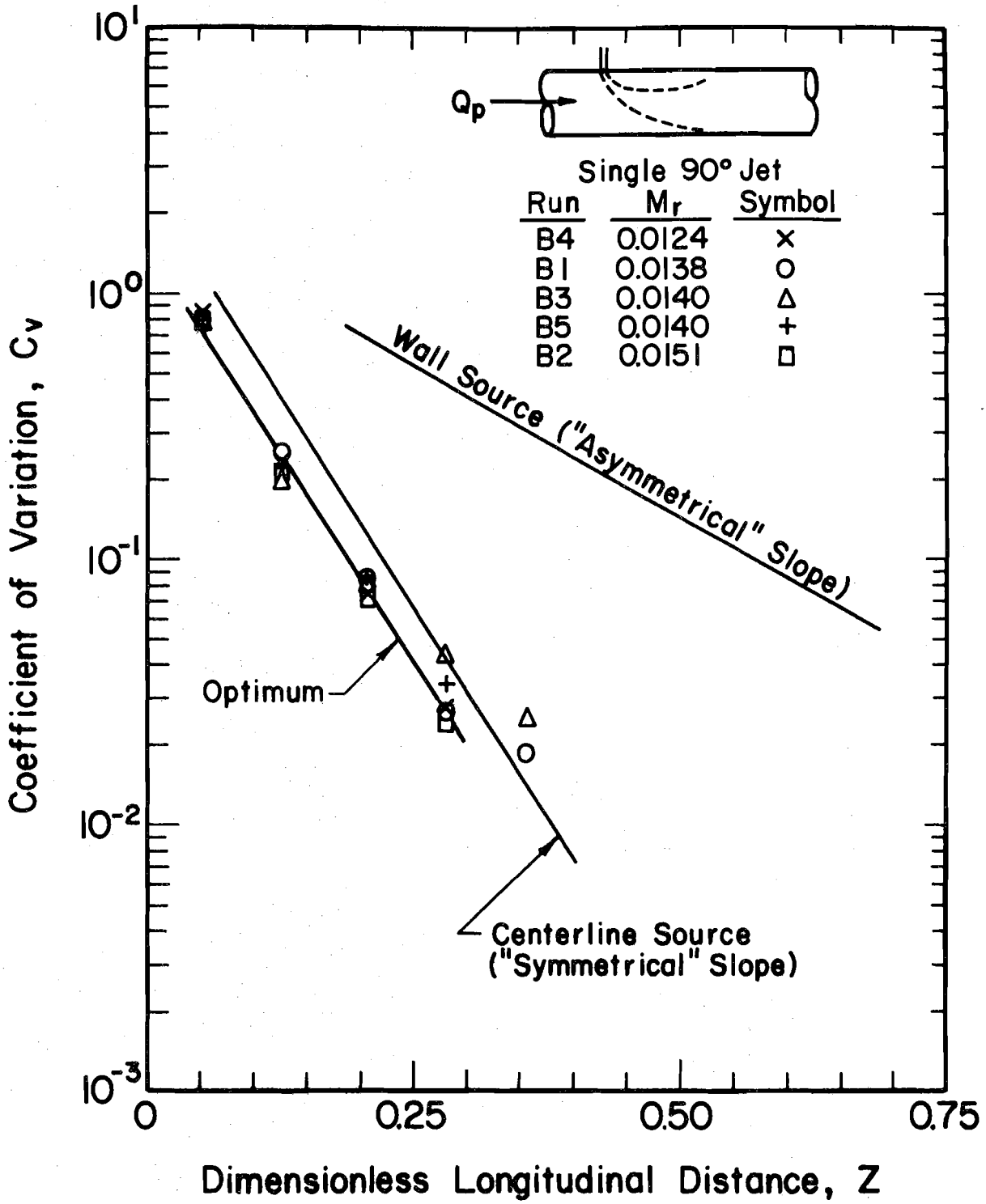

Fig. 4.1 - Coefficient of variation for single 90^o jet

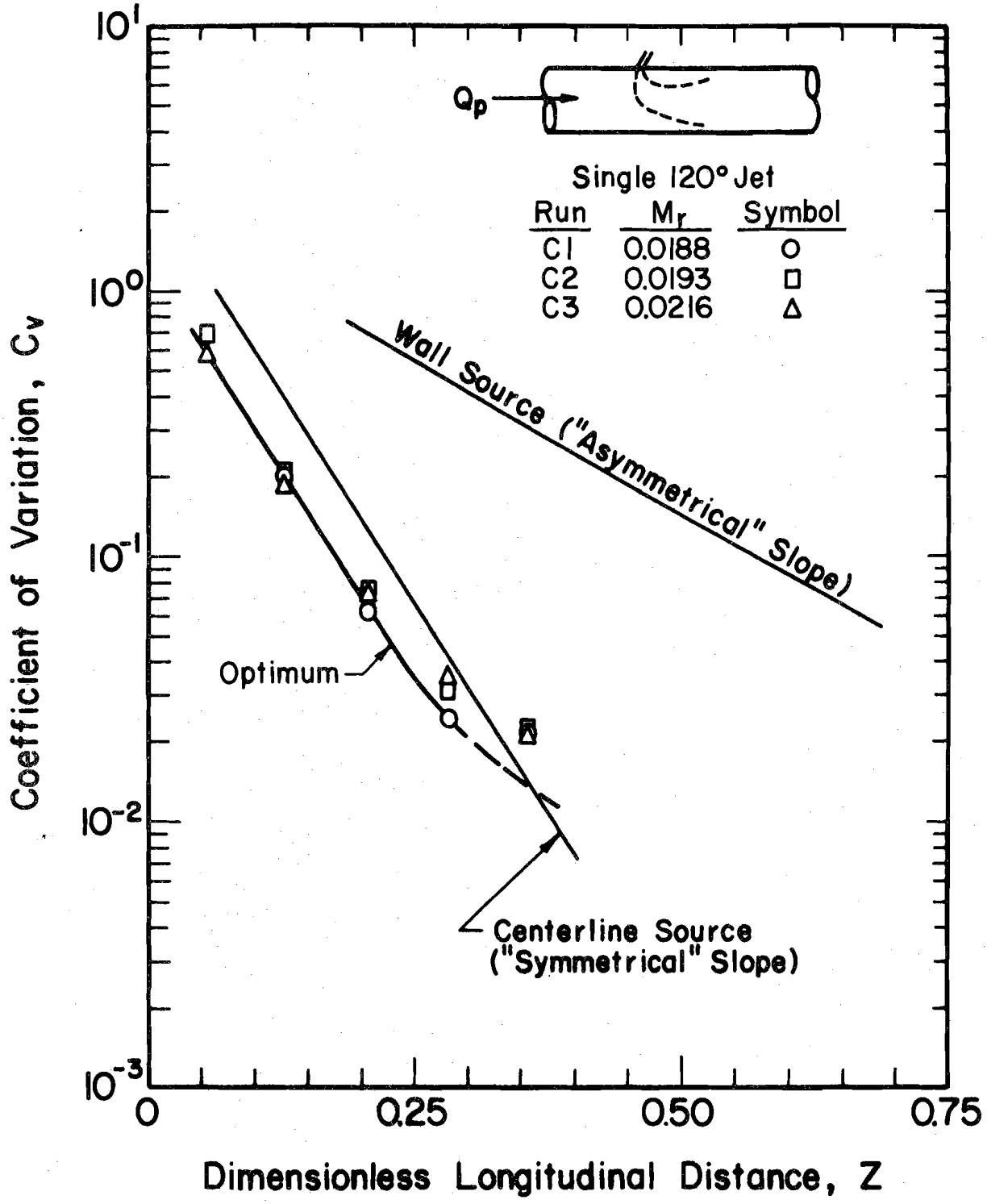

Fig. 4.2 - Coefficient of variation for single 120^0 jet

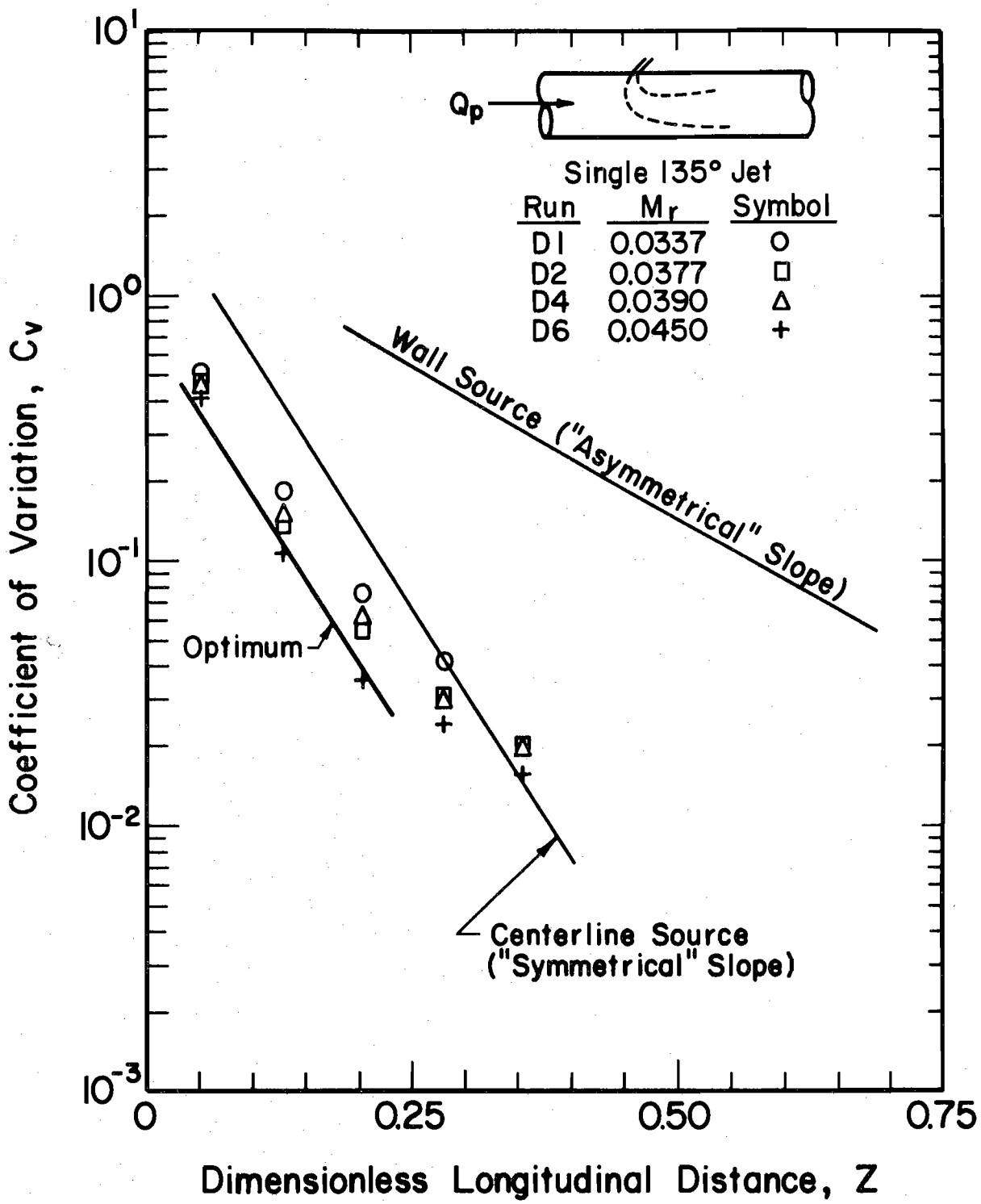

Fig. 4.3 - Coefficient of variation for single 135^0 jet

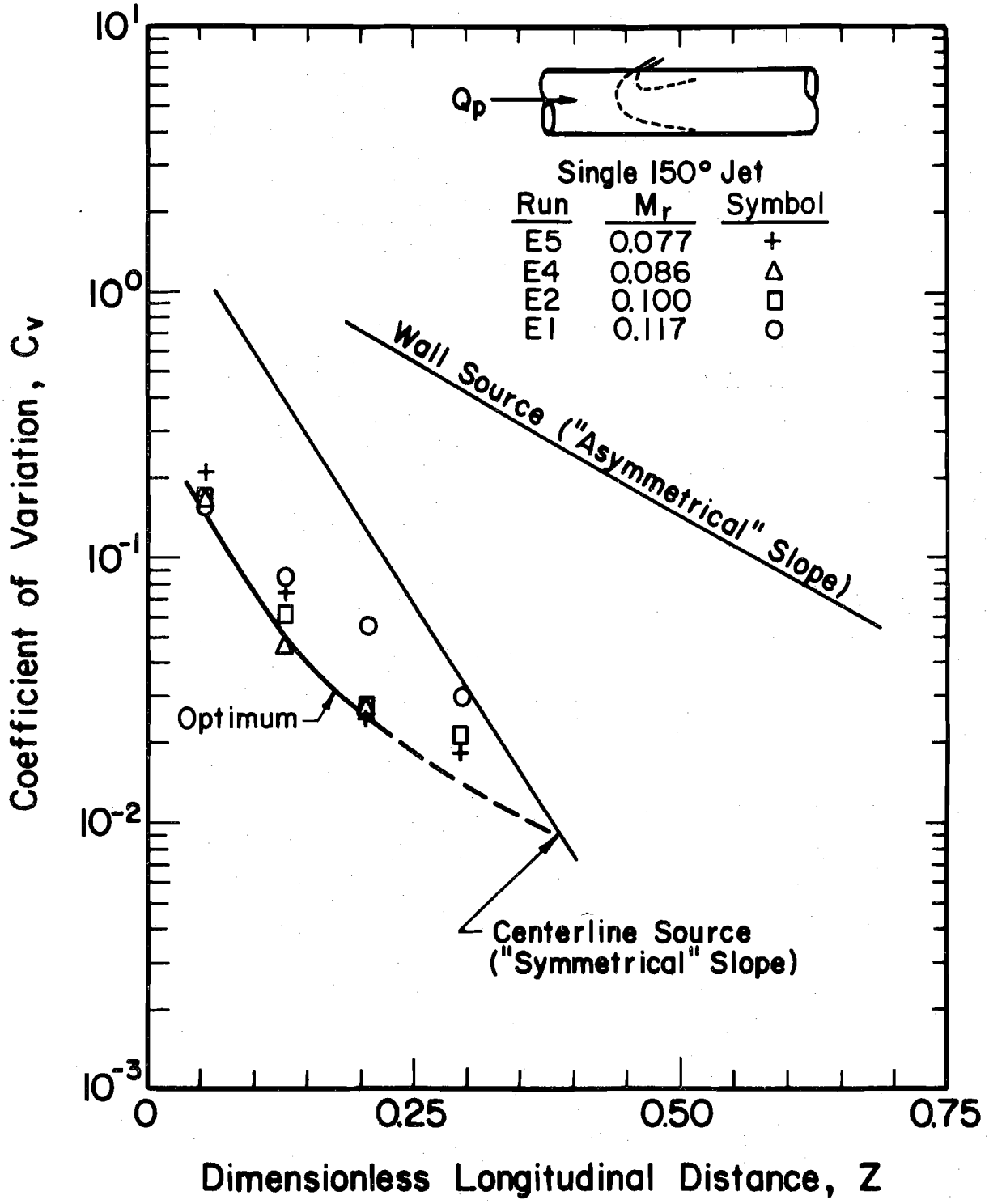

Fig. 4.4 - Coefficient of variation for single 150° jet

diameter. Fig. 4.5 shows this behavior in the concentration distributions while Fig. 4.6 shows a case with an overpenetrating jet.

The concentration data show that it became progressively more difficult to maintain transverse symmetry of the jet as α was increased. The results of this asymmetry can be seen in that the C_v values for $\alpha = 135^o$ and 150^o and for the last 2 or 3 measurement stations tend to break away from a line with the "symmetrical" slope. The concentration distributions for Run D6 appear to be more nearly symmetrical in the transverse direction than most of the distributions for the larger α values. This nearly symmetrical situation may be the reason that the C_v values (Fig. 4.3) for Run D6 are noticeably smaller than for the other runs with $\alpha = 135^o$.

In some cases the optimum M_r had to be identified by interpolation. For example, for $\alpha = 90^o$, the concentration data showed a slight underpenetration at Stations 3 and 4 for $M_r = 0.0124$ and a slight over-penetration at the same stations for $M_r = 0.0138$ and 0.0140. Thus, M_r^* was estimated to be 0.013. This value is 17% lower than the value given by Ger and Holley (1974). Part of the difference may be due to the fact that the present value was selected by interpolation. Part of the difference may also be due to the slight misalignment of the jets in Ger and Holley's (1974) work, as discussed in Section 4.3.

By following the same procedure of studying C_v and concentration data, the M_r^* value was selected for each α. The values are given in Table 4.1 along with the value of Z_m, i.e. Z at which $C_v = 0.03$ for $M_r = M_r^*$. (See Section 4.1.3.)

Series E for $\alpha = 150^o$ was the only series in which M_r values significantly greater than M_r^* were used. The C_v data (Fig. 4.4) tend to indicate that using $M_r > M_r^*$ could give more mixing and smaller C_v values for small Z than existed for $M_r = M_r^*$. This behavior could have been due to the increase

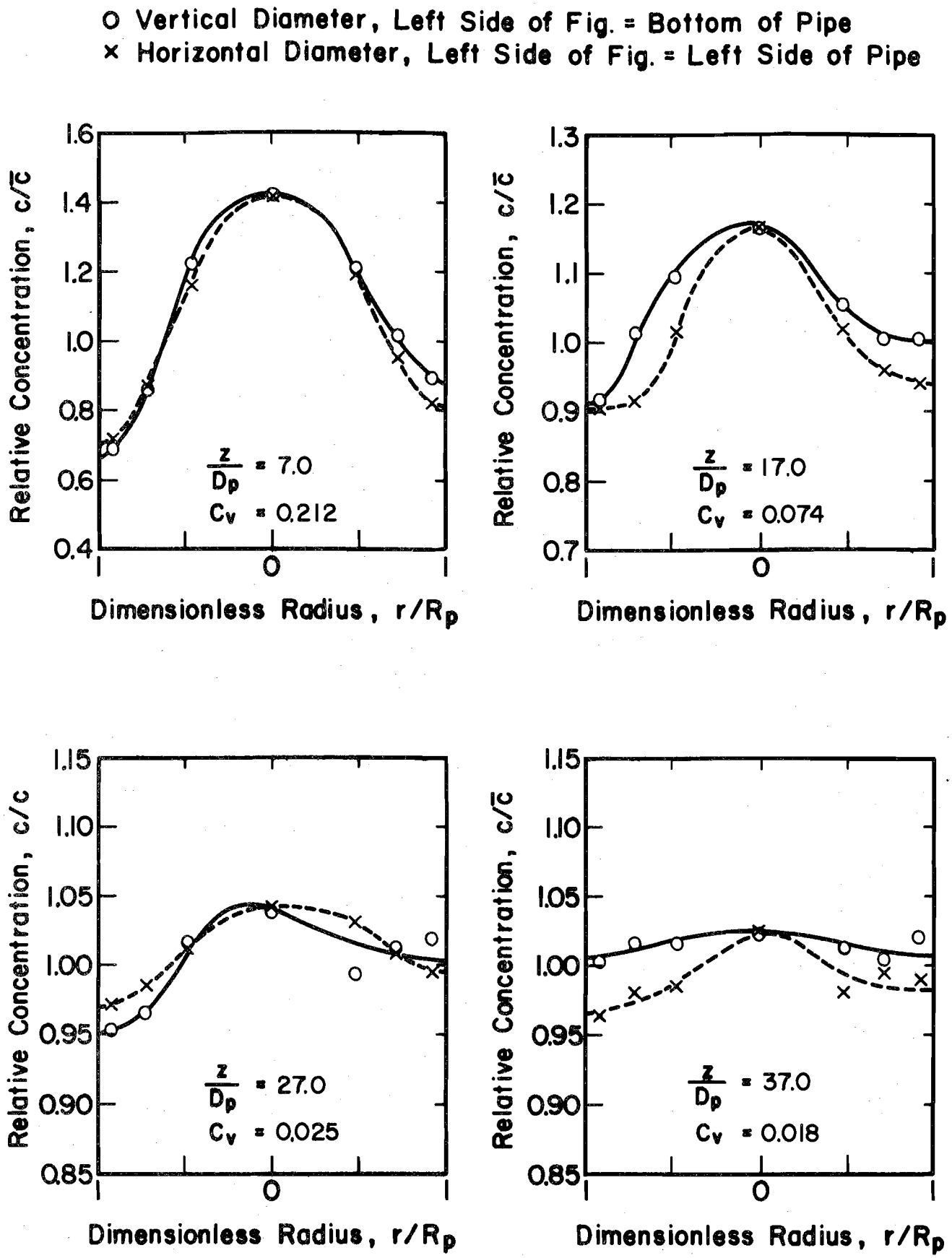

Fig. 4.5 - Concentration distributions for a single 150° jet (Run E5)

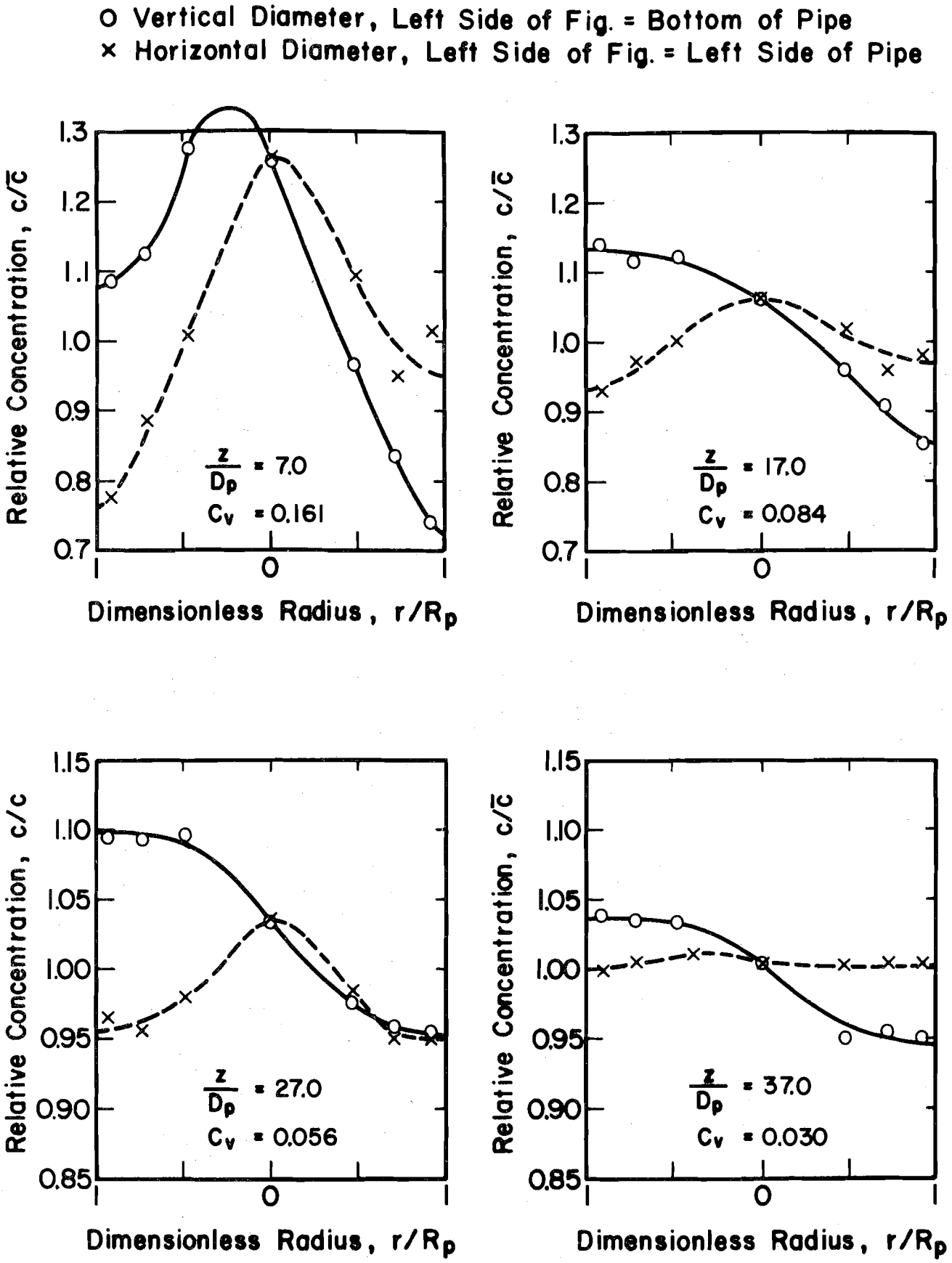

Fig. 4.6 - Concentration distributions for a single 150° jet (Run E1)

Table 4.1 SUMMARY OF OPTIMUM SINGLE JET INJECTIONS

Angle of Injection α	Optimum Momentum Ratio M_r^*	Dimensionless Mixing Distance Z_m
90^o	0.013	0.275
120^o	0.019	0.260
135^o	0.045	0.225
150^o	0.080	0.175

Z_m = Z for C_v = 0.03

in jet mixing as M_r increased. However, using $M_r > M_r^*$ gave asymmetrical concentration distributions so that the C_v curves tended to have a smaller slope for large Z and gave larger mixing distances than $M_r = M_r^*$ if the mixing distance is based on a small value of C_v (say 0.03). There is some slight indication of this behavior for Series B and C (Figs. 4.1 and 4.2). For Series D, there were no experiments with $M_r > M_r^*$. In fact, the concentration distributions indicate that the maximum M_r used for Series D may have been slightly too small to be M_r^*.

4.1.3 Effect of α on the Mixing Distance

Another objective of the single jet experiments was to determine how much reduction in the mixing distance could be achieved by increasing α. The value of Z for C_v = 0.03 was chosen as the point where the mixing distances were to be compared for each of the α angles. The mixing distances determined using C_v on the order of 0.02 or smaller would not have been reliable because the C_v values begin to reflect the random measurement errors rather than the uniformity of the concentration distribution.

The non-dimensional mixing distances, Z_m, as defined by $C_v = 0.03$ for each α are also included in Table 4.1. A graph of Z_m and M_r^* vs α is given in Fig. 4.7. The 150^o angle of injection produced the minimum mixing distance of approximately 0.175 using a M_r^* of 0.080, as compared to the mixing distance at 0.275 for the 90^o angle of injection using a M_r^* of 0.013. By using an injector oriented at $\alpha = 150^o$ instead of $\alpha = 90^o$, a 35% decrease in Z_m could be realized under optimum conditions. However, for a given ambient flow rate, the momentum of the optimum 150^o jet must be increased by a factor of six above the momentum of the optimum 90^o jet. Figures 4.8 and 4.9 are photographs of the optimum 90^o and 150^o jets. The photographs were taken at the point of injection and show the jet trajectory and initial mixing region for each α. A visual comparison of the cross sectional dye distributions indicated that the optimum 150^o jet had undergone more initial mixing than the optimum 90^o jet. Thus, an optimum 150^o jet injection produces a shorter mixing distance than an optimum 90^o jet injection if the ambient mixing characteristics are similar for each injector orientation.

4.2 DUAL JET INJECTIONS

In order to determine the improvement which could be obtained in mixing by using multiple injections, experiments were conducted using two diametrically opposed 90^o jets flush with the pipe wall. Angles of injection other than 90^o and injections with three or more jets were not studied experimentally for reasons given in Section 4.5. The two 90^o jets issued into uniform fully-established turbulent pipe flow, and the same momentum ratio was used for both jets in an attempt to have symmetry with respect to the horizontal diameter. The normalized concentration data for each of the dual jet experiments are given in Appendix A.

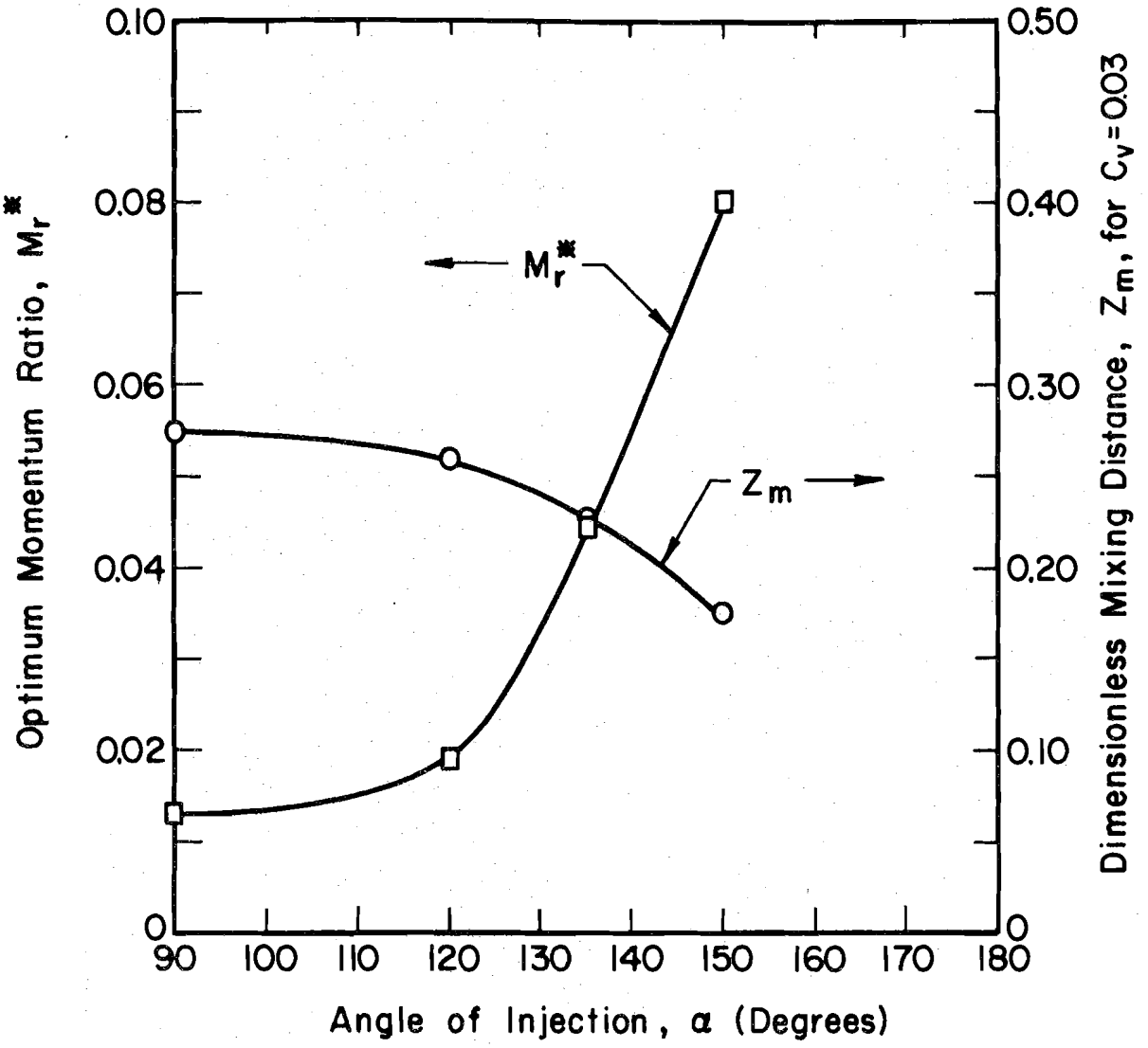

Fig. 4.7 - Optimum momentum ratios and mixing distances for single jet injections ranging from $\alpha = 90^o$ to 150^o

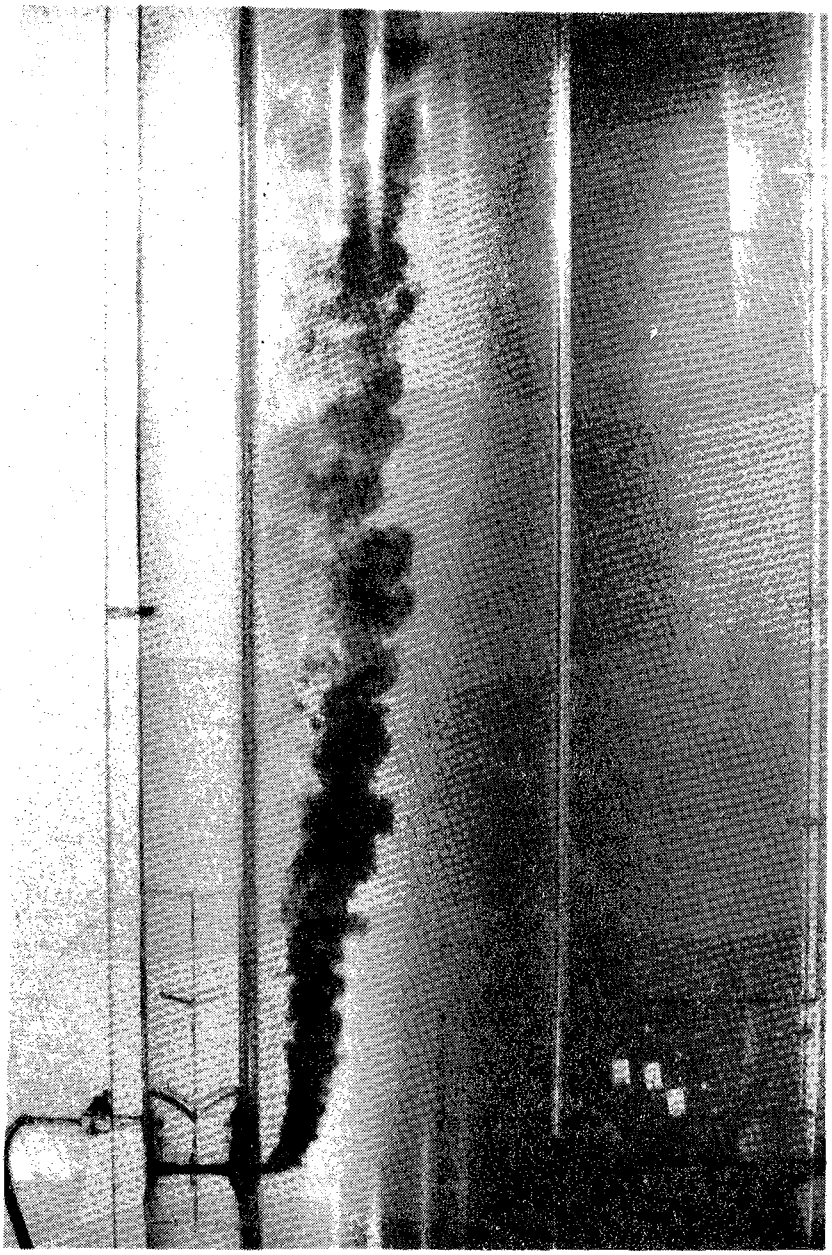

Fig. 4.8 - Photograph of optimum single 90^{o} jet

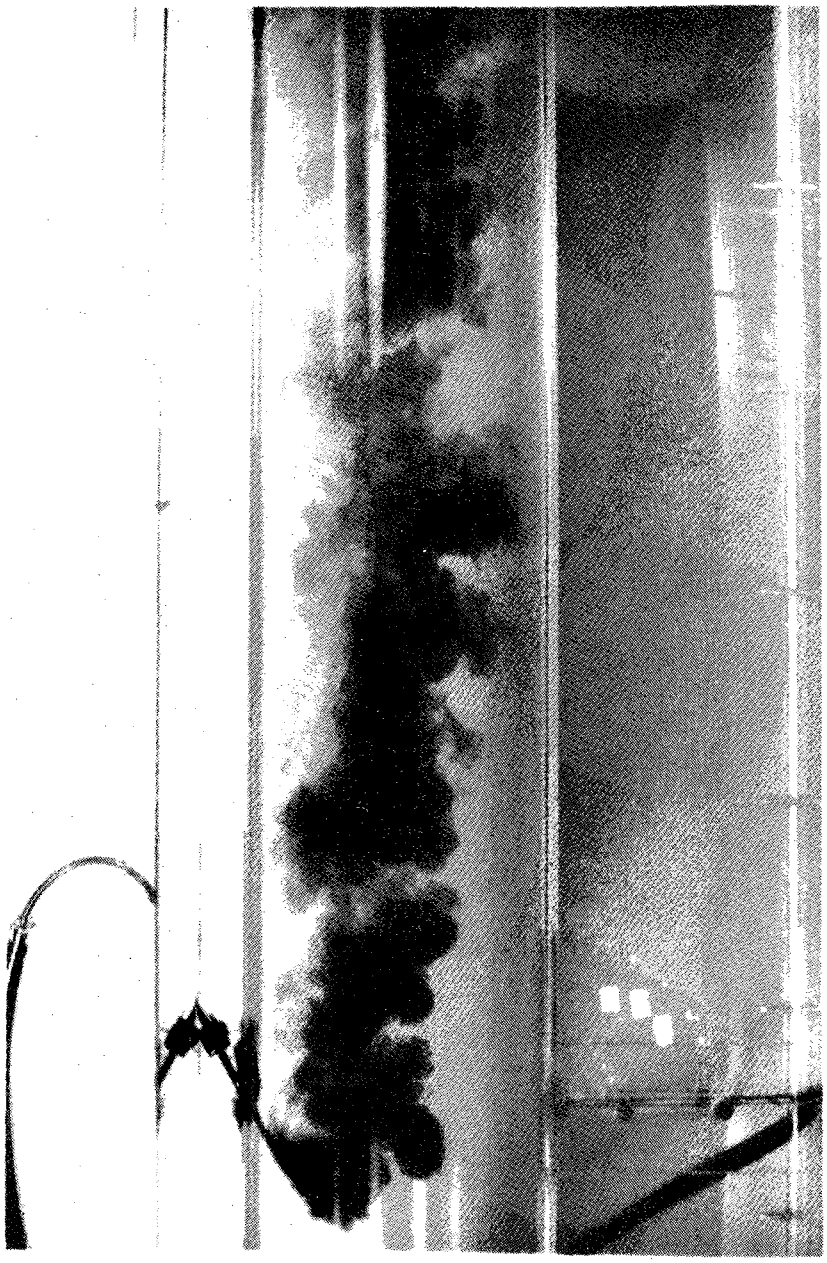

Fig. 4.9 - Photograph of optimum single 150^{o} jet

4.2.1 Coefficient of Variation

The coefficient of variation was obtained from the concentration data given in Appendix A. The graph of log C_v vs Z for various M_r values is shown in Fig. 4.10. Because the injectors were located on the top and bottom of the pipe, the maximum concentrations occurred along the vertical diameter and the minimum concentrations occurred along the horizontal diameter. Therefore, the measured concentrations represented either the maximum or the minimum value for each subarea, rather than representing an average value. Consequently, C_v calculated using only 13 points was slightly larger than the actual C_v. The errors due to orientation of the sampling diameters relative to the nonuniform concentration distribution decreased with increasing distance downstream and therefore should have had a negligible effect on the evaluation on the mixing distance based on small C_v values, say $C_v < 0.05$.

4.2.2 Optimum Momentum Ratio

(For the two jet injections, M_r refers to the momentum ratio for each jet, not to the combined momentum.)

From Fig. 4.10 and from studying graphs of the concentration distributions which are tabulated in Appendix A, the optimum momentum ratio, M_r^*, was determined to be in the range of 0.006 to 0.010. Unfortunately, for two reasons, it was not possible to determine M_r^* more precisely. One of the reasons is that the mixing was rapid enough that most of the concentration distributions at Station 4 (Z = 0.281) for $0.006 \leq M_r \leq 0.010$ showed little variation from the average concentration and significant scatter in the data points. Therefore, the C_v values at Station 4 for $0.006 \leq M_r \leq 0.010$ were so small that they may be primarily representative of random errors rather than of degree of mixing. The second reason is that there are some apparent

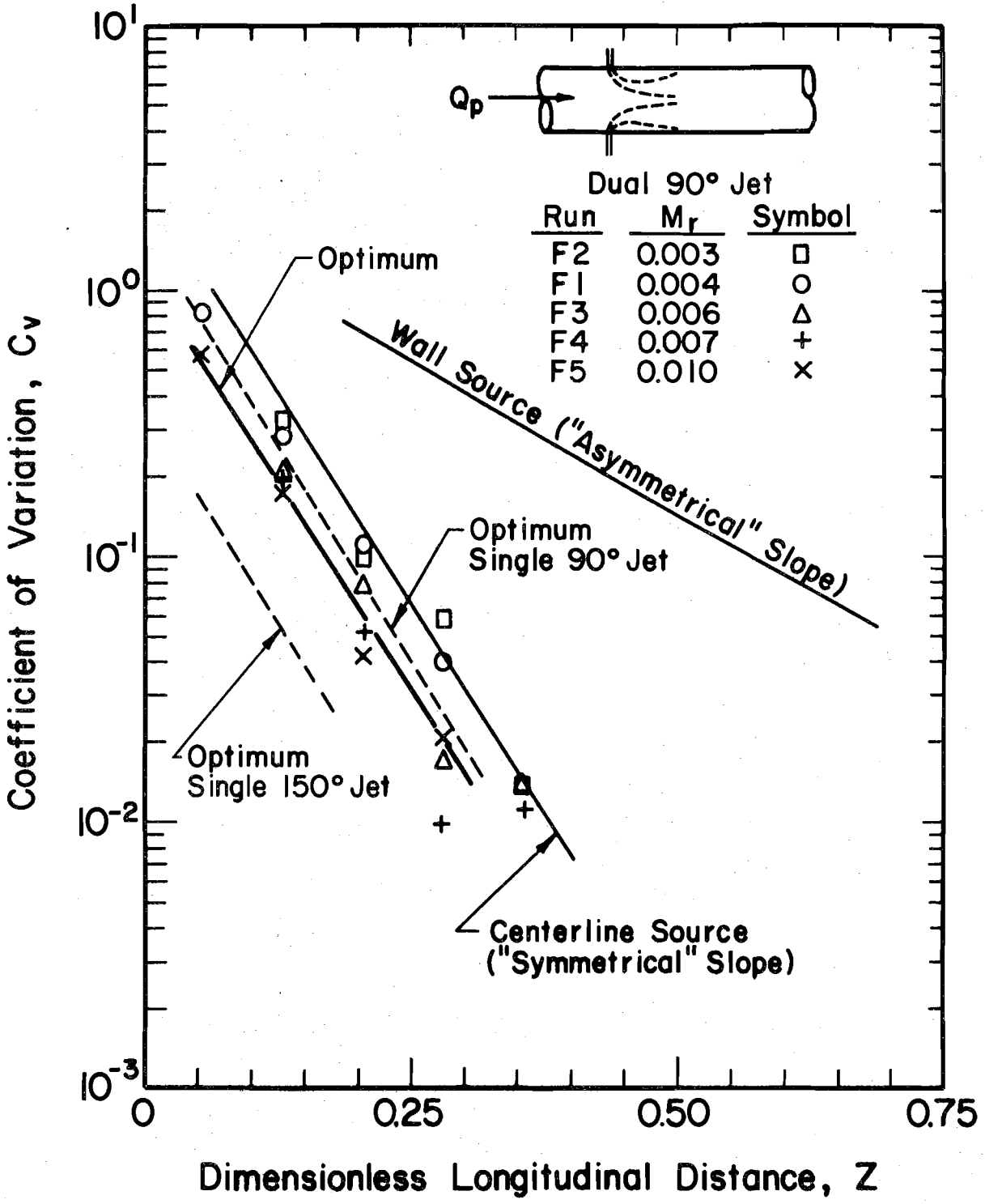

Fig. 4.10 - Coefficient of variation for dual 90° jets

inconsistencies in the C_v values at Station 3 (Z = 0.205). If the C_v value for Run F3 were correct in indicating a trend away from the "symmetrical" slope, then C_v at station 4 should have been about 0.03 or greater and therefore could have been measured with minor experimental error, but such was not the case. For Run F5, the slope indicated by the C_v values for Stations 2 and 3 (Z = 0.129 to 0.205) is steeper than the "symmetrical" slope and therefore apparently unrealistic. It was assumed that C_v for Station 3 (Z = 0.205) was too small for Run F5 since the values for Stations 1 and 2 (Z = 0.053 and 0.129) fell on a line having the "symmetrical" slope and therefore tended to support each other. An inspection of the concentration distributions did not help to identify the M_r^* since the distributions all had the same general characteristics for Runs F3, F4 and F5. The C_v values give slight support to selection of 0.010 as the optimum M_r since Run F5 had the lowest C_v at Station 2 and as mentioned, the slope from Station 1 to Station 2 is the "symmetrical" slope.

From Fig. 4.10, for M_r = 0.010 the dimensionless mixing distance, Z_m, defined by C_v = 0.03 was found to be 0.225 for the dual 90° jet injections. An optimum, single 135° jet injection produced a similar mixing distance (0.225), but required an M_r^* of 0.019.

4.2.3 Comparison With Two Point Sources

The experiments with a single jet injection indicated that using the optimum momentum ratio produced concentration distributions which were symmetrical about the pipe center line at large Z's and which, in a sense, could therefore be viewed as being produced by a virtual centerline source located upstream of the actual injection location. The centerline is the optimum location for a single passive source, so that the results for a

single jet indicated that optimum injection was obtained when the momentum ratio was sufficient to carry the center of the injected tracer to the optimimum location of a passive source. (Also see Fig. 2.1 and related discussion in Section 2.2.)

In view of these results for a single injection, the analytical solution (Holley, 1977; Holley and Ger, 1978) for mixing downstream of point sources was used to determine the optimum location for two point sources located on opposite halves of the same diameter with each source being a distance $\rho' = r'/R_p$ from the centerline. The variation of Z_m for $C_v = 0.03$ is illustrated in Fig. 4.11. From the figure, a minimum mixing distance of 0.237 occurred for $\rho' = 0.53$, which is virtually the quarter point of the diameter. From this analytical approach, it was assumed that M_r for the dual jets should be adjusted to produce jets which penetrate to the quarter points of the diameter. Eq. 2.15 was used to estimate the required M_r. If sub-1 represents jets penetrating to the centerline ($y/D_p = 1/2$) and sub-2 represents jets penetrating to the quarter points ($y/D_p = 1/4$), then from Eq. 2.15,

$$\frac{M_{r,1}}{M_{r,2}} = \left[\frac{\frac{1}{2}}{\frac{1}{4}}\right]^2 = 4$$

Since $M_{r,1} = 0.013$ (Section 4.1.2), then $M_{r,2} = 0.0033$.

Based on this reasoning, Runs F1 and F2 were conducted with $M_r = 0.003$ and 0.004. However, the C_v values (Fig. 4.10) for small Z (Stations 1, 2 and 3) were only slightly smaller than would be expected for two wall sources and were therefore larger than the calculated values for two sources at $\rho' = 0.53$. Also, at Station 4, the C_v values indicated a trend breaking away from the "symmetrical" slope. The apparent reasons for these results can be seen in the concentration distributions in Fig. 4.12. The distributions for the vertical diameter for Stations 1 and 2 do not show symmetry

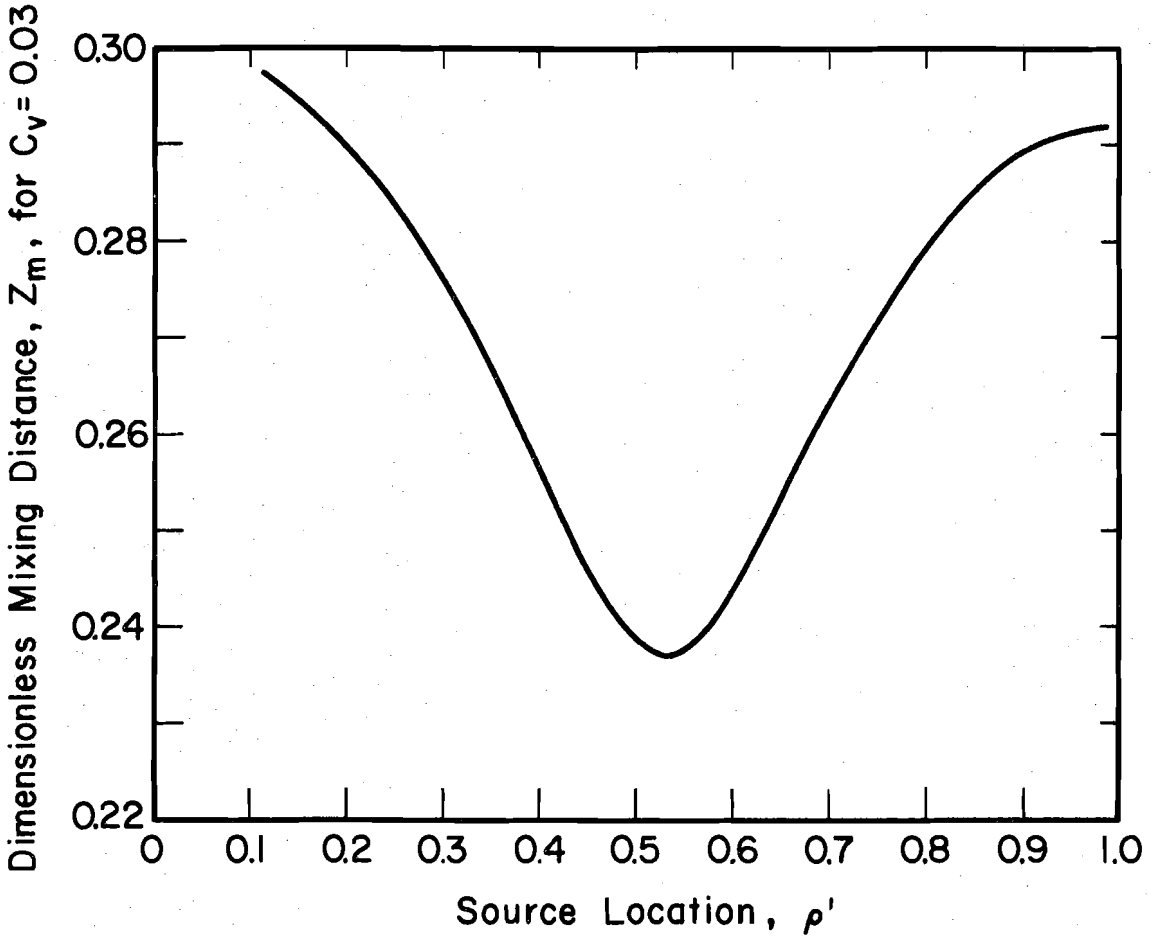

Fig. 4.11 - Calculated mixing distance for two point sources on the same diameter

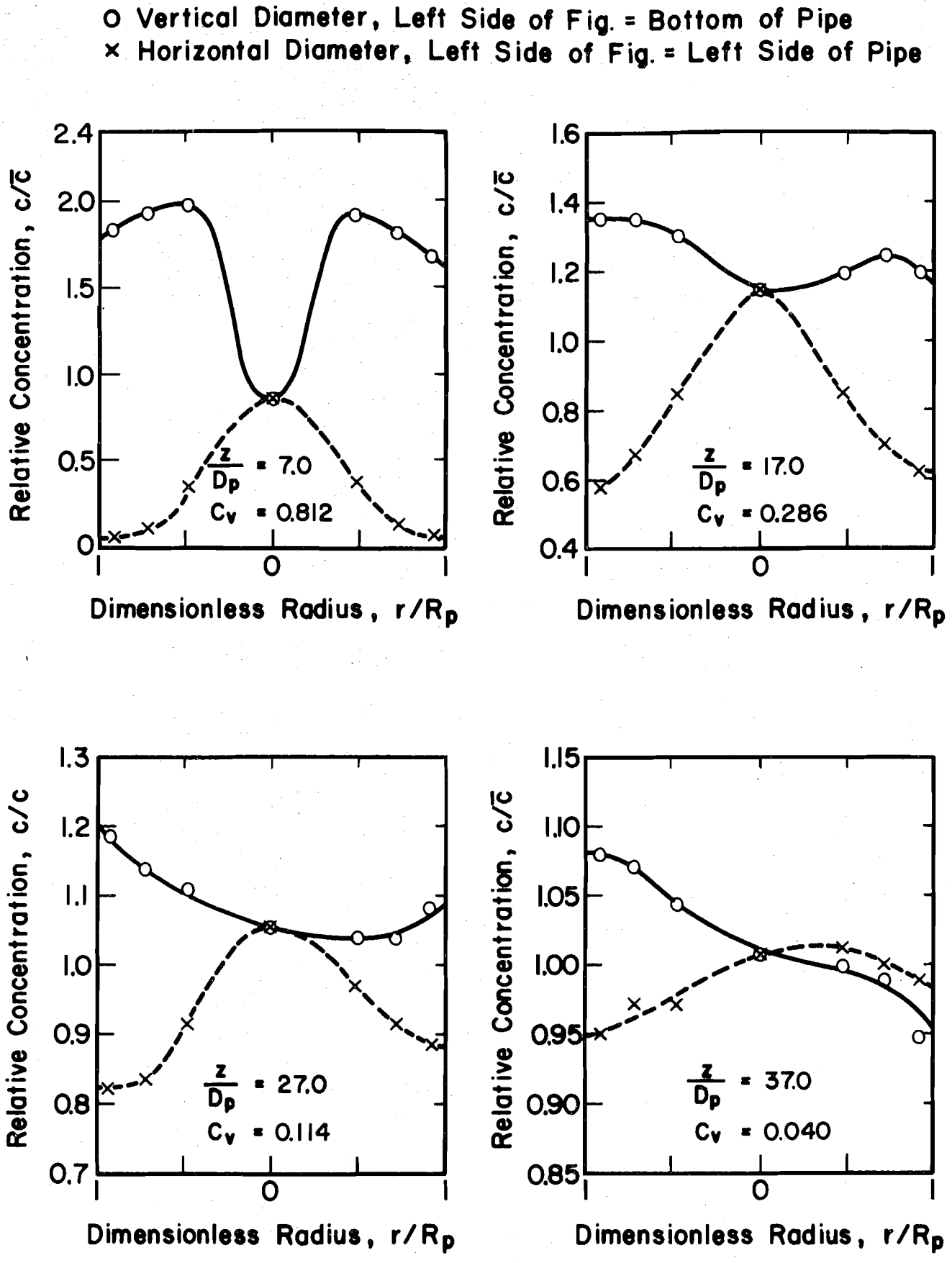

Fig. 4.12 - Concentration distributions for dual 90° jets (Run F1)

about the quarter points but rather have significantly higher concentrations at the wall than at the centerline. From all of the distributions given in Appendix A for runs F1 through F8, it can be seen, in spite of the efforts even under laboratory conditions to achieve symmetry about the horizontal diameter, that such symmetry was not achieved.

The concentration distributions in Fig. 4.13 for M_r = 0.010 are typical of the results for Runs F3 - F5 with M_r = 0.006 - 0.010 and indicate that optimum conditions for uniform flow were obtained by causing the jets to penetrate somewhat past the quarter points of the diameter. With the maximum concentration between the quarter points and the centerline, the ambient diffusion caused the maximum concentration to move to the centerline. The reason for this behavior can be seen by visualizing a two-peak concentration distribution (similar to the one for the vertical diameter for Station 1 in Fig. 4.12). Diffusion moves mass from the two regions of high concentration to the three regions of low concentration. If the jets penetrate past the quarter points, then the concentration on the centerline will be higher than the concentration at the walls (contrary to Station 1 in Fig. 4.12). The diffusion from the large concentrations will "fill in" the distribution in the center of the pipe faster than at the walls since there is less to "fill in". Then diffusion will take place only toward the wall and the maximum concentration will be in the central portion of the pipe. Apparently, since it is not possible to obtain the precise symmetry which existed in the computations leading to Fig. 4.11, the practical optimum is for penetration past the quarter points of the diameter to obtain distributions as shown in Fig. 4.13.

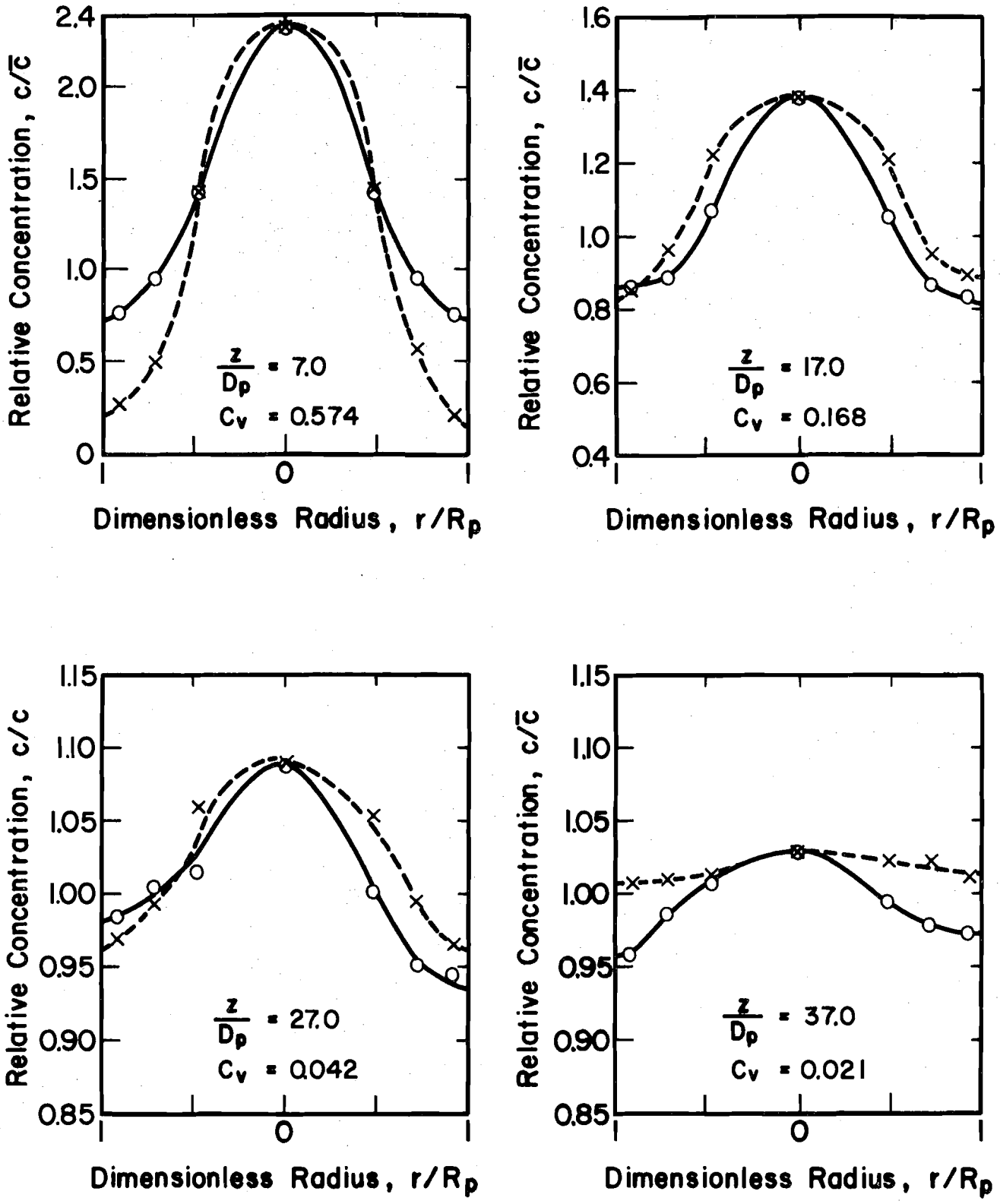

Fig. 4.13 - Concentration distributions for dual 90° jets (Run F8)

4.3. EFFECTS OF JET MISALIGNMENT

Figure 2.1 shows C_v calculated from the analytical solution of the mass balance equation (Section 2.3) for single point sources located between the pipe wall and centerline. Inspection of the results indicates that the mixing distance as defined by Z for some C_v is more sensitive to a source's being off the center a short distance than to being moved inward from the pipe wall a short distance. For example, the mixing distance as defined by Z_m for $C_v = 0.03$ is 75% larger for a source located at $\rho' = 0.10$ than for a source located at $\rho' = 0.0$. However, very little change in the mixing distance occurs for a source located at $\rho' = 0.80$ rather than at $\rho' = 1.00$.

This analytical evaluation of the effect which a slight misplacement of a centerline point source would have on the mixing distance is an indication that the mixing distance for a jet issuing into the pipe would also be rather sensitive to the concentration distribution immediately downstream from the initial mixing zone and therefore to the transverse alignment of the jet. Sensitivity tests per se were not run for the jet-type injection, but during the process of attempting to find M_r^* for a variety of injection configurations, it became apparent that the mixing was sensitive to jet alignment. Even with the utmost attention given to the alignment, it was difficult to obtain a concentration distribution which was symmetrical about the vertical diameter. With care, the jet could be aligned well enough so that the slight asymmetry was not evident in the C_v vs Z graphs for $C_v \geq 0.03$ for the single jet injections. The distance which a concentration distribution can deviate from the center before the asymmetry effect becomes significant could not be determined accurately without measuring the concentration distributions in more detail than was done for this study. Nevertheless, the concentration distributions for an optimum 90^o single jet in the present work were compared to the distributions of an optimum 90^o single jet slightly off center (Ger and Holley,

1974) and indicated that missing the center of the pipe can be critical (Fig. 3.9). The closest that the peak concentration got to the centerline for the 90^{o} jet studied by Ger and Holley (1974) was $r/D_p = 0.15$ at $Z/D_p = 4$. Z_m for $C_v = 0.03$ was 55% larger for Ger and Holley's optimum 90^{o} single jet than for a similar injection in this study.

The discussion thus far has dealt with injections into an ambient flow with essentially no secondary currents or swirling motion. The symmetry which has been considered actually requires symmetry of both the flow and the injection. Since secondary currents exist in most pipes, the flow may not be symmetrical with respect to the centerline and even a high degree of accuracy in aligning the jets may not produce the symmetry necessary to achieve the same rates of mixing as measured in the laboratory. The possible influence of secondary currents on the mixing are considered further in Section 4.4 and in Chapter 5.

4.4 TESTS WITH SECONDARY CURRENTS IN THE AMBIENT FLOW

For the experiments described in the two previous sections, care was taken (Section 3.1) to minimize secondary currents in the test reach. However, in actual pipe lines, the presence of secondary currents is common and could significantly influence the mixing process and the mixing distance. To investigate this possible influence, a swirling motion was induced in the flow by placing a three-bladed, fixed propeller in the pipe upstream of the point of injection (Section 3.6). The resulting secondary current consisted of a single cell swirl which was approximately symmetrical with respect to the centerline (Fig 3.11).

Single ($M_r = 0.014$) and dual ($M_r = 0.010$) 90^{o} jet injections were used to compare the mixing characteristics with and without the swirl. The semi-log graph of C_v vs z/D_p is presented in Fig. 4.14. C_v was not plotted

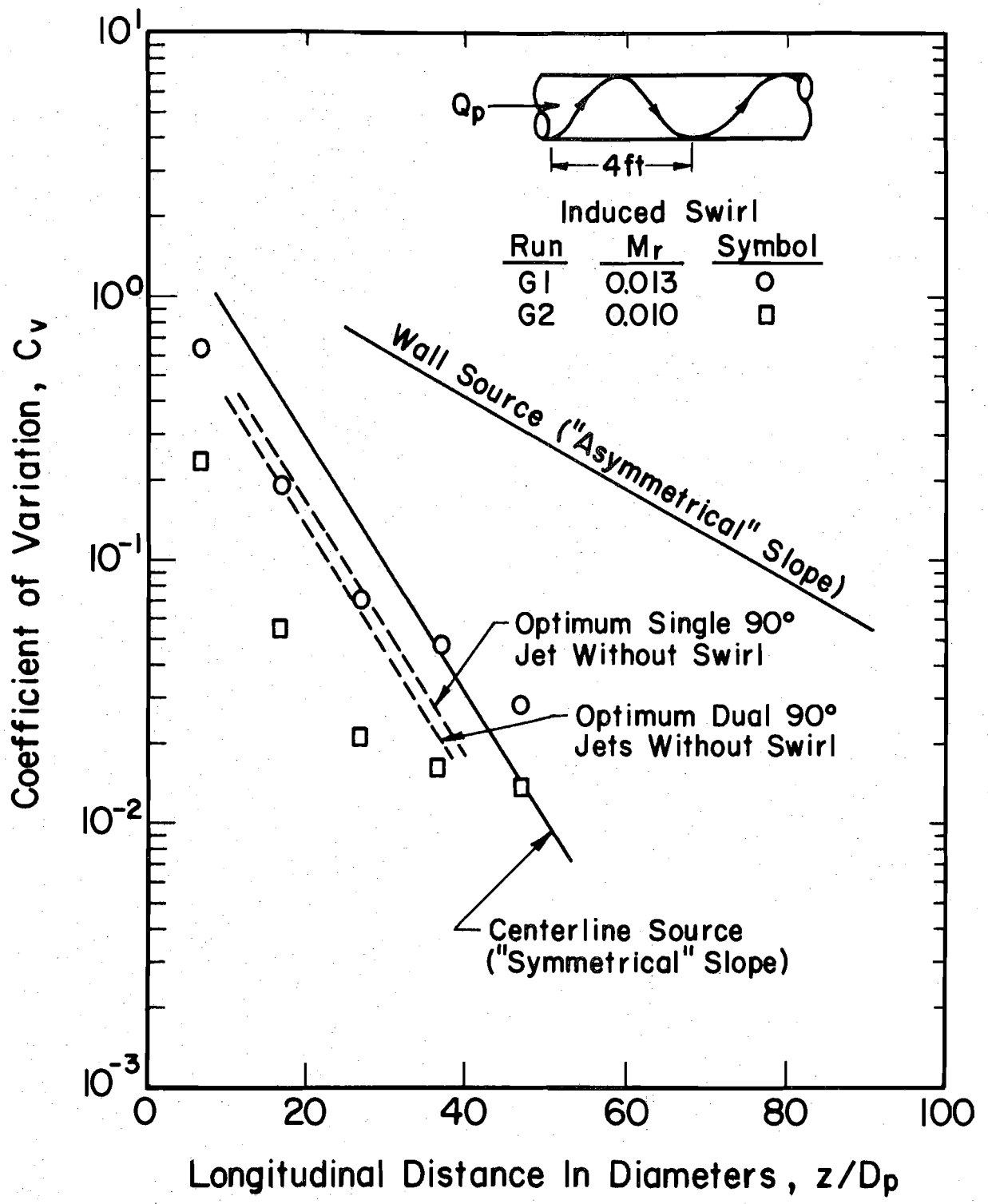

Fig. 4.14 - Coefficient of variation for single and dual 90^0 jets with induced swirl

against Z because Eq. 2.7 indicates that at a given cross section and for a given pipe flow velocity, Z is proportional to e_r. The propeller changed the structure of the pipe flow and thus may have changed e_r compared to the previous tests. Experiments were not conducted to find the actual e_r; therefore, Z could not be used to characterize the longitudinal distance.

A comparison (Fig. 4.13) of the single 90^o jet with and without the secondary current shows that the swirling motion caused the log C_v vs z/D_p curve to break away from the "symmetrical" slope sooner than for the condition with no swirl. The concentration distributions (Appendix A) showed that the swirl apparently deflected the jet toward the side of the pipe and thereby caused an asymmetrical distribution. Thus, even though the propeller probably increased e_r, the asymmetry increased the mixing distance.

For multi-cell secondary currents (for example, Rouse, 1961), a single jet could still be deflected from the centerline and asymmetry could result, depending on the orientation of the jet relative to the cells of the secondary current.

A comparison of the C_v values for two 90^o jets (M_r = 0.010) issuing into a flow with and without a single cell secondary current (Fig 4.14) indicated that unlike the single jet injection where the secondary current increased the mixing distance, the swirl decreased the mixing distance for this dual jet arrangement. There is too little data to obtain a definite explanation for this observed decrease in mixing distance, but the explanation might be as follows: With no secondary currents, the two jets approached each other and the two concentrations distributions which resulted from the initial mixing merged together about the centerline (see discussion in Section 4.2.3). With the single cell swirl in the flow, the top and bottom jets were deflected in opposite directions so that they did not merge at the

center and therefore produced a greater amount of initial mixing, i.e. a more "spread out" concentration distribution at the end of the initial mixing zone. This explanation is not incompatible with two observed characteristics. The first is that the slope of the log C_v vs. z/D_p curve for small z/D_p is approximately parallel to the "symmetrical" slope. This behavior indicates that the ambient mixing was taking place at approximately the same rate both without and with the swirl and therefore that the shorter mixing distance must have been due primarily to an increase in initial mixing. The second observed characteristic relates to the concentration distributions. With only 13 points, the details of the distributions can not be definitely established, but the available values are not incompatible with a bimodal distribution having maximum concentrations at the upper right and lower left parts of the pipe at $z/D_p = 7$ (Station 1). This type of distribution would indicate that the two jets were kept separate by the swirl.

4.5 OTHER MULTIPLE-JET INJECTIONS

4.5.1 Uniform Flow

The results from the dual 90^o jets did not indicate a significant decrease in the mixing distance as compared to the single 90^o jet for uniform flow (Fig. 4.10). It was assumed that any decrease which could be obtained by using two jets with $\alpha > 90^o$ instead of one jet would be on the same order of magnitude as the decrease for $\alpha = 90^o$. Therefore, dual jet injections for $\alpha > 90^o$ did not seem justified for uniform flow conditions.

Holley (1977) has shown for equally spaced wall sources that there is only a small reduction in the calculated mixing distance (Z_m) when using three sources instead of two and that there is no reduction in Z_m when using four or more wall sources instead of three. In view of these results, and in view of the facts that (a) the optimum condition for two jets corresponded to the concentration distributions' merging at the center of the pipe

and (b) the optimum two jet injection gave only a small reduction in Z_m compared to the optimum single jet (Fig. 4.10), it appeared that there would probably be only marginal further reduction in Z_m by using three or more jets.

4.5.2 Flow With Secondary Currents

Most natural pipe flows have secondary currents rather than being truly uniform. Because of the various types of secondary flows which can exist, it is difficult to generalize on possible interactions of jet injections and secondary currents. Nevertheless, some secondary currents (Section 4.4) destroy the symmetry required to achieve the rates of mixing which existed for the optimum conditions with uniform flow (Sections 4.1 and 4.2). Thus, even though the use of three or four injections gives only small reductions in Z_m compared to one or two injections for uniform flow, Fig. 4.14 shows that the use of two injections provides a definite advantage compared to one injection in a particular flow with a secondary current. Thus, at least for some flows, it might be expected that the use of two or more injections would provide a sort of factor of safety against possible effects of secondary currents on Z_m. However, there is not enough data presently available to quantify this possible effect.

5. APPLICATIONS

5.1 PUMP MIXING

This report has not dealt with the use of pumps for mixing; nevertheless pump mixing deserves some mention even though there is apparently very little data on mixing achieved in a pump. One study (Clayton, 1964) has shown that nearly complete mixing (less than 2% variation in concentration) was obtained in a mixed-flow pump with a 20-in. discharge line and with a flow of 8.2 cfs. The injection was made at the bell-mouth suction port which was submerged in a sump.

The efficiency of pumps gives one indication that pumps should serve as rapid-mixing chambers. If a pump has an efficiency of 80%, then 80% of the energy input goes into producing the flow through the pump and the piping system while 20% is lost in various ways with the primary part of the loss being in the generation of turbulence. It is this turbulence that produces the mixing and the fact that a significant part of the energy goes into turbulence indicates that mixing should be rapid. On the other hand, turbines generally have very high efficiencies so that there is very little turbulence, and therefore very little mixing, generated in a turbine.

If a pump is being considered for mixing, the considerations should include possible volitalization of the additive due to low pressures in the pump and possible corrosion of metal parts, deterioration of seals, etc. due to the concentrations of the additive in the pump.

5.2 PIPE MIXING

If speed of mixing is not important and if sufficient pipe length is available, then a simple injection at or near the pipe wall may be all that is required. Figs. 2.1 and 3.8 show that a distance corresponding to $Z \simeq 1.0$

will produce enough mixing to give C_v = 0.01 when there is negligible density difference between the fluid in the pipe and the injected fluid. The corresponding maximum deviation from the average concentration would be less than 2% (Holley, 1977). For a friction factor of 0.02, Z of 1.0 corresponds to 147 pipe diameters (Eq. 2.8 with Sc_t = 1.0), or f = 0.01 gives 208 diameters for Z = 1.0.

If there is not sufficient pipe length to accomplish the mixing by ambient mixing or if more rapid mixing is required for chemical or biological reasons, then jet injections could be considered. When it is desirable to use a combination of initial mixing due to the injection and ambient mixing due to the pipe flow, the selection of the best injection system for promoting rapid mixing in a specific application requires consideration of at least six design factors:

1) required degree of uniformity or required coefficient of variation for the additive,
2) the speed with which mixing needs to be accomplished,
3) pipe length available for mixing,
4) hydraulics of the pipe flow, i.e. the friction factor and secondary current pattern,
5) accessibility of the injection region and possible problems installing and operating an injection system, and
6) availability of power for the injection.

In general, the required degree and speed of mixing will depend on the particular application. For example, when using the method of dilution for measuring discharge in a pipe, it may be advantageous to measure the tracer at only one point in the pipe flow at a cross section where C_v is small, say less than 0.01. As C_v decreases, one concentration measurement gets closer to the average concentration, but there is little to be gained

by specifying C_v significantly smaller than the measurement accuracy. For other applications such as adding disinfectants to water supplies, larger C_v values may be acceptable.

The pipe length available for mixing must be determined. Some injection configurations may be excluded from consideration because the flow distance required to reach the specified C_v is longer than the available pipe length. For established, uniform flows with negligible secondary currents, the results in Section 4.1 and 4.2 may be used to estimate the distance required to obtain a certain degree of mixing for the optimum momentum ratios for injections with one and two jets. For example, for two jets with $M_r = 0.010$, $C_v = 0.10$ would be achieved at $Z \simeq 0.17$ and $C_v = 0.01$ at $Z \simeq 0.33$. For $f = 0.015$, using Eq. 2.8 with $Sc_t = 1.0$, $Z = 0.17$ corresponds to $z/D_p = 29$. Similarly, $Z = 0.33$ gives $z/D_p = 56$. For a 3-ft diameter pipe with a velocity of 5 fps and with 1-in. diameter injection tubes with $M_r = 0.010$, the injection velocity and discharge for each jet could be calculated from

$$M_r = \left(\frac{V_j D_j}{V_p D_p} \right)^2 = 0.010 \qquad (5.1)$$

$$V_j = \sqrt{0.010} \; \frac{V_p D_p}{D_j} = 18.0 \text{fps} \qquad (5.2)$$

$$Q_j = A_j V_j = 0.098 \text{ cfs} \qquad (5.3)$$

Power requirements are considered in Section 5.3.

As mentioned in Sections 4.4 and 4.5, many flows have significant secondary currents which can destroy the symmetry that is necessary to achieve the optimum rates of mixing discussed in Sections 4.1 and 4.2. Some experimental results were obtained for a flow with a

particular type of secondary current, but that current was a rather strong, single cell swirl and the results for that case are not necessarily indicative of the behavior in other situations. On the basis of present information, in order to achieve the most rapid possible mixing with jet injections, it would appear to be advisable to use two or more jets equally spaced around the pipe periphery, with each jet having M_r of approximately 0.010. The use of additional jets provides a sort of factor of safety against the unknown influences of secondary currents which might exist in the flow. Similarly, there are some indications in the results presented in Section 4.2 for two-jet injections in flows with no secondary currents that $M_r = 0.006$ may produce almost as much effect on the mixing distance as $M_r = 0.010$, but using $M_r = 0.010$ also provides some factor of safety. As mentioned in Section 4.5, for pipe flows with natural secondary currents, there is a sparsity of data on the behavior of jet injections and more research is needed on this topic.

5.3 POWER REQUIREMENT

The power requirement (P_j) for supplying the kinetic energy to the jets can be written in dimensionless form as

$$\frac{P_j}{P_p} = \frac{N\gamma Q_j \frac{V_j^2}{2g}}{\gamma Q_p \frac{V_p^2}{2g}} = N\, M_r^{3/2} \frac{D_p}{D_j} \qquad (5.4)$$

where P_p = power in kinetic energy of pipe flow

Q = discharge

V = velocity

D = diameter

sub p = pipe

sub j = jet

N = number of jets

Eq. 5.4 shows that P_j decreases as D_j increases for a given pipe flow and given M_r. See Fig. 5.1 for P_j/P_p for various injection conditions.

Eq. 5.4 gives only the power required for the velocity head of the jet. A major additional head requirement could come from the need to pump the jet against the internal pressure in high pressure lines. However, this head requirement can be eliminated by a closed system where the fluid for the jet injection is extracted from the pipe. Then a small power, high pressure pump could be used to inject a concentrated tracer (additive) into the closed system, as shown in Fig. 5.2. The injection should be made in the by-pass line so as to assure complete mixing before the jet enters the main pipe. This mixing could be accomplished by injecting upstream of the pump, as illustrated in Fig. 5.2, or by providing sufficient length of the by-pass line. Friction losses and pump efficiency must also be included in a calculation of total power requirement.

To illustrate the use of Eq. 5.4, assume that two jets with 1 in. diameters are to be used to obtain M_r = 0.010 in a 10 ft. diameter pipe with a flow velocity of 5 fps. The value of P_j would be 1690 ft-lb/sec or 3.1 hp. Pump efficienty has not been included in these considerations. Using D_j of 2 in. would reduce the required power by a factor of 2 for the same M_r.

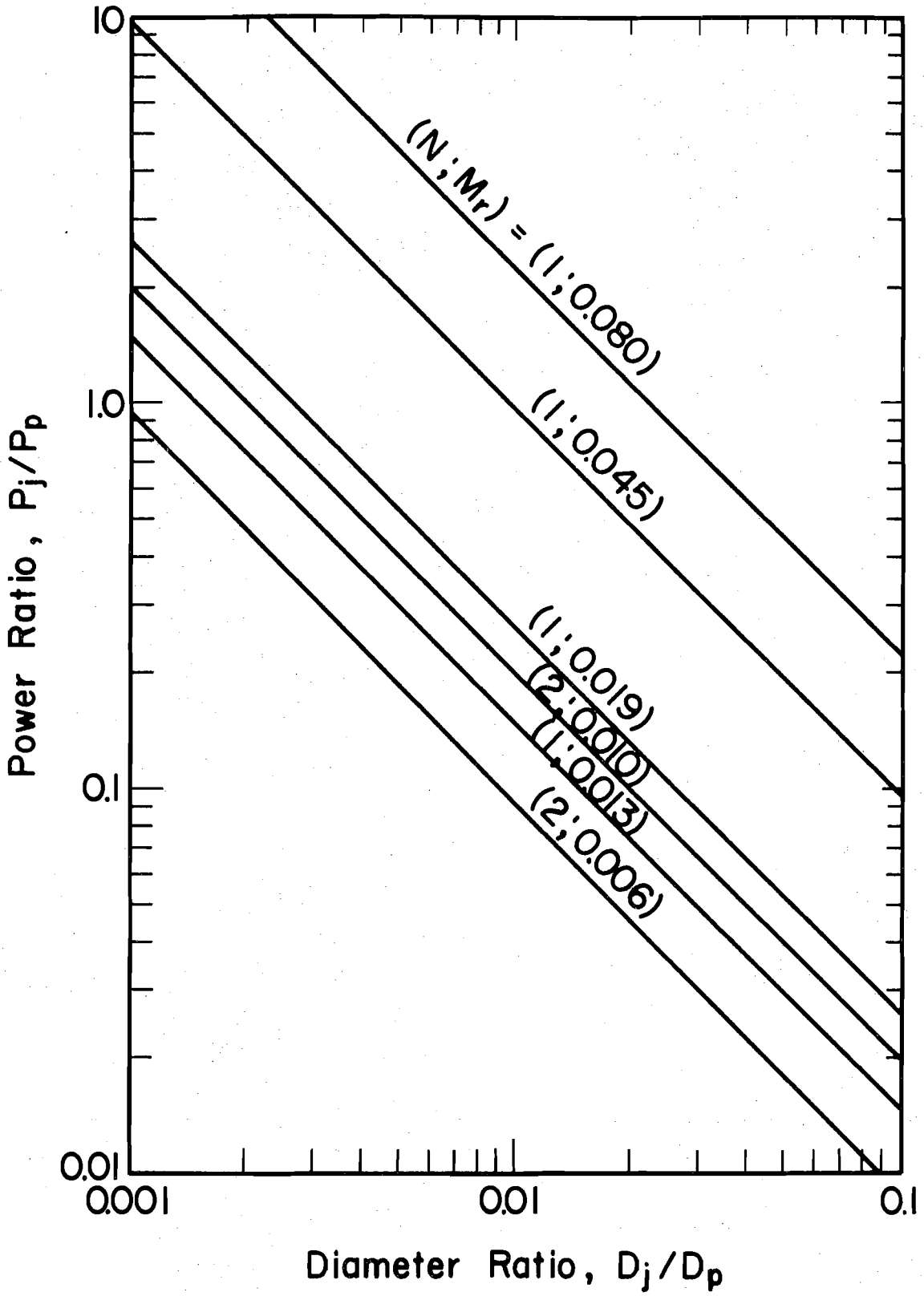

Fig. 5.1 - Dimensionless power requirements

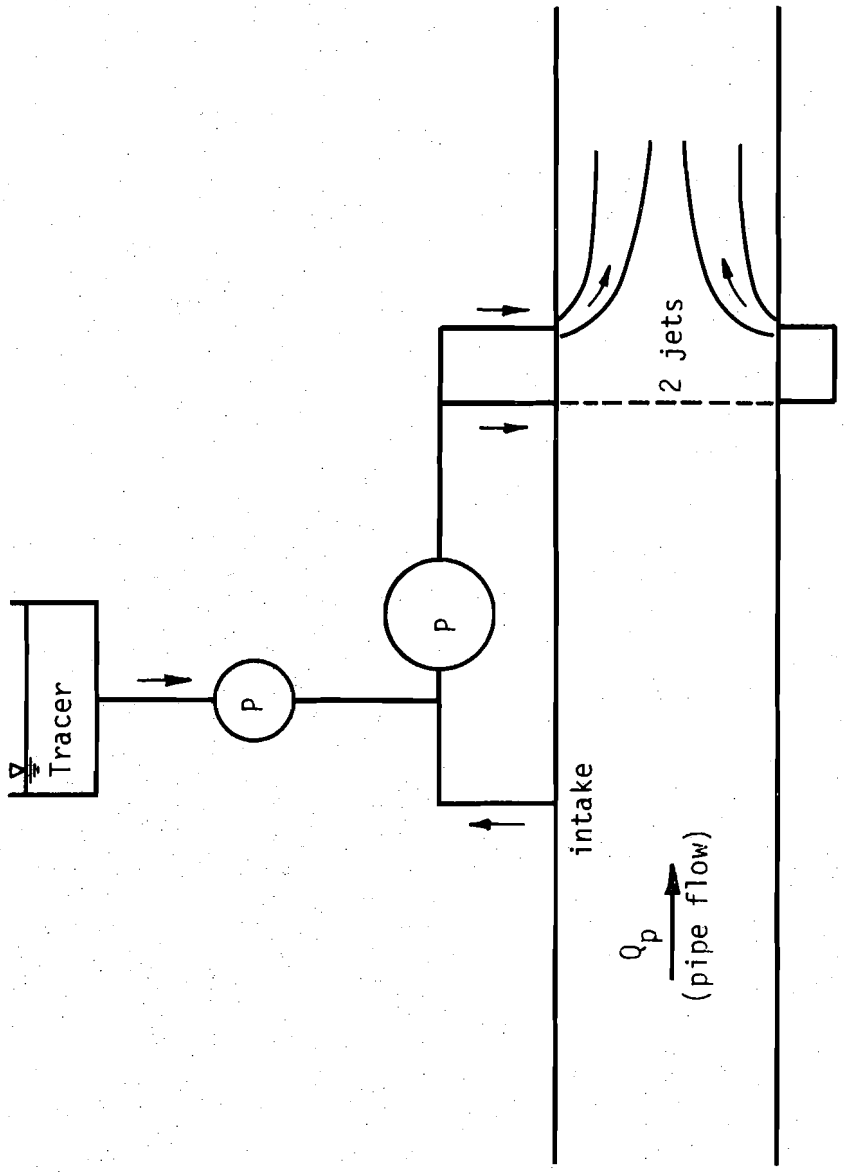

Fig. 5.2 - Schematic diagram of injection into by-pass line

6. CONCLUSIONS

When injecting a miscible fluid into a flow in a pipe, the use of jet injections can speed the mixing relative to that which would take place just due to the ambient flow. The jets can be at the pipe wall and therefore do not require that any appurtenances or devices be placed inside the pipe.

In this study, laboratory experiments were conducted to investigate the effectiveness of jet-induced mixing in pipe flows. The coefficient of variation (C_v) of the concentration distribution was used as a measure of the degree of mixing at a given cross section. The dimensionless mixing distance (Z_m) was defined as the flow distance required to obtain $C_v = 0.03$. Increases in the effectiveness of the jet mixing produced decreases in Z_m and vice-versa. As in previous studies, this work also found, for uniform pipe flow with a given number and orientation of jets, that the ratio (M_r) of the jet momentum flux to the pipe-flow momentum flux is the parameter which is indicative of the mixing induced by the jets. For a single jet oriented at various angles to the ambient flow, the moment ratios for optimum mixing and the corresponding mixing distances are given in Table 4.1. Increasing the angle of injection from 90^o (cross flow) to 150^o (almost counterflow) decreased the optimum Z_m by 35% but at the cost of a large increase in the momentum ratio and in the power requirement. Under many circumstances, it might not be practical to consider any angle of injection other than 90^o.

Experiments were also conducted with two diametrically opposed 90^o jets in uniform flow. Optimum mixing was obtained with the momentum ratio for each jet being on the order of one-half of the optimum momentum ratio for a single jet injection. Thus, even though the use of two jets did

not produce a significant decrease in the mixing distance compared to a single jet, the two jets would require less total power than a single jet. Furthermore, limited experiments in a pipe flow with an induced secondary current, indicated that the use of two or more jets for the injection would provide a sort of factor of safety against the effects which unknown secondary currents could have on the jets and on the mixing process.

REFERENCES

Chilton, T.H., and Genereaus, R.P., American Institute of Chemical Engineers Transactions, Vol. 25, 1930, pp. 102-122.

Clayton, C.G., "The Use of a Pump to Reduce Mixing Length in the Dilution Method of Flow Measurement," Rept. AERE-R 4623, Wantage Research Laboratory, AERE, Wantage, Berks, England, 9 p., 1964.

Clayton, C.G., Ball, A.M. and Spackman, R., "Dispersion and Mixing during Turbulent Flow of Water in a Circular Pipe", Isotope Research Division, Wantage Research Laboratory, Wantage, Berkshire, Report AERE-R 5569, 1968, p. 31.

Evans, G.V., "A Study of Diffusion in Turbulent Pipe Flow", Journal of Basic Engineering, ASME, Vol. 89D, 1967, pp. 624-632.

Fan, L.N., "Turbulent Buoyant Jets into Stratified or Flowing Ambient Fluids", W.M. Keck Laboratory of Hydraulics and Water Resources, California Institute of Technology, Pasadena, 196 p., 1967.

Filmer, R.W. and Yevdjevich, V.M., "The Use of Tracers in Making Accurate Discharge Measurements in Pipelines", Report CER66RWF-VMY 38, Colorado State University , Fort Collins, 1966, p. 90.

Ger, A.M., and Holley, E.R., "Turbulent Jets in Crossing Pipe Flow", Hydraulic Engineering Series Report 30, University of Illinois at Urbana-Champaign, 1974, p. 198.

Holley, E.R. and Ger, A.M., "Circumferential Diffusion in Pipe Mixing", Journal of the Hydraulics Division, ASCE, Vol. 104, No. HY4, April, 1978, pp. 471-485.

Holley, E.R., "Dilution Method of Discharge Measurement in Pipes", Proceedings of the Flow Measurement Symposium, National Bureau of Standards Special Publ. 484, October 1977, pp. 395-421.

Jordan, D.W., "A Theoretical Study of the Diffusion of Tracer Gas in an Airway", Quarterly Journal of Mechanics and Applied Mathematics, Vol. 14, 1961, pp. 203-222.

Morgan, W.D., Brinkworth, B.J., and Evans, G.V., "Upstream Penetration of an Enclosed Counterflowing Jet", Ind. Eng. Chem., Fundam., Vol. 15, No. 2, 1976, pp. 125-127.

Rouse, H., Fluid Mechanics for Hydraulic Engineers, Dover, New York, 422 p., 1961.

APPENDIX

The data from each of the experimental runs are given below. The value given for each measurement point is the time-averaged concentration (c) at a particular point in the cross section divided by the cross sectional average concentration ($\bar{c}$). The locations and numbering scheme of the thirteen measurement points are shown in Fig. A-1. For both the wall sources and the injections, the distance from the point of injection to each sampling station is given in Table A-1 in both pipe diameters (z/D_p) and dimensionless longitudinal distances (Z).

Table A-1 - Location of the Sampling Stations

	Wall Source		Jet Injection	
Sampling Station	z/Dp	Z[1]	z/Dp	Z
1	6.17	0.047	7.00	0.053
2	16.17	0.123	17.00	0.129
3	26.17	0.199	27.00	0.205
4	36.17	0.275	37.00	0.281
5	46.17	0.351	47.00	0.357
6	66.17	0.503	67.00	0.509
7	86.17	0.655	87.00	0.660
8	106.17	0.807	107.00	0.812

[1]Defined by Eqs. 2.7 and 2.8.

Run A1 Single Wall Source (22 May 1978) R_p = 32,500 M_r = 0.00038

Cross Section	C_v	1	2	3	4	5	6	7	8	9	10	11	12	13
3	0.783	0.014	0.071	0.221	0.914	1.953	2.391	2.569	0.758	0.784	0.809	0.846	0.838	0.832
5	0.352	0.444	0.452	0.551	0.976	1.425	1.533	1.573	1.008	0.981	1.003	1.030	1.049	0.976
6	0.159	0.757	0.777	0.848	1.050	1.209	1.270	1.270	0.977	0.965	0.965	0.972	0.965	0.977
7	0.083	0.858	0.870	0.901	1.000	1.080	1.099	1.139	0.961	0.981	1.000	1.016	1.036	1.060
8	0.035	0.951	0.945	0.970	1.007	1.045	1.063	1.052	0.979	0.983	0.996	1.001	1.007	1.001

Run A2 Single Wall Source (29 May 1978) R_p = 37,300 M_r = 0.00038

Cross Section	C_v	1	2	3	4	5	6	7	8	9	10	11	12	13
3	0.792	0.079	0.142	0.236	1.027	2.053	2.441	2.551	0.761	0.690	0.768	0.772	0.734	0.748
5	0.304	0.475	0.509	0.608	0.950	1.337	1.422	1.473	1.090	1.052	1.049	1.025	1.005	1.005
6	0.170	0.758	0.772	0.844	1.019	1.225	1.276	1.313	0.994	1.025	0.947	0.937	0.947	0.943

Run B1 Single 90° jet (13 June 1978) R_p = 35,300 M_r = 0.0138

Cross Section	C_v	1	2	3	4	5	6	7	8	9	10	11	12	13
2	0.254	0.718	0.929	1.335	1.554	1.020	0.867	0.785	0.809	0.882	1.239	1.250	0.913	0.700
3	0.083	0.923	1.007	1.110	1.199	1.048	0.996	0.972	0.910	0.969	1.026	1.037	0.910	0.894
4	0.026	0.979	0.987	1.014	1.058	0.987	1.004	0.971	0.989	0.995	1.048	1.018	0.971	0.981
5	0.019	0.983	0.987	0.994	1.020	1.016	1.030	1.027	1.011	1.003	0.994	0.987	0.963	0.987

Run B2 Single 90° jet (18 October 1978) R_p = 31,500 M_r = 0.0151

Cross Section	C_v	1	2	3	4	5	6	7	8	9	10	11	12	13
1	0.798	0.101	0.285	1.375	3.051	1.543	0.934	0.733	0.299	0.561	1.500	1.768	0.603	0.248
2	0.210	0.870	1.015	1.386	1.446	0.983	0.831	0.811	0.761	0.904	1.119	1.141	0.939	0.794
3	0.070	1.010	1.027	1.147	1.147	0.974	0.939	0.925	0.965	0.928	0.971	1.018	1.001	0.948
4	0.024	1.019	1.002	1.029	1.008	0.967	0.950	0.960	1.016	1.004	1.007	1.030	1.013	0.996

Run B3 Single 90° jet (27 October 1978) R_p = 32,8000 M_r = 0.0140

Cross Section	C_v	1	2	3	4	5	6	7	8	9	10	11	12	13
1	0.786	0.098	0.390	1.716	2.896	1.376	0.819	0.617	0.294	0.559	1.702	1.696	0.621	0.216
2	0.204	0.966	1.073	1.418	1.414	0.931	0.802	0.834	0.793	0.989	1.088	1.056	0.828	0.810
3	0.086	1.083	1.098	1.128	1.093	0.905	0.858	0.865	0.981	1.011	1.030	1.042	0.976	0.932
4	0.045	1.057	1.066	1.090	1.043	0.967	0.947	0.955	0.967	0.982	0.996	0.990	0.962	0.979
5	0.025	1.022	1.034	1.032	0.995	0.955	0.965	0.956	1.016	1.007	1.004	0.998	1.007	1.010

Run B4 Single 90° Jet (1 November 1978) R_p = 33,500 M_r = 0.0124

Cross Section	C_v	1	2	3	4	5	6	7	8	9	10	11	12	13
1	0.867	0.025	0.233	1.129	3.238	1.646	1.075	0.750	0.175	0.540	1.556	1.844	0.595	0.193
2	0.238	0.733	0.910	1.335	1.539	1.055	0.916	0.903	0.747	0.875	1.165	1.199	0.900	0.723
3	0.075	0.932	1.001	1.094	1.207	1.039	0.990	0.970	0.932	0.946	1.015	0.987	0.970	0.917
4	0.028	0.958	0.973	0.999	1.057	1.024	0.999	1.004	0.999	1.013	1.042	0.993	0.966	0.973

Run B5 Single 90° Jet (8 November 1978) R_p = 34,300 M_r = 0.0140

Cross Section	C_v	1	2	3	4	5	6	7	8	9	10	11	12	13
1	0.816	0.066	0.317	1.467	3.054	1.506	0.890	0.726	0.265	0.615	1.779	1.611	0.490	0.213
2	0.229	0.864	1.001	1.424	1.510	0.997	0.874	0.818	0.813	0.901	1.147	1.078	0.859	0.717
3	0.085	1.022	1.074	1.148	1.140	0.956	0.883	0.875	0.942	0.973	1.049	1.051	0.952	0.934
4	0.034	1.047	1.049	1.060	1.032	0.971	0.963	0.951	0.978	1.006	0.991	0.983	0.995	0.974
5	0.032	1.012	1.032	1.032	1.000	0.959	0.951	0.923	1.005	1.015	1.025	1.020	1.003	1.023

Run C1 Single 120° Jet (October 9 1978) R_p = 37,500 M_r = 0.0188

Cross Section	C_v	1	2	3	4	5	6	7	8	9	10	11	12	13
2	0.208	0.728	0.891	1.312	1.429	1.086	1.008	1.002	0.787	0.853	1.139	1.146	0.886	0.734
3	0.064	0.911	0.986	1.095	1.127	1.004	0.971	0.961	0.920	0.955	1.044	1.064	1.013	0.948
4	0.025	0.972	0.979	1.024	1.048	1.012	0.998	1.008	0.966	0.971	1.005	1.030	1.012	0.974
5	0.022	0.955	0.963	0.990	1.016	1.016	1.012	1.015	0.972	0.994	1.004	1.030	1.017	1.017

Run C2 Single 120° Jet (13 September 1978) R_p = 36,100 M_r = 0.0193

Cross Section	C_v	1	2	3	4	5	6	7	8	9	10	11	12	13
1	0.702	0.059	0.247	1.121	2.618	1.637	1.105	0.893	0.406	0.765	1.655	1.613	0.605	0.276
2	0.210	0.653	0.798	1.174	1.468	1.097	1.018	0.966	0.845	0.923	1.174	1.184	0.927	0.774
3	0.076	0.900	0.921	1.056	1.179	1.061	1.029	1.006	0.944	1.006	1.032	1.032	0.934	0.898
4	0.032	0.932	0.956	0.983	1.039	0.991	0.991	0.997	0.986	0.993	1.036	1.047	1.036	1.015
5	0.023	0.971	0.979	0.992	1.047	1.023	1.023	1.036	0.979	0.986	0.992	1.001	0.992	0.982

Run C3 Single 120° Jet (15 September 1978) R_p = 35,100 M_r = 0.0216

Cross Section	C_v	1	2	3	4	5	6	7	8	9	10	11	12	13
1	0.595	0.170	0.491	1.501	2.324	1.375	0.929	0.704	0.426	0.748	1.480	1.640	0.808	0.405
2	0.185	0.834	0.907	1.328	1.382	1.038	0.914	0.901	0.758	0.936	1.126	1.134	0.938	0.805
3	0.073	1.051	1.096	1.134	1.127	0.980	0.965	0.947	0.920	0.947	0.989	0.986	0.931	0.929
4	0.035	1.028	1.039	1.059	1.010	0.960	0.943	0.936	0.986	1.015	1.013	1.019	1.013	0.979
5	0.022	1.016	1.021	1.037	1.001	0.960	0.964	0.977	1.001	1.028	1.007	0.994	0.994	1.001

Run D1 Single 135° Jet (20 September 1978) R_p = 36,500 M_r = 0.0337

Cross Section	C_v	1	2	3	4	5	6	7	8	9	10	11	12	13
1	0.529	0.135	0.379	1.127	2.074	1.403	0.998	0.863	0.559	0.916	1.608	1.560	0.880	0.498
2	0.178	0.633	0.811	1.106	1.356	1.093	1.003	1.019	0.870	0.966	1.151	1.183	0.939	0.870
3	0.076	0.850	0.877	1.010	1.145	1.056	1.040	1.051	0.941	0.981	1.050	1.047	0.978	0.973
4	0.043	0.899	0.922	0.963	1.047	1.031	1.030	1.030	0.988	1.006	1.035	1.023	1.013	1.013

Run D2 Single 135° Jet (2 October 1978) R_p = 35,600 M_r = 0.0377

Cross Section	C_v	1	2	3	4	5	6	7	8	9	10	11	12	13
1	0.462	0.252	0.535	1.212	1.976	1.222	0.916	0.754	0.579	0.920	1.441	1.589	1.010	0.593
2	0.140	0.739	0.858	1.114	1.280	1.008	0.984	0.944	0.897	0.934	1.120	1.190	1.005	0.928
3	0.055	0.878	0.958	1.012	1.100	1.038	1.021	1.003	0.941	0.949	1.016	1.062	1.010	1.015
4	0.030	0.939	0.960	0.992	1.034	1.018	1.020	1.019	0.953	0.986	1.012	1.034	1.020	1.013
5	0.020	0.985	0.986	1.012	1.012	1.017	1.026	1.023	0.956	0.967	0.996	1.005	1.007	1.007

Run D3 Single 135° Jet (6 October 1978) R_p = 34,800 M_r = 0.0382

Cross Section	C_v	1	2	3	4	5	6	7	8	9	10	11	12	13
1	0.434	0.321	0.529	1.205	1.893	1.229	0.840	0.710	0.635	0.990	1.503	1.507	0.990	0.648
2	0.140	0.776	0.820	1.026	1.296	1.096	0.980	0.939	0.920	0.991	1.177	1.131	0.964	0.882
3	0.050	0.870	0.960	1.027	1.095	1.033	1.015	1.015	0.965	0.973	1.028	1.030	0.991	0.999
4	0.024	0.942	0.968	0.990	1.028	1.023	1.016	1.026	0.987	0.981	1.005	1.026	1.008	1.001
5	0.023	0.977	0.999	1.002	1.026	1.040	1.021	1.037	0.965	0.981	0.978	0.985	0.996	0.993

Run D4 Single 135° Jet (9 October 1978) R_p = 35,600 M_r = 0.0390

Cross Section	C_v	1	2	3	4	5	6	7	8	9	10	11	12	13
1	0.464	0.260	0.505	1.239	1.984	1.242	0.895	0.701	0.669	1.016	1.493	1.534	0.882	0.582
2	0.144	0.708	0.822	1.068	1.296	1.087	1.013	0.979	0.938	0.991	1.127	1.115	0.988	0.867
3	0.062	0.855	0.910	0.980	1.099	1.039	1.023	1.016	0.969	0.989	1.064	1.054	0.987	1.016
4	0.029	0.948	0.946	1.008	0.992	1.040	1.043	1.035	0.993	1.009	1.015	1.005	0.983	0.983
5	0.020	0.958	0.963	0.981	1.003	1.017	1.017	1.011	0.989	1.017	1.011	1.019	1.011	1.003

Run D5 Single 135° Jet (11 October 1978) R_p = 35,400 M_r = 0.0446

Cross Section	C_v	1	2	3	4	5	6	7	8	9	10	11	12	13
1	0.433	0.276	0.560	1.237	1.878	1.143	0.832	0.696	0.650	1.017	1.465	1.573	0.966	0.708
2	0.127	0.752	0.799	1.074	1.217	1.033	0.966	0.964	0.903	0.970	1.126	1.151	1.030	1.016
3	0.053	0.885	0.932	1.007	1.088	1.044	1.021	1.009	0.948	0.961	1.040	1.044	0.997	1.024
4	0.028	0.959	0.975	0.983	1.036	1.044	1.027	1.025	0.959	0.969	0.989	1.015	1.021	0.998
5	0.272	0.973	0.987	1.007	1.026	1.040	1.042	1.037	0.958	0.970	0.984	0.998	0.989	0.988

Run D6 Single 135° Jet (13 October 1978) R_p = 33,200 M_r = 0.0450

Cross Section	C_v	1	2	3	4	5	6	7	8	9	10	11	12	13
1	0.411	0.319	0.695	1.295	1.809	1.088	0.733	0.622	0.744	0.961	1.482	1.533	1.026	0.695
2	0.103	0.846	0.914	1.123	1.221	0.992	0.914	0.918	0.941	0.968	1.078	1.125	1.023	0.938
3	0.035	0.936	0.969	1.014	1.050	0.993	0.953	0.962	1.014	1.016	1.050	1.027	1.025	0.991
4	0.024	0.986	1.016	1.031	1.044	0.998	1.018	1.010	0.949	0.983	1.000	1.000	1.000	0.965
5	0.015	0.966	0.993	0.993	0.993	0.986	0.999	0.991	1.012	1.023	1.021	1.020	0.999	1.005

Run E1 Single 150° Jet (15 November 1978) R_p = 32,400 M_r = 0.1170

Cross Section	C_v	1	2	3	4	5	6	7	8	9	10	11	12	13
1	0.161	1.084	1.125	1.277	1.260	0.970	0.838	0.740	0.775	0.875	1.006	1.089	0.947	1.014
2	0.083	1.141	1.116	1.119	1.057	0.960	0.906	0.855	0.924	0.971	0.996	1.019	0.960	0.979
3	0.056	1.097	1.092	1.097	1.034	0.977	0.960	0.955	0.964	0.955	0.980	0.986	0.952	0.952
4	0.030	1.039	1.036	1.034	1.004	0.950	0.955	0.947	1.000	1.006	1.020	1.000	1.006	1.003

Run E2 Single 150° Jet (22 November 1978) R_p = 32,400 M_r = 0.1009

Cross Section	C_v	1	2	3	4	5	6	7	8	9	10	11	12	13
1	0.164	0.850	0.998	1.235	1.300	1.122	0.929	0.860	0.712	0.817	1.102	1.119	1.005	0.955
2	0.063	1.035	1.061	1.094	1.127	1.015	0.973	0.967	0.900	0.917	1.005	0.973	0.973	0.959
3	0.027	1.025	1.013	1.029	1.026	0.970	0.961	0.959	0.965	0.979	1.016	1.015	1.022	1.020
4	0.023	1.033	1.036	1.041	1.015	0.999	0.996	0.996	0.957	0.975	0.989	0.989	0.986	0.989

Run E3 Single 150° Jet (24 November 1978) R_p = 31,500 M_r = 0.0916

Cross Section	C_v	1	2	3	4	5	6	7	8	9	10	11	12	13
1	0.156	0.907	1.025	1.256	1.299	1.094	0.939	0.835	0.737	0.838	1.058	1.101	0.960	0.950
2	0.070	1.060	1.042	1.100	1.114	1.019	0.976	0.970	0.836	0.913	0.990	1.006	0.983	0.990
3	0.026	1.021	1.037	1.028	1.031	0.975	0.975	0.957	0.968	0.973	1.000	1.018	1.001	1.015
4	0.028	1.040	1.043	1.043	1.017	1.005	1.005	0.994	0.948	0.962	0.978	0.997	0.982	0.988
5	0.016	1.006	1.012	1.006	0.995	0.975	0.963	0.989	0.992	1.012	1.014	1.003	1.012	1.021

Run E4 Single 150° Jet (27 November 1978) R_p = 31,200 M_r = 0.0868

Cross Section	C_v	1	2	3	4	5	6	7	8	9	10	11	12	13
1	0.155	0.831	1.019	1.237	1.326	1.072	0.905	0.864	0.789	0.895	1.118	1.092	0.961	0.891
2	0.046	1.025	1.020	1.075	1.092	1.005	0.947	0.954	0.940	0.965	1.006	1.020	0.954	0.998
3	0.027	1.016	1.052	1.045	1.037	0.999	0.981	0.990	0.968	0.983	0.997	0.974	0.979	0.981

Run E5 Single 150° Jet (27 November 1978) R_p = 31,200 M_r = 0.0773

Cross Section	C_v	1	2	3	4	5	6	7	8	9	10	11	12	13
1	0.211	0.691	0.860	1.218	1.416	1.203	1.009	0.894	0.719	0.871	1.164	1.190	0.948	0.817
2	0.073	0.912	1.015	1.095	1.165	1.056	1.004	1.007	0.904	0.912	1.015	1.019	0.958	0.938
3	0.025	0.953	0.966	1.018	1.039	0.993	1.012	1.019	0.969	0.984	1.013	1.030	1.010	0.995
4	0.018	1.003	1.018	1.018	1.024	1.015	1.006	1.021	0.963	0.981	0.986	0.981	0.994	0.990

Run F1 Two 90° Jets (6 February 1979) R_p = 36,800 M_r 0.0040

Cross Section	C_v	1	2	3	4	5	6	7	8	9	10	11	12	13
1	0.811	1.831	1.925	1.961	0.845	1.906	1.793	1.676	0.047	0.115	0.342	0.379	0.124	0.056
2	0.285	1.356	1.347	1.296	1.138	1.188	1.240	1.196	0.570	0.669	0.836	0.839	0.703	0.624
3	0.113	1.186	1.144	1.110	1.055	1.040	1.040	1.084	0.823	0.835	0.916	0.969	0.913	0.885
4	0.040	1.080	1.071	1.044	1.006	0.991	0.984	0.947	0.949	0.969	0.972	1.011	0.990	0.986

Run F2 Two 90° Jets (10 February 1979) R_p = 37,600 M_r = 0.0045

Cross Section	C_v	1	2	3	4	5	6	7	8	9	10	11	12	13
2	0.262	1.262	1.217	1.258	1.296	1.199	1.190	1.131	0.544	0.670	0.927	0.945	0.729	0.635
3	0.089	1.099	1.087	1.052	1.083	1.061	1.057	1.052	0.809	0.858	0.944	1.016	0.948	0.933
4	0.053	1.033	1.037	1.037	1.048	1.037	1.052	1.052	0.889	0.916	0.939	0.995	0.989	0.977
5	0.016	1.002	1.004	1.002	1.002	0.992	1.002	0.996	0.969	0.969	0.996	1.020	1.029	1.017

Run F3 Two 90° Jets (13 February 1979 R_p = 38,800 M_r = 0.0035

Cross Section	C_v	1	2	3	4	5	6	7	8	9	10	11	12	13
2	0.295	1.294	1.275	1.267	1.194	1.238	1.270	1.291	0.565	0.657	0.868	0.863	0.658	0.562
3	0.092	1.083	1.083	1.068	1.052	1.083	1.100	1.083	0.833	0.881	0.970	0.983	0.902	0.883
4	0.053	1.042	1.052	1.035	1.032	1.042	1.063	1.063	0.914	0.926	0.948	0.971	0.968	0.945
5	0.010	0.986	0.990	0.987	1.002	1.002	1.003	1.003	0.987	0.994	1.007	1.011	1.016	1.013

Run F4 Two 90° Jets (13 February 1979) R_p = 40,100 M_r = 0.0030

Cross Section	C_v	1	2	3	4	5	6	7	8	9	10	11	12	13
2	0.326	1.355	1.347	1.258	1.082	1.249	1.370	1.349	0.581	0.644	0.821	0.796	0.597	0.551
3	0.100	1.106	1.085	1.080	1.018	1.018	1.126	1.105	0.844	0.869	0.959	0.955	0.914	0.858
4	0.057	1.052	1.036	1.047	1.033	1.057	1.056	1.072	0.907	0.928	0.970	0.973	0.945	0.925
5	0.014	0.983	0.988	0.983	0.983	1.000	1.011	1.013	0.986	1.006	1.006	1.000	1.016	1.026

Run F5 Two 90° Jets (17 February 1979) R_p = 33,200 M_r = 0.0040

Cross Section	C_v	1	2	3	4	5	6	7	8	9	10	11	12	13
2	0.268	1.259	1.271	1.256	1.176	1.224	1.226	1.224	0.602	0.715	0.937	0.870	0.660	0.586
3	0.105	1.104	1.110	1.092	1.089	1.095	1.080	1.086	0.843	0.896	0.958	0.936	0.875	0.839
4	0.034	1.046	1.015	1.021	1.020	1.015	1.032	1.027	0.986	0.991	1.005	0.972	0.946	0.924
5	0.035	1.017	1.046	1.036	1.024	1.019	1.040	1.037	0.964	0.976	0.974	0.968	0.950	0.948

Run F6 Two 90° Jets (20 February 1979) R_p = 31,000 M_r = 0.0060

Cross Section	C_v	1	2	3	4	5	6	7	8	9	10	11	12	13
2	0.197	1.092	1.136	1.199	1.283	1.157	1.102	1.082	0.685	0.786	1.058	0.995	0.753	0.673
3	0.075	1.021	1.046	1.067	1.103	1.079	1.052	1.061	0.879	0.924	0.992	0.992	0.906	0.879
4	0.017	1.010	0.998	1.003	1.025	1.012	1.022	0.998	0.974	0.983	1.017	1.001	0.989	0.968
5	0.013	0.985	0.978	0.983	0.990	0.984	1.001	1.008	1.005	1.017	1.017	1.019	1.009	1.005

Run F7 Two 90° Jets (22 February 1979) R_p = 30,700 M_r = 0.0070

Cross Section	C_v	1	2	3	4	5	6	7	8	9	10	11	12	13
2	0.198	1.117	1.161	1.190	1.338	1.138	1.052	1.038	0.712	0.819	1.026	1.005	0.732	0.673
3	0.051	1.011	1.041	1.053	1.112	1.027	0.986	0.989	0.935	0.948	1.014	1.017	0.936	0.933
4	0.009	0.994	1.004	1.002	1.000	0.990	0.986	0.991	0.990	1.002	1.007	1.021	1.000	1.014
5	0.011	0.986	0.998	0.993	1.001	0.991	0.991	0.981	1.007	1.007	1.019	1.016	1.007	1.005

Run F8 Two 90° Jets (6 March 1979) R_p = 27,500 M_r = 0.0100

Cross Section	C_v	1	2	3	4	5	6	7	8	9	10	11	12	13
1	0.574	0.748	0.946	1.422	2.327	1.437	0.953	0.737	0.269	0.489	1.440	1.460	0.564	0.209
2	0.168	0.858	0.885	1.069	1.380	1.055	0.858	0.814	0.852	0.961	1.219	1.203	0.954	0.893
3	0.041	0.982	1.002	1.013	1.088	1.000	0.949	0.942	0.968	0.990	1.058	1.051	0.993	0.963
4	0.021	0.959	0.975	1.007	1.027	0.992	0.978	0.974	1.007	1.010	1.012	1.023	1.023	1.012

Run G1 Induced Swirl, Single 90° Jet(13 April 1979) R_p = 31,300 M_r = 0.0140

Cross Section	C_v	1	2	3	4	5	6	7	8	9	10	11	12	13
1	0.638	0.016	0.042	0.084	0.645	1.211	1.622	1.744	1.469	1.069	0.472	1.320	1.643	1.666
2	0.191	0.834	0.884	0.986	1.043	0.982	0.960	0.930	0.777	0.810	0.828	1.354	1.299	1.311
3	0.070	1.026	1.076	1.132	1.098	0.911	0.909	0.901	0.982	1.002	1.043	0.983	0.990	0.948
4	0.048	0.923	0.908	0.942	1.013	1.073	1.040	1.042	0.994	0.980	0.992	1.043	1.022	1.028
5	0.028	0.994	0.989	1.000	1.015	0.996	0.989	0.959	1.048	1.055	1.033	0.976	0.977	0.970

Run G2 Induced Swirl, Two 90° Jets, (17 April 1979) R_p = 30,000 M_r = 0.0100

Cross Section	C_v	1	2	3	4	5	6	7	8	9	10	11	12	13
1	0.235	0.605	0.749	0.610	0.929	0.965	1.228	1.012	1.084	1.289	0.841	1.133	1.315	1.240
2	0.052	0.956	0.971	1.017	1.021	0.960	0.933	1.003	0.945	0.983	0.968	1.044	1.092	1.108
3	0.021	0.960	0.975	0.992	1.010	0.999	0.990	1.005	1.007	1.040	1.037	1.005	0.992	0.987
4	0.016	0.971	0.983	0.983	1.011	1.023	1.023	1.014	0.980	0.990	1.011	1.002	1.005	1.005
5	0.013	0.971	0.989	0.992	0.989	0.998	0.995	0.995	1.001	1.013	1.013	1.010	1.007	1.026

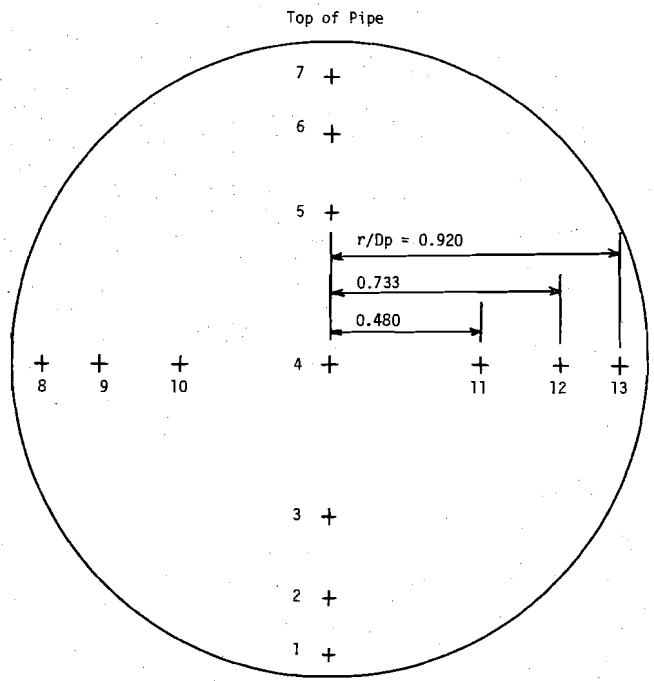

Fig. A-1 - Location of 13 measurement points in the pipe cross section